# DISSEMINATION OF *Yersinia pestis* DURING BUBONIC PLAGUE

Rodrigo Javier Gonzalez

A dissertation submitted to the faculty at The University of North Carolina at Chapel Hill in partial fulfillment of the requirements for the degree of Doctor in Philosophy in the Department of Microbiology and Immunology.

Chapel Hill 2014

Approved by:

Peggy Cotter

William E. Goldman

Thomas H. Kawula

Zhi Liu

Virginia L. Miller

## ABSTRACT

Rodrigo Javier Gonzalez: Dissemination of *Yersinia pestis* during bubonic plague
(Under the direction of Virginia L. Miller)

*Yersinia pestis* is a highly virulent bacterial pathogen with remarkable abilities to disseminate in a host. The ability of this Gram-negative bacterium to spread and replicate in its host results in high morbidity and mortality in humans. Bubonic plague is the most prevalent form of the disease and develops after *Y. pestis* is deposited into the skin of a susceptible host. Little is known about the events that occur after inoculation into the skin and that result in movement of bacteria to the lymph node that drains this site. Similar questions surround how the bacteria progress beyond the lymph node to survive systemically. This work focused on the use of a murine model and a fully virulent strain of plague to gain insights into how *Y. pestis* interacts with the host during dissemination. We describe an imaging approach to study bacterial dissemination in mice (*Chapter 2*). In this chapter, a bioluminescent strain of *Y. pestis* was used to track bacterial spread in mice by bioluminescence imaging using different routes of infection. We also studied the major events that define dissemination from the skin into the lymph node and that result in systemic dissemination (*Chapter 3*). We found that dissemination of *Y. pestis* into lymph nodes is restricted by a bottleneck that defines the final population that colonizes the host. By using confocal microscopy, we tracked bacteria at different stages of infection and identified important sites where host-pathogen interactions occur. Lastly, we established the importance of

an intradermal model of inoculation we implemented after comparing it with a subcutaneous model that has been traditionally used in the field (*Chapter 4*).

Our study contributes significantly to the understanding of host-pathogen interaction during bacterial infections. More specifically, our findings provide important information that advances our knowledge on *Y. pestis* pathogenesis and how the bacterium disseminates inside a host. Because of the scope of our research, these findings have relevant implications to fields as diverse as bacterial pathogenesis, cutaneous immunity, and vaccine development.

## DEDICATION

I dedicate this work to all the people that have supported me in any way during my career. This includes my mother, the rest of my family, and the many friends I have accumulated through the years. This also includes the researchers that have served as my mentors in the different branches of research I have explored and the professors that contributed to my formation as a biologist. Besides obtaining invaluable support from them to advance in my field, I also obtained extremely valuable lessons that will be essential for my future career.

## ACKNOWLEDGEMENTS

I am particularly thankful to Virginia L. Miller for her interest in my development as a researcher and in the advancement of my career. Her commitment and dedication to research and academia, along with other qualities, served as an example for me to follow.

I would also like to thank Kim Walker for her constant support during experimental design and critical review of the publications that derive from this work.

# TABLE OF CONTENTS

## LIST OF TABLES

## LIST OF FIGURES

## LIST OF ABBREVIATIONS

BHI: Brain and heart infusion

BLI: Bioluminescence imaging

BSL3: Biosafety level three laboratory

Carb: Carbenicillin

CFU: Colony forming units

DC: Dendritic cell

GFP: Green fluorescent protein

hpi: Hours post inoculation

ID: Intradermal

IP: Intraperitoneal

IV: Intravenous

Kan: Kanamycin

LN: Lymph node

O.D.: Optical density

PAMP: Pathogen associated molecular pattern

PRR: Pathogen recognition receptor

RFP: Red fluorescent protein

ROS: Reactive oxygen species

SC: Subcutaneous

T3SS: Type three secretion system

Yaps: Yersinia autotransporters

Yops: Yersinia outer proteins

WHO: World Health Organization

WT: Wild type

# CHAPTER 1: *Yersinia pestis* AND PLAGUE

## 1.1. Overview

*Yersinia pestis* is a Gram-negative bacterium and the etiological agent of plague (Stenseth et al., 2008). Mainly because of historical reasons, plague is one of the most widely recognized bacterial diseases. Three of the deadliest pandemics in history were caused by *Y. pestis*, making this pathogen a source of fear as well as a reminder of the threat that infectious diseases represent (Zietz and Dunkelberg, 2004). While the antibiotic era brought the threat of plague pandemics to an end, *Y. pestis* still circulates worldwide in animal reservoirs (Gage and Kosoy, 2005). These reservoirs represent a threat to human populations that live in close proximities and are the source of occasional outbreaks. More important concerns are raised when the potential use of *Y. pestis* as a bioweapon is taken into account (Inglesby et al., 2000). In addition, further concerns derive from reports describing the existence of antibiotic resistant strains in nature (Galimand et al., 2006).

Bubonic plague is the most prevalent form of the disease. It originates from the bite of an infectious flea; as it attempts to feed, it deposits bacteria into the skin (Wimsatt and Biggins, 2009). Despite many years of research, little is understood about how *Y. pestis* interacts with mammalian hosts at the cellular and molecular level. This is especially true during bacterial dissemination from the skin into deeper tissues. Little is known about the specific responses of the skin to *Y. pestis*.

Bacterial interactions with the host components have been addressed mostly *in vitro* rather than *in vivo*. In addition, because of the challenges of working with fully virulent *Y. pestis*, most of the research has been conducted with attenuated strains. For these reasons, the interactions of *Y. pestis* with the immune response, specifically with the phagocytes, are not fully elucidated. Moreover, the use of less than ideal approaches to study plague has generated ideas that are widespread in the field. However, these ideas might have little in common with observations made in a biologically relevant system where all the components of infection are taken into account.

### 1.2. Natural history of plague

In 1894, Alexander Yersin isolated the causative agent of plague, a bacterium later known under the name of *Yersinia pestis*. Many years later, Yersin himself proposed a connection between plague and rats, an idea that was expanded by Paul-Louis Simond. Simond proposed a central role of fleas in transmission but was not able to show convincing evidence (Zietz and Dunkelberg, 2004). The flea hypothesis was confirmed in 1914 when Bacot and Martin described *Y. pestis* in the digestive tract of fleas. The conclusion of their report was that bacteria survived in fleas forming aggregates that blocked the proventriculus of the insect (Bacot and Martin, 1914). This blockage was demonstrated to be important for efficient bacterial transmission from flea to host. With this, centuries of unfruitful speculation on the causes of plague were over and the paradigm of plague infections was established.

Ricardo Jorge made an early observation with important consequences for plague persistence. Jorge demonstrated that *Y. pestis* was maintained in animal reservoirs in the wild, establishing plague as a zoonosis (Zietz and Dunkelberg, 2004). Besides explaining the occurrence of sudden outbreaks, this finding meant that control and elimination of plague would be a difficult, if not impossible task to accomplish. Indeed, plague currently exists in many parts of the globe, mainly in rodent reservoirs. The prevalence of *Y. pestis* in wild animals has been termed sylvatic plague. In addition to the role of rodents in the maintenance of *Y. pestis*, other animals are affected by the bacteria and may contribute to plague persistence. Lagomorphs (hares and rabbits), ungulates (hoofed mammals), marsupials, carnivores, primates, among others, have been described to succumb to infection (Gage and Kosoy, 2005). Cold blooded animals and birds do not appear to be susceptible to the disease. Sylvatic plague is also important because high spread episodes in animals (epizootics) result in the substantial lost of members of a species. In the United States, plague is distributed in areas inhabited by more than half of the animals considered endangered (Biggins and Kosoy, 2001). Species that are susceptible to the disease, such as the black footed ferret (*Mustela nigripes*), are considered endangered because of plague (Matchett et al., 2010).

How the bacteria are maintained during inter-epizootic cycles is at the moment one of the most important questions in the plague field. This is relevant because it is during epizootics when humans are at high risk, as they can acquire the fleas that abandon dead animals and that look for new sources of blood. Many

hypotheses have been proposed but little research has been done to test them. One possibility is that the bacteria survive in hosts that are less susceptible to the effects of the disease and, thus, play the role of healthy carriers. It has been suggested that latency can occur during the winter in ground squirrels during hibernation (Bizanov and Dobrokhotova, 2007). These carriers could start new cycles of transmission once they are active in the spring. Another possibility is that fleas can remain infected with *Y. pestis* for long periods, during which their ability to transmit the bacteria varies. In this case, epizootics would be observed only during the periods where optimal transmission by the flea takes place, a phenomenon perhaps triggered by changes in temperature, humidity, or availability of a specific nutrient in a bloodmeal. In agreement with this hypothesis, it has been shown that the source of blood can affect many factors of flea transmission (Eisen et al., 2008). Feeding fleas on different sources (rat, mouse, and rabbit) affected bacterial loads and the ability of fleas to remain infected. Lastly, a bacterial dormant stage in the environment has also been proposed. Few studies have addressed this idea but one in particular claims to have found an induced dormant state in low temperature water (Pawlowski et al., 2011).

Other less conventional hypotheses have been proposed regarding maintenance of *Y. pestis* in natural settings, but are not generally accepted due to a lack of data to support them. One such hypothesis proposes that specific genes allow the bacteria to survive and continue colonizing an animal after death (Easterday et al., 2011). This could allow the bacteria to survive over extended

periods and perhaps to be transmitted to a carrion-eating animal with equal or less susceptibility to *Y. pestis*.

One or many of the scenarios mentioned above could contribute to the maintenance of sylvatic plague but so far none of them have been established as relevant. Determining how *Y. pestis* survives during inter-epizootic events could potentially be the next most important discovery in the field.

### 1.3. Epidemiology

Vague descriptions of the spread of plague date back from ancient times. It was only in the 14th century, during the pandemic known as the Black Death, when more detailed descriptions about disease spread and prevalence were written. These are the first examples where prevalence could be linked to symptoms that are more or less compatible with plague. Very detailed documents exist from the centuries that followed the Black Death. Worth mentioning are the records of the Venetian government, which made substantial efforts to control epidemics of plague. During the 17$^{th}$ and 16$^{th}$ centuries, the city of Venice relied on a remarkably well-structured set of strategies to prevent plague outbreaks (Konstantinidou et al., 2009). These strategies included isolation of sick individuals to separate islands, which constitutes the first example of government control over a population to prevent disease spread. As a result, the Venetian republic was one of the very few territories in Europe and Asia that, to some extent, was able to control plague. In spite of such epidemiological control, plague continued to have devastating effects during the next several centuries.

*Y. pestis* is considered to be responsible for three major pandemics in history: The Justinian Plague, The Black Death, and the Third Pandemic (Zietz and Dunkelberg, 2004). Despite the large number of epidemics caused by *Y. pestis*, humans are considered incidental hosts. Most human cases are caused by fleabites in plague endemic foci (Perry and Fetherston, 1997). Transmission to humans can only be linked to specific groups of animals, since only some of the flea species that parasitize them can also feed on human blood. Squirrels, which carry fleas that feed on humans, are the major source of infections in the United States (Perry and Fetherston, 1997). Besides fleabites, other less common means of transmission exist. Ingestion of raw meat from camel resulted in infection of five individuals in the middle east (Abdulaziz A Bin Saeed, 2005). *Y. pestis* was isolated from left over meat and from fleas found in the surroundings where the camel was kept. This case is an example of a rare manifestation of the disease termed pharyngeal plague that is caused by ingestion of bacteria. Other uncommon means of transmission include handling of infected carcasses (Wong et al., 2009). A field biologist acquired the bacteria in the United States during a dissection of a mountain lion found dead in the wild. The researcher was found dead in his house and *Y. pestis* bacilli were isolated from his body and from the carcass of the mountain lion.

The World Health Organization (WHO) reported that the number of suspected and confirmed human cases of plague worldwide from 1994 to 2003 was 28,530 (Table 1.1) (Butler, 2009; WHO, 2004). The number of deaths reported was 2015. This number might not be accurate because isolated cases are typically not

reported. Africa is the most affected continent but plague foci exist in every continent. Of importance is the reappearance of cases where the disease had not been seen in many years. Eighteen cases of bubonic plague were reported in 2003 in Algeria, a country that had no reported cases in the previous 50 years (Bertherat et al., 2007). Because of similar increases in reported cases in other countries, plague has been categorized as a re-emerging infectious disease. It has been suggested, however, that amplification and regression of existing sylvatic foci drive this apparent re-emergence (Duplantier et al., 2005). Whether this is true or new foci are starting to emerge is unknown.

Lastly, a role of climate change in plague cases around the world has been proposed. This hypothesis states that raising temperatures can influence the three factors that are important for plague transmission: fleas, hosts, and bacteria (Ben Ari et al., 2011). At a small scale, temperature can influence the ability of bacteria to replicate and perhaps to efficiently colonize fleas. At a higher scale, temperature affecting local weather can affect flea and rodent density. At an even higher scale, temperature can increase the probability of primary hosts establishing contacts with secondary hosts such as humans (Ben Ari et al., 2011).

### 1.4. Clinical manifestations and treatment

Depending on the route of bacterial entrance to the body, plague can be identified as bubonic, pneumonic, and septicemic. Each route varies in early clinical manifestations but all can result in bacterial dissemination into the bloodstream.

*1.4.1. Bubonic plague*

Bubonic plague is the most prevalent form of the disease and it takes place after bacteria penetrate the skin (Smego et al., 1999). This can occur when individuals handle contaminated material and experience skin abrasions, or most commonly, after the bite of an infected flea (Wimsatt and Biggins, 2009). Mortality rates range between 50 to 90% (Dennis and Staples, 2009; Prentice and Rahalison, 2007).

During the early stages of infection, pustules can develop in the area of contact. Disease progresses as *Y. pestis* abandons the skin and moves into the lymph node that drains this site (Sebbane et al., 2005). The bacteria that reach this compartment replicate at remarkably high rates. Colonization of lymph nodes results in severe inflammation causing major enlargement of the tissue (Smego et al., 1999). Enlarged lymph nodes are termed buboes, and constitute the hallmark of bubonic plague. From the Middle Ages on, the presence of buboes is one of the most important signs of bubonic plague infections (Walløe, 2008). Because fleabites take place more commonly in the extremities, buboes are typically found in the inguinal and axillary regions of the body (Smego et al., 1999).

Symptoms of bubonic plague include high fever, myalgia, malaise and painful buboes (Crook and Tempest, 1992). During the late stages of infection, *Y. pestis* escapes into the blood stream. This can happen through direct entrance of bacteria into the blood from the vessels that irrigate the lymph nodes. Alternatively, bacterial can escape through efferent lymphatic vessels to eventually reach the thoracic duct. This is the largest lymphatic vessel and the major collector of lymph from

other vessels of the body. It serves as a connection between the lymphatic system and systemic circulation as it drains into the left subclavian vein. The escape of *Y. pestis* from the lymph node is one of the most understudied aspects of plague. It is unknown if specific genes are upregulated in this compartment to either invade local blood vessels or to guarantee easy escape from efferent lymphatic vessels.

Once systemic dissemination occurs, the typical symptoms of sepsis are observed. Necrosis in the skin or other parts of the body such as entire limbs can occur. Digital gangrene has also been observed (Anisimov and Amoako, 2006). This is thought to be caused by bacterial blockage of capillary vessels, which results in irregular blood irrigation to the affected areas. Death is mainly caused by circulatory collapse and extended internal hemorrhage. In some cases, colonization of the lungs develops into secondary pneumonic plague, which can be an alternative cause of death.

*1.4.2. Pneumonic plague*

Pneumonic plague is the only form of the disease that can be transmitted person-to-person and is considered the most lethal manifestation of plague (Dennis and Staples, 2009). A plague patient with bacteria in the lungs can expel bacteria-containing particles, which in turn can be inhaled by a naïve individual. This individual most likely will develop primary pneumonic plague. Patients succumb in four to seven days after initial contact with the bacteria. Without prophylaxis, mortality rates are nearly 100%. Because *Y. pestis* can be acquired through aerosols, the use of fully virulent strains in research is restricted to biosafety level 3 (BSL3) laboratories. Furthermore, aerosol dispersion poses a threat to public

health as it provides the possibility that *Y. pestis* could be used as a bioweapon (Inglesby et al., 2000). For this reason, *Y. pestis* is currently categorized as a tier one select agent, which entails tight regulations for those who handle the bacteria in any setting.

A murine model of infection suggests that pneumonic plague progresses in two phases (Lathem et al., 2005). The pre-inflammatory phase is characterized by high levels of bacterial replication in the lung, and the absence of a local immune response. This is followed by a pro-inflammatory phase, when cytokine production, neutrophil influx, and disruption of the lung architecture are observed. The effects of this pro-inflammatory phase are responsible for pneumonia and death. Septic shock caused by bacterial escape to the bloodstream might also contribute to death.

During the pro-inflammatory phase, patients experience an array of symptoms. These symptoms include coughing, myalgia, malaise and weakness (Crook and Tempest, 1992). As pneumonia progresses, shortness of breath, chest pain and bloody or purulent sputum are observed. Other symptoms might include diarrhea and vomiting. Hemorrhages in the lung fill air spaces with blood, causing hemorrhagic pneumonia. Stridor and cyanosis precede terminal events, which include respiratory and circulatory collapse, and bleeding diathesis (Anisimov and Amoako, 2006).

### *1.4.3 Septicemic plague*

Septicemic plague derives from skin inoculations that result in direct passage of bacteria to the bloodstream (Dennis and Staples, 2009). In septicemic plague,

patients do not display any of the lymphatic tissue-related symptoms, such as appearance of buboes. Laboratory intradermal models of infection using mice rarely result in septicemic plague. However, this changes when flea-murine models are employed. Flea infections have been reported to result in septicemic plague with no apparent lymph node involvement (Sebbane et al., 2006). It is challenging to determine if these cases are truly septicemic plague. This is because the criteria used to establish septicemic cases rely mainly on the absence of bubo formation. While a true direct passage from skin into blood might occur, an alternative explanation could be elimination of bacteria in lymph nodes after they have escaped to the bloodstream. Along with pneumonic plague, patients that experience septicemic plague rarely survive (Dennis and Staples, 2009).

*1.4.4 Treatment*

The three forms of the disease described above result in high morbidity and mortality. Up until the antibiotic era, patient care relied on strategies mostly based on superstition or archaic medicine. In more recent times, treatments such as the application of local antiseptics and incision of buboes were efficacious in a few patients (Anisimov and Amoako, 2006). However, high levels of efficacy were only reached with the use of sulfanilamide antibiotics (Carman, 1938). The use of tetracycline, streptomycin, chloramphenicol, and more recently, gentamicin and amikacin, are currently recommended to treat plague patients (Anisimov and Amoako, 2006). While these antibiotics are easy to administer, mortality is still not uncommon. This is mainly because of misdiagnosis that derives from the subtle and unspecific early symptoms of plague (i.e. myalgia, fever, malaise).

Misdiagnosis typically leads to delayed administration of prophylaxis, making these drugs inefficacious because bacterial numbers in circulation are too large. Important concerns have been raised because of reports that describe antibiotic resistant strains circulating in nature (Hinnebusch et al., 2002).

## 1.5. *Yersinia pestis* pathogenesis and host response

The genus *Yersinia* includes 15 species and belongs to the Enterobacteriaceae family (Zhou and Yang, 2009). Three species of this genus are considered pathogenic to humans: *Y. enterocolitica*, *Y. pseudotuberculosis* and *Y. pestis*. The first two are enteric pathogens that are acquired via food-oral routes. *Y. pestis* is a non-motile coccobacillus that shares a very high DNA sequence similarity with *Y. pseudotuberculosis* (Dennis and Staples, 2009). It is thought that *Y. pestis* emerged from a *Y. pseudotuberculosis* clone and subsequently acquired multiple genetic traits (Hinnebusch, 2005). These traits gave the bacterium the ability to survive in a new life cycle that involved a flea vector and that resulted in high pathogenicity to mammals. The three major pandemics thought to be caused by *Y. pestis* are associated with specific biovars. These three biovars are Antiqua, Medievalis, and Orientalis and are associated with the Justinian plague, the Black Death, and the Third Pandemic, respectively (Prentice and Rahalison, 2007). The strain used in this work, CO92, belongs to the biovar Orientalis (Parkhill et al., 2001).

### *1.5.1. Virulence factors*

*Y. pestis* and *Y. pseudotuberculosis* diverge in ways that include gene inactivations, deletions, additions, and chromosomal rearrangements (Perry and

Fetherston, 1997). *yadA* and *inv* constitute examples of gene inactivations. The proteins encoded by these two genes are important for *Y. pseudotuberculosis* to cause enteric disease by helping the bacteria with adhesion and invasion of enteric tissues. These two genes are inactivated (present as pseudogenes) in *Y. pestis*, a trait that is thought to reflect a switch from an enteric to a vector-born lifestyle (Hinnebusch, 1997).

All pathogenic yersiniae carry the plasmid pCD1 (also known as pYV), which carries genes that encode the Ysc type III secretion system (T3SS) apparatus and the *Yersinia* outer proteins (Yops) secreted by it (Bleves and Cornelis, 2000). These genes are essential for abrogating immune responses of the host and, elimination of the pCD1 plasmid results in avirulent strains (Huang et al., 2006). Many of the Yops have been suggested to play specific roles during infection: YopE has been shown to interfere with actin polymerization of phagocytic cells; YopH is thought to induce apoptosis; YopM is suggested to be important to prevent blood clot formation. Many of the Yops are not fully characterized and their function remains to be confirmed *in vivo* (Amedei et al., 2011).

In addition to pCD1, *Y. pestis* carries the plasmid pPla (also known as pPCP1 or pPst) (Hinnebusch, 1997). This plasmid carries the plasminogen activator gene *pla*, which encodes a factor with proteolytic properties. This gene is involved in fibrinolytic and plasmocoagulase activities of *Y. pestis*. *pla* has been shown to be essential for *Y. pestis* to cause pneumonic plague (Lathem et al., 2007) and flea-derived bubonic plague (Sebbane et al., 2006). The same plasmid also carries *pst*

(bacteriocin pesticin), and *pim* (pesticin immunity protein) (Perry and Fetherston, 1997).

A third plasmid, pFra (also known as pMT1), carries *ymt* (murine toxin) and *caf1* (capsular antigen) (Zhou et al., 2006). Their functions are not fully understood but most studies agree that Caf1 acts an antiphagocytic factor. The importance of this protein, however, has been shown to depend on the genetic background of the host in experiments using a murine model of bubonic plague (Weening et al., 2011).

Another gene that has been shown to be important to abrogate innate immune responses is *psaA* (pH6 antigen). As with *caf1*, this gene is thought to prevent phagocytosis (Huang and Lindler, 2004). Mutants lacking the *psaA* gene showed attenuation during mouse infections (Weening et al., 2011; Zav'yalov et al., 1996).

### *1.5.2. Innate immunity and bubonic plague*

The immune response to pathogens can be specific (termed adaptive) or non-specific (termed innate). Innate immune responses are those that are activated against general stimuli that serve as cues for the body to identify invaders. These cues are termed pathogen associated molecular patterns (PAMPs) and are molecules that serve as building blocks of essential components of pathogens (Vance et al., 2009). They are detected in the host by pattern recognition receptors (PRRs), which results in the activation of a myriad of systems whose goal is to eliminate infection (Diacovich and Gorvel, 2010). While adaptive responses are extremely important for controlling many pathogens, they are not thought to play a relevant role during normal plague infections. Adaptive immunity starts when

specialized cells process molecules produced by a specific pathogen. Long-lasting immune responses are then generated specifically against the pathogens that carry such molecules. Establishing an adaptive immune response requires approximately two weeks. This is twice the time it takes for plague-infected animals to succumb to disease (Lathem et al., 2005; Sebbane et al., 2005). For this reason, innate immunity is the only branch of the immune response that is believed to be relevant to plague pathogenesis and will be the focus of this section.

Innate immune responses consist of physical barriers, immune molecules, and immune cells (Akira et al., 2006). Infection starts when bacteria break the physical barriers that protect the body from the environment. Epithelial tissues are examples of these barriers, as they prevent entry of bacteria into the body. Upon entrance, the bacteria themselves or the damage caused to the surrounding cells trigger the release of molecules that serve mostly as alert signals (Nestle et al., 2009). The most important molecules the innate immune system uses to combat pathogens are complement and cytokines (Kumar et al., 2011; Shi and Pamer, 2011). The functions of these molecules are diverse. They can serve as chemoattractants to cells of the immune response; modulate expression of genes that will favor pathogen elimination; or adhere directly to a pathogen to facilitate phagocytosis. Upon cytokine release, cellular-mediated responses are activated. These responses rely on specialized lineages of cells with many properties that allow them to eliminate intruders. These cells include macrophages, dendritic cells (DC), neutrophils, natural killer cells, mast cells, and monocytes (Abraham and St John, 2010; Kolaczkowska and Kubes, 2013; Nestle et al., 2009; Rescigno, 2002; Shi

and Pamer, 2011; Slauch, 2011). Bacterial killing can be achieved by the release of molecules that are detrimental to the pathogen. However, killing of bacteria mostly occurs intracellularly, after phagocytosis. Any cell of the innate immune response that can engulf invaders is termed a phagocyte. Some of these cells are also called professional antigen presenting cells. This is because they present molecules from degraded pathogens to T cells in lymph nodes (Alvarez et al., 2008). Antigen presentation in lymph nodes marks the beginning of adaptive immune responses. DCs are the epitome of antigen presenting cells and, thus, are considered a link between innate and adaptive immunity (Ueno et al., 2007).

Another important aspect of innate immunity is inflammation. This mechanism of defense can act as a physical barrier to dissemination. In addition, inflamed tissues release alarm signals, which are molecules that alert the body about the invasion of a pathogen (Kolaczkowska and Kubes, 2013).

The ability of *Y. pestis* to prevent phagocytosis is perhaps its most important trait. *Y. pestis* shows multiple genetic traits that reflect the importance of host cellular-mediated responses to infection (Durand et al., 2010). Based on the degrees of attenuation obtained by the use of deletion mutant strains, the T3SS apparatus and some of its translocated proteins have been shown to be the most important virulence factors of *Y. pestis* (Aepfelbacher et al., 2007). Abrogation of cellular-mediated innate immune responses is probably the most important activity of *Y. pestis* to survive in the host (DeLeo and Hinnebusch, 2005). The bacteria can affect basic activities of a phagocytic cell, such as movement, or its ability to produce cytokines to recruit other cells. For this reason, the proteins that help the

bacteria accomplish this function are simply known as antiphagocytic factors. In a murine model of plague using a reporter system to identify cells targeted by T3SS, Marketon et al. found that neutrophils, macrophages and DCs were injected by the apparatus (Marketon et al., 2005). In intranasal models that mimic pneumonic plague, similar results were shown but the most important group targeted was neutrophils (Pechous et al., 2013).

The great majority of plague studies that address interactions with host cells have been conducted *in vitro* using tissue culture cell lines. The most extensively studied cell lineage for these studies is macrophages. This is perhaps because macrophage cells and macrophage-like cell lines are readily available and relatively easy to work with. Macrophage phagocytosis of *Y. pestis* grown at a temperature of 26°C has been extensively documented (Janssen and Surgalla, 1969). This is a temperature at which *Y. pestis* grows inside a flea and one that is not conducive to expression of antiphagocytic factors. Most reports affirm that *Y. pestis* survives and replicates inside macrophages (Cavanaugh and Randall, 1959; Pujol and Bliska, 2003; Straley and Harmon, 1984). However, the most recent literature emphasizes survival rather than growth (Amedei et al., 2011; Klein et al., 2012). This is perhaps because of high variability that exists between cell lines and because observations of substantial intracellular growth are hard to replicate (Ponnusamy and Clinkenbeard, 2012). While interactions with macrophages have been assessed in a few *in vivo* murine models, attenuated strains or routes that are not biologically relevant are typically used (Charnetzky and Shuford, 1985), making the conclusions somewhat limited.

Neutrophils are the second most common phagocyte used to study plague pathogenesis (Shannon et al., 2013; Spinner et al., 2013). These cells are considered the most efficient lineage of the innate response to control any bacteria (Kobayashi et al., 2005). As with macrophages, most plague research involving neutrophils has relied on *in vitro* approaches. Although there are some disagreements among different studies, it is largely believed that *Y. pestis* is susceptible in one way or another to the microbicidal effects of neutrophils (Pujol and Bliska, 2005). It has been proposed that ingested *Y. pestis* are eliminated by neutrophils regardless of the presence of T3SS. Moreover, extracellular bacteria appear to survive in a T3SS dependent manner (Spinner et al., 2008). For this reason, it is thought that preventing neutrophil recruitment is beneficial for *Y. pestis*. The outer membrane protein Ail has been suggested to contribute to preventing neutrophil recruitment (Hinnebusch et al., 2011). Survival in neutrophils has also been reported and is dependent on the two component system PhoPQ (O'Loughlin et al., 2010). Recent work using an intradermal murine model of bubonic plague imaged neutrophil recruitment into the skin (Shannon et al., 2013). In this study, a robust neutrophil response was seen in the dermis during the first four hours of infection. The study reported bacteria residing inside neutrophils in the skin as well as subversion of neutrophil functions against bacteria at this site. In addition, it was proposed that *Y. pestis*-containing neutrophils are engulfed by macrophages (Spinner et al., 2013). This process, termed efferocytosis, has been documented in other infections. Efferocytosis has been shown to have major implications for the transport of pathogens such as *Leishmania* to lymph nodes

(Peters et al., 2008; Silva, 2010). In summary, *Y. pestis* might be eliminated by neutrophils in some cases and might be able to survive inside them as well. These contradictory properties of the bacteria might reflect adaptations of *Y. pestis* to the specific conditions used during experiments. They may also reflect how little we understand about neutrophil biology and, perhaps, even diversification.

An active role of DCs during bubonic plague infections has been suggested (Velan et al., 2006; Zhang et al., 2008). This is because these cells move antigen from the skin to lymph nodes and could be used by the bacteria to disseminate inside the body (Rescigno, 2002; Weiner and Glomski, 2012). However, very little research on the interactions of *Y. pestis* with DCs has been conducted. This could be because of the technical challenges that working with this group of cells entails. DCs exist in very low numbers in the body and their isolation in high enough quantities for experiments is difficult (Inaba et al., 2001). In addition, DCs exist in a myriad of subgroups whose functions are unknown. It is difficult to determine what is the most appropriate subgroup to use when addressing a specific question (Kadowaki et al., 2001). While different reports have looked at some aspects of *Y. pestis* interactions with dendritic cells, *in vitro* approaches were used in most of them (Lindner et al., 2007; Robinson et al., 2008; Velan et al., 2006; Zhang et al., 2008). In the same study that determined neutrophil recruitment to the dermis, Shannon et al. also assessed the role of DCs during infection (Shannon et al., 2013). The study reports a very modest recruitment of DCs into the dermis and little interaction of these cells with *Y. pestis*. The report concludes that DCs are not likely to play a relevant role during infection.

### 1.6. Dissemination from the skin

Based on its anatomy and physiology, the skin can be divided into three main layers: epidermis, dermis, and hypodermis or subcutaneous space. The epidermis is in direct contact with the environment and is devoid of blood and lymphatic vessels (Combadiere and Liard, 2011). The dermis is the most active layer of the skin, physiologically and immunologically (Nestle et al., 2009; Teunissen et al., 2012). The dermis possesses high numbers of blood vessels, lymphatic vessels, and cells of the innate immune response. The presence of these three elements makes the dermis unique in its responses to invading microorganisms (Mathers and Larregina, 2006; Teunissen et al., 2012). The hypodermis contains blood and lymphatic vessels but in low densities. Furthermore, the lymphatic vessels in this layer of the skin vary considerably from those found in the dermis. The lymphatic vessels found in the dermis, termed superficial lymphatics, are adapted to readily take lymph from the surrounding tissue. The lymphatic vessels found in the hypodermis, termed deeper lymphatics or collectors, are surrounded by a basement membrane and smooth muscle cells (Shayan et al., 2006). These two elements make deeper lymphatics less efficient in the uptake of surrounding fluid. Furthermore, the lack of resident immune cells in the hypodermis makes this layer of the skin a less immunologically competent site in comparison with the dermis (Bonnotte et al., 2003; Combadiere and Liard, 2011).

Very little research has been done regarding how arthropods obtain blood from a mammal and it is not well understood what kind of lesion a flea produces when probing the skin to take a bloodmeal (Hinnebusch, 2005). A blood feeding

arthropod can insert a sucking mouthpart (proboscis) into the skin and feed directly from a blood vessel. Alternatively, specialized mouthparts can cut into the skin, which produces a lesion filled with fluids from which the arthropod can feed. While fleas possess cutting mouthparts, it is not known if they can be used to obtain blood directly from blood vessels or if they damage the surrounding area to obtain a bloodmeal. Most research has been done on mosquitoes, which were thought to probe directly into blood vessels to obtain blood. Recent intravital imaging experiments have shown that while that does occur, mosquitoes can also feed from other sites of the skin where blood accumulates as they probe (Choumet et al., 2012). This shows that the question of how a flea feeds might be a very complex one and how little we understand about how bacteria are deposited into the skin. Most research agrees, however, that the preferred site for blood feeding arthropods to obtain a meal is the dermis, and not the subcutaneous space (Chong et al., 2013). This has also been suggested specifically for plague (Hinnebusch, 2005; Sebbane et al., 2006). Determining how exactly the flea inoculates *Y. pestis* is critical for understanding the first moments of dissemination. If bacteria are deposited into blood vessels, they will disseminate in a direct route that goes from flea into blood. If, on the other hand, fleas probe on the surrounding tissue, bacteria must disseminate in a skin-lymph-blood route. Most of the research conducted so far suggests that the latter is a closer description of what happens during bubonic plague (Sebbane et al., 2005).

One of the most important questions in infectious diseases is how pathogens move from the initial site of contact with the host into deeper organs. Because of

technological limitations, however, direct approaches to address this question are not readily available. Two possibilities exist as to how bacteria travel from the skin to lymph nodes through lymphatics. The first possibility involves bacteria traveling with the flow of lymph. In this case, bacteria are deposited into the skin and the pressure of lymph itself, along with the contractions of lymphatic vessels could drive movement to lymph nodes (Hegde et al., 2011). Knowledge on the lymphatic system in general is very limited, and the physiology of particle movement through it is not well understood. Perhaps for this reason, the possibility of pathogens moving with the flow of lymph in lymphatic vessels is scarcely addressed in the literature.

The second possibility is that pathogens travel from the site of inoculation into lymph nodes inside phagocytic cells. This idea is the most widely accepted in fields beyond plague research. However, this notion is, with very few exceptions, merely speculative. In the case of plague, the most accepted model states that upon inoculation, *Y. pestis* does not yet express antiphagocytic factors and thus, it is susceptible to phagocytosis. This has lead to the notion that *Y. pestis* has an intracellular phase during early stages of infection. Moreover, it has been proposed that intracellular phases are necessary for the bacteria to travel from the skin to the lymph node that drains this site (Zhou et al., 2006). This is based on the normal function of antigen presenting cells, which travel to lymph nodes once they have engulfed antigen. In this way, *Y. pestis* would reach the lymph node using a phagocyte as a Trojan horse (Weiner and Glomski, 2012). Once in the lymph node, the bacteria could exit the phagocytic cell for further colonization of this

compartment. A “Trojan Horse” model of bacterial dissemination has been proposed for other pathogens (Guidi-Rontani, 2002). However, the model has received only modest experimental support (Mihret, 2012). An alternative model of dissemination has been proposed for *Bacillus anthracis*. In this alternative model, in addition to intracellularly, bacteria can also disseminate freely without the need of a phagocytic cell (Weiner and Glomski, 2012). Supporting a phagocyte-free model, a study on *Salmonella abortusovis* found that during the first 90 minutes of dissemination, 80% of bacteria are found in lymph vessels traveling freely to lymph nodes (Bonneau et al., 2006).

Recent advances in *in vivo* work and imaging are opening the possibilities of studying in more detail *Y. pestis* dissemination from the skin to the lymph nodes. Much experimental support will be needed for the field to accept a model where an intracellular stage is not required for bacteria to disseminate from the skin into lymph nodes and deeper organs.

### 1.8. Significance

Bacterial infections are detrimental to human health and can be lethal. While some research has been conducted on bacteria or the immune response, studies that describe the interactions of both are scarce. This is important because of the appearance of antibiotic resistance in many bacterial species that affect humans. New strategies to treat bacterial infections are needed but the lack of information on the physiology of host-pathogen interactions has been an impediment to advances. The threat of bacterial infections to human health is essentially defined by the capacity of bacteria to disseminate in the host. The remarkable ability of *Y.*

*pestis* to cause disease is strictly linked to its proficiency to disseminate in the host. This makes it an ideal model to study bacterial dissemination. Understanding *Y. pestis* dissemination has the potential of providing valuable information that will result in new strategies to control or even prevent bacterial infections. In addition, studying host-pathogen interactions *in vivo* provides invaluable information with relevant implications to other fields such as vaccine development.

### 1.7. Figures and Tables

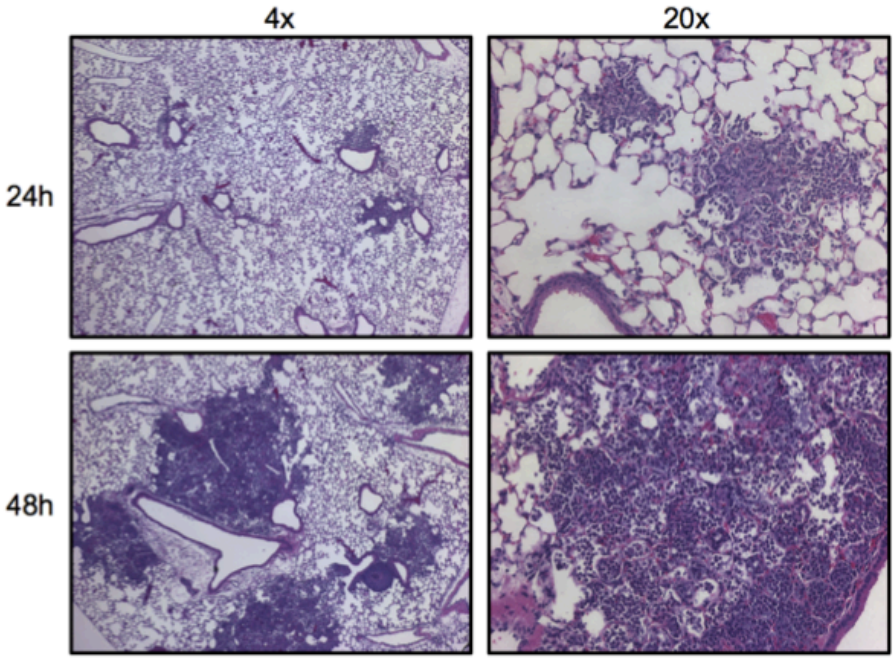


**Figure 1.1. Inflammation of the lung during pneumonic plague.**
During a pre-inflammatory phase, bacterial growth and little or no damage to the lung architecture is observed. At later time points (48 hours after intranasal inoculation), high levels of inflammation are detected. Image from (Pechous et al., 2013).

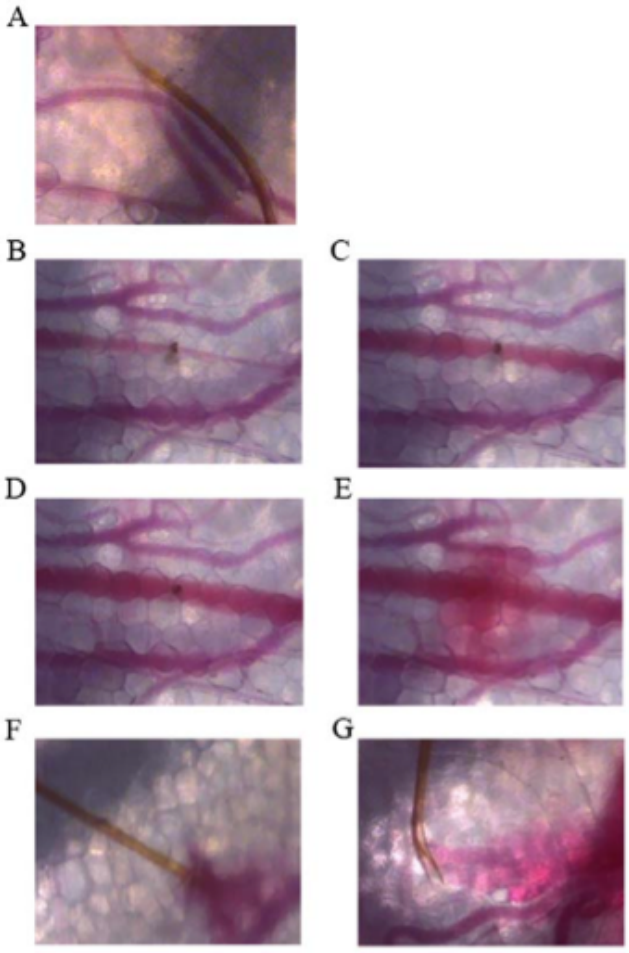


**Figure 1.2. Skin micrographs showing mosquito-feeding patterns.**
(A) Proboscis inside blood vessel. (B-E) Proboscis inserted perpendicular to the blood vessel. (F and G) types of blood feeding: proboscis located in the pool of blood (F) and sucking up blood from a pool of blood distant from the blood vessel. Blood vessels appear pink and the proboscis appears brown. Image from (Choumet et al., 2012).

| Country | Number of cases | Case-fatality rate (%) |
|---|---|---|
| **Congo** | 3619 | 10 |
| **Tanzania** | 3527 | 7 |
| **Mozambique** | 2387 | 1 |
| **Vietnam** | 1331 | 6 |
| **Malawi** | 900 | 2 |
| **Uganda** | 654 | 17 |
| **Peru** | 631 | 3 |
| **Zimbabwe** | 417 | 8 |
| **China** | 357 | 7 |

**Table 1.1: Cases of human plague in 1994-2003 in the countries that reported >100 confirmed or suspected cases.**
Adapted from (Butler, 2009)

## REFERENCES


Abdulaziz A Bin Saeed, N.A.A.-H.R.E.F. (2005). Plague from Eating Raw Camel Liver. Emerging Infect Dis *11*, 1456.

Abraham, S.N., and St John, A.L. (2010). Mast cell-orchestrated immunity to pathogens. Nat Rev Immunol *10*, 440–452.

Aepfelbacher, M., Trasak, C., and Ruckdeschel, K. (2007). Effector functions of pathogenic *Yersinia* species. Thromb Haemost *98*, 521–529.

Akira, S., Uematsu, S., and Takeuchi, O. (2006). Pathogen recognition and innate immunity. Cell *124*, 783–801.

Alvarez, D., Vollmann, E.H., and Andrian, von, U.H. (2008). Mechanisms and consequences of dendritic cell migration. Immunity *29*, 325–342.

Amedei, A., Niccolai, E., Marino, L., and D'Elios, M.M. (2011). Role of immune response in *Yersinia pestis* infection. J Infect Dev Ctries *5*, 628–639.

Anisimov, A.P., and Amoako, K.K. (2006). Treatment of plague: promising alternatives to antibiotics. Journal of Medical Microbiology *55*, 1461–1475.

Bacot, A.W., and Martin, C.J. (1914). LXVII. Observations on the mechanism of the transmission of plague by fleas. J Hyg (Lond) *13*, 423–439.

Ben Ari, T., Neerinckx, S., Gage, K.L., Kreppel, K., Laudisoit, A., Leirs, H., and Stenseth, N.C. (2011). Plague and climate: scales matter. PLoS Pathog *7*, e1002160.

Bertherat, E., Bekhoucha, S., Chougrani, S., Razik, F., Duchemin, J.B., Houti, L., Deharib, L., Fayolle, C., Makrerougrass, B., Dali-Yahia, R., et al. (2007). Plague reappearance in Algeria after 50 years, 2003. Emerging Infect Dis *13*, 1459–1462.

Biggins, D.E., and Kosoy, M.Y. (2001). Influences of introduced plague on North American mammals: implications from ecology of plague in Asia. Journal of Mammalogy *82*, 906–916.

Bizanov, G., and Dobrokhotova, N.D. (2007). Experimental infection of ground squirrels (*Citellus pygmaeus* Pallas) with *Yersinia pestis* during hibernation. J Infect *54*, 198–203.

Bleves, S., and Cornelis, G.R. (2000). How to survive in the host: the *Yersinia* lesson. Microbes Infect *2*, 1451–1460.

Bonneau, M., Epardaud, M., Payot, F., Niborski, V., Thoulouze, M.-I., Bernex, F., Charley, B., Riffault, S., Guilloteau, L.A., and Schwartz-Cornil, I. (2006). Migratory monocytes and granulocytes are major lymphatic carriers of *Salmonella* from tissue

to draining lymph node. J Leukoc Biol *79*, 268–276.

Bonnotte, B., Gough, M., Phan, V., Ahmed, A., Chong, H., Martin, F., and Vile, R.G. (2003). Intradermal injection, as opposed to subcutaneous injection, enhances immunogenicity and suppresses tumorigenicity of tumor cells. Cancer Research *63*, 2145–2149.

Butler, T. (2009). Plague into the 21st century. Clin. Infect. Dis. *49*, 736–742.

Carman, J.A. (1938). Prontosil in the treatment of oriental plague. East African Med J *14*, 362–366.

Cavanaugh, D., and Randall, R. (1959). The role of multiplication of *Pasteurella pestis* in mononuclear phagocytes in the pathogenesis of flea-borne plague. J Immunol *83*, 348–363.

Charnetzky, W.T., and Shuford, W.W. (1985). Survival and growth of *Yersinia pestis* within macrophages and an effect of the loss of the 47-megadalton plasmid on growth in macrophages. Infect Immun *47*, 234–241.

Chong, S.Z., Evrard, M., and Ng, L.G. (2013). Lights, Camera, and Action: Vertebrate Skin Sets the Stage for Immune Cell Interaction with Arthropod-Vectored Pathogens. Front Immunol *4*, 286.

Choumet, V., Attout, T., Chartier, L., Khun, H., Sautereau, J., Robbe-Vincent, A., Brey, P., Huerre, M., and Bain, O. (2012). Visualizing non infectious and infectious Anopheles gambiae blood feedings in naive and saliva-immunized mice. PLoS ONE *7*, e50464.

Combadiere, B., and Liard, C. (2011). Transcutaneous and intradermal vaccination. Hum Vaccin *7*, 811–827.

Crook, L.D., and Tempest, B. (1992). Plague. A clinical review of 27 cases. Arc Intern Med *152*, 1253–1256.

DeLeo, F.R., and Hinnebusch, B.J. (2005). A plague upon the phagocytes. Nat Med *11*, 927–928.

Dennis, D.T., and Staples, J.E. (2009). Plague. 597–611.

Diacovich, L., and Gorvel, J.-P. (2010). Bacterial manipulation of innate immunity to promote infection. Nat Rev Micro *8*, 117–128.

Duplantier, J.-M., Duchemin, J.-B., Chanteau, S., and Carniel, E. (2005). From the recent lessons of the Malagasy foci towards a global understanding of the factors involved in plague reemergence. Vet Res *36*, 437–453.

Durand, E.A., Maldonado-Arocho, F.J., Castillo, C., Walsh, R.L., and Mecsas, J.

(2010). The presence of professional phagocytes dictates the number of host cells targeted for Yop translocation during infection. Cell Microbiol *12*, 1064–1082.

Easterday, W.R., Kausrud, K.L., Star, B., Heier, L., Haley, B.J., Ageyev, V., Colwell, R.R., and Stenseth, N.C. (2011). An additional step in the transmission of *Yersinia pestis*? Isme J *6*, 231–236.

Eisen, R.J., Vetter, S.M., Holmes, J.L., Bearden, S.W., Montenieri, J.A., and Gage, K.L. (2008). Source of host blood affects prevalence of infection and bacterial loads of *Yersinia pestis* in fleas. J Med Entomol *45*, 933–938.

Gage, K.L., and Kosoy, M.Y. (2005). Natural history of plague: perspectives from more than a century of research. Annu Rev Entomol *50*, 505–528.

Galimand, M., Carniel, E., and Courvalin, P. (2006). Resistance of *Yersinia pestis* to antimicrobial agents. Antimicrob Agents Chemother *50*, 3233–3236.

Guidi-Rontani, C. (2002). The alveolar macrophage: the Trojan horse of *Bacillus anthracis*. Trends Microbiol *10*, 405–409.

Hegde, N.R., Kaveri, S.V., and Bayry, J. (2011). Recent advances in the administration of vaccines for infectious diseases: microneedles as painless delivery devices for mass vaccination. Drug Discov. Today *16*, 1061–1068.

Hinnebusch, B.J. (1997). Bubonic plague: a molecular genetic case history of the emergence of an infectious disease. J Mol Med *75*, 645–652.

Hinnebusch, B.J. (2005). The evolution of flea-borne transmission in *Yersinia pestis*. Curr Issues Mol Bio *7*, 197–212.

Hinnebusch, B.J., Jarrett, C.O., Callison, J.A., Gardner, D., Buchanan, S.K., and Plano, G.V. (2011). Role of the *Yersinia pestis* Ail protein in preventing a protective polymorphonuclear leukocyte response during bubonic plague. Infect Immun *79*, 4984–4989.

Hinnebusch, B.J., Rosso, M.-L., Schwan, T.G., and Carniel, E. (2002). High-frequency conjugative transfer of antibiotic resistance genes to *Yersinia pestis* in the flea midgut. Mol Microbiol *46*, 349–354.

Huang, X.-Z., and Lindler, L.E. (2004). The pH 6 antigen is an antiphagocytic factor produced by *Yersinia pestis* independent of *Yersinia* outer proteins and capsule antigen. Infect Immun *72*, 7212–7219.

Huang, X.-Z., Nikolich, M.P., and Lindler, L.E. (2006). Current trends in plague research: from genomics to virulence. Clin Med Res *4*, 189–199.

Inaba, K., Swiggard, W.J., Steinman, R.M., Romani, N., and Schuler, G. (2001). Isolation of dendritic cells. Curr Prot Imm / Edited by John E Coligan [Et Al] *Chapter 3*, Unit3.7.

Inglesby, T.V., Dennis, D.T., Henderson, D.A., Bartlett, J.G., Ascher, M.S., Eitzen, E., Fine, A.D., Friedlander, A.M., Hauer, J., Koerner, J.F., et al. (2000). Plague as a biological weapon: medical and public health management. Working Group on Civilian Biodefense. Jama *283*, 2281–2290.

Janssen, W.A., and Surgalla, M.J. (1969). Plague bacillus: survival within host phagocytes. Science *163*, 950–952.

Kadowaki, N., Ho, S., Antonenko, S., Malefyt, R.W., Kastelein, R.A., Bazan, F., and Liu, Y.J. (2001). Subsets of human dendritic cell precursors express different toll-like receptors and respond to different microbial antigens. J Exp Med *194*, 863–869.

Klein, K.A., Fukuto, H.S., Pelletier, M., Romanov, G., Grabenstein, J.P., Palmer, L.E., Ernst, R., and Bliska, J.B. (2012). A Transposon Site Hybridization Screen Identifies galU and wecBC as Important for Survival of *Yersinia pestis* in Murine Macrophages. J Bacteriol *194*, 653–662.

Kobayashi, S.D., Voyich, J.M., Burlak, C., and DeLeo, F.R. (2005). Neutrophils in the innate immune response. Arch Immunol Ther Exp (Warsz.) *53*, 505–517.

Kolaczkowska, E., and Kubes, P. (2013). Neutrophil recruitment and function in health and inflammation. Nat Rev Immunol *13*, 159–175.

Konstantinidou, K., Mantadakis, E., Falagas, M.E., Sardi, T., and Samonis, G. (2009). Venetian rule and control of plague epidemics on the Ionian Islands during 17th and 18th centuries. Emerging Infect Dis *15*, 39–43.

Kumar, H., Kawai, T., and Akira, S. (2011). Pathogen recognition by the innate immune system. Int Rev Immunol *30*, 16–34.

Lathem, W.W., Crosby, S.D., Miller, V.L., and Goldman, W.E. (2005). Progression of primary pneumonic plague: a mouse model of infection, pathology, and bacterial transcriptional activity. Proc Natl Acad Sci USA *102*, 17786–17791.

Lathem, W.W., Price, P.A., Miller, V.L., and Goldman, W.E. (2007). A plasminogen-activating protease specifically controls the development of primary pneumonic plague. Science *315*, 509–513.

Lindner, I., Torruellas-Garcia, J., Torrvellas-Garcia, J., Kolonias, D., Carlson, L.M., Tolba, K.A., Plano, G.V., and Lee, K.P. (2007). Modulation of dendritic cell differentiation and function by YopJ of *Yersinia pestis*. Eur J Immunol *37*, 2450–2462.

Marketon, M.M., DePaolo, R.W., DeBord, K.L., Jabri, B., and Schneewind, O. (2005). Plague bacteria target immune cells during infection. Science *309*, 1739–1741.

Matchett, M.R., Biggins, D.E., Carlson, V., Powell, B., and Rocke, T. (2010). Enzootic plague reduces black-footed ferret (*Mustela nigripes*) survival in Montana. Vector Borne Zoonotic Dis *10*, 27–35.

Mathers, A.R., and Larregina, A.T. (2006). Professional antigen-presenting cells of the skin. Immunol Res *36*, 127–136.

Mihret, A. (2012). The role of dendritic cells in *Mycobacterium tuberculosis* infection. Virulence *3*, 654–659.

Nestle, F.O., Di Meglio, P., Qin, J.-Z., and Nickoloff, B.J. (2009). Skin immune sentinels in health and disease. Nat Rev Immunol *9*, 679–691.

O'Loughlin, J.L., Spinner, J.L., Minnich, S.A., and Kobayashi, S.D. (2010). *Yersinia pestis* two-component gene regulatory systems promote survival in human neutrophils. Infect Immun *78*, 773–782.

Parkhill, J., Wren, B.W., Thomson, N.R., Titball, R.W., Holden, M.T., Prentice, M.B., Sebaihia, M., James, K.D., Churcher, C., Mungall, K.L., et al. (2001). Genome sequence of *Yersinia pestis*, the causative agent of plague. Nature *413*, 523–527.

Pawlowski, D.R., Metzger, D.J., Raslawsky, A., Howlett, A., Siebert, G., Karalus, R.J., Garrett, S., and Whitehouse, C.A. (2011). Entry of *Yersinia pestis* into the viable but nonculturable state in a low-temperature tap water microcosm. PLoS ONE *6*, e17585.

Pechous, R.D., Sivaraman, V., Price, P.A., Stasulli, N.M., and Goldman, W.E. (2013). Early host cell targets of *Yersinia pestis* during primary pneumonic plague. PLoS Pathog *9*, e1003679.

Perry, R.D., and Fetherston, J.D. (1997). *Yersinia pestis*--etiologic agent of plague. Clin. Microbiol. Rev. *10*, 35–66.

Peters, N.C., Egen, J.G., Secundino, N., Debrabant, A., Kimblin, N., Kamhawi, S., Lawyer, P., Fay, M.P., Germain, R.N., and Sacks, D. (2008). *In vivo* imaging reveals an essential role for neutrophils in leishmaniasis transmitted by sand flies. Science *321*, 970–974.

Ponnusamy, D., and Clinkenbeard, K.D. (2012). *Yersinia pestis* intracellular parasitism of macrophages from hosts exhibiting high and low severity of plague. PLoS ONE *7*, e42211.

Prentice, M.B., and Rahalison, L. (2007). Plague. Lancet *369*, 1196–1207.

Pujol, C., and Bliska, J.B. (2003). The ability to replicate in macrophages is conserved between *Yersinia pestis* and *Yersinia pseudotuberculosis*. Infect Immun *71*, 5892–5899.

Pujol, C., and Bliska, J.B. (2005). Turning *Yersinia* pathogenesis outside in: subversion of macrophage function by intracellular yersiniae. Clin Immunol *114*, 216–226.

Rescigno, M. (2002). Dendritic cells and the complexity of microbial infection. Trends Microbiol *10*, 425–461.

Robinson, R.T., Khader, S.A., Locksley, R.M., Lien, E., Smiley, S.T., and Cooper, A.M. (2008). *Yersinia pestis* evades TLR4-dependent induction of IL-12(p40)2 by dendritic cells and subsequent cell migration. J Immunol *181*, 5560–5567.

Sebbane, F., Gardner, D., Long, D., Gowen, B.B., and Hinnebusch, B.J. (2005). Kinetics of disease progression and host response in a rat model of bubonic plague. Am J Pathol *166*, 1427–1439.

Sebbane, F., Jarrett, C.O., Gardner, D., Long, D., and Hinnebusch, B.J. (2006). Role of the *Yersinia* pestis plasminogen activator in the incidence of distinct septicemic and bubonic forms of flea-borne plague. Proc Natl Acad Sci USA *103*, 5526–5530.

Shannon, J.G., Hasenkrug, A.M., Dorward, D.W., Nair, V., Carmody, A.B., and Hinnebusch, B.J. (2013). *Yersinia pestis* Subverts the Dermal Neutrophil Response in a Mouse Model of Bubonic Plague. MBio *4*, e00170–13..

Shayan, R., Achen, M.G., and Stacker, S.A. (2006). Lymphatic vessels in cancer metastasis: bridging the gaps. Carcinogenesis *27*, 1729–1738.

Shi, C., and Pamer, E.G. (2011). Monocyte recruitment during infection and inflammation. Nat Rev Immunol *11*, 762–774.

Silva, M.T. (2010). When two is better than one: macrophages and neutrophils work in concert in innate immunity as complementary and cooperative partners of a myeloid phagocyte system. J Leukoc Biol *87*, 93–106.

Slauch, J.M. (2011). How does the oxidative burst of macrophages kill bacteria? Still an open question. Mol Microbiol *80*, 580–583.

Smego, R.A., Frean, J., and Koornhof, H.J. (1999). Yersiniosis I: microbiological and clinicoepidemiological aspects of plague and non-plague *Yersinia* infections. Eur J Clin Microbiol Infect Dis. *18*, 1–15.

Spinner, J.L., Cundiff, J.A., and Kobayashi, S.D. (2008). *Yersinia pestis* type III secretion system-dependent inhibition of human polymorphonuclear leukocyte function. Infect Immun *76*, 3754–3760.

Spinner, J.L., Winfree, S., Starr, T., Shannon, J.G., Nair, V., Steele-Mortimer, O., and Hinnebusch, B.J. (2013). *Yersinia pestis* survival and replication within human neutrophil phagosomes and uptake of infected neutrophils by macrophages. J Leukoc Biol.

Stenseth, N.C., Atshabar, B.B., Begon, M., Belmain, S.R., Bertherat, E., Carniel, E., Gage, K.L., Leirs, H., and Rahalison, L. (2008). Plague: past, present, and future. PLoS Med *5*, e3.

Straley, S.C., and Harmon, P.A. (1984). *Yersinia pestis* grows within phagolysosomes in mouse peritoneal macrophages. Infect Immun *45*, 655–659.

Teunissen, M.B.M., Haniffa, M., and Collin, M.P. (2012). Insight into the immunobiology of human skin and functional specialization of skin dendritic cell subsets to innovate intradermal vaccination design. Curr Top Microbiol Immunol *351*, 25–76.

Ueno, H., Klechevsky, E., Morita, R., Aspord, C., Cao, T., Matsui, T., Di Pucchio, T., Connolly, J., Fay, J.W., Pascual, V., et al. (2007). Dendritic cell subsets in health and disease. Immunol Rev *219*, 118–142.

Vance, R.E., Isberg, R.R., and Portnoy, D.A. (2009). Patterns of pathogenesis: discrimination of pathogenic and nonpathogenic microbes by the innate immune system. Cell Host Microbe *6*, 10–21.

Velan, B., Bar-Haim, E., Zauberman, A., Mamroud, E., Shafferman, A., and Cohen, S. (2006). Discordance in the effects of *Yersinia pestis* on the dendritic cell functions manifested by induction of maturation and paralysis of migration. Infect Immun *74*, 6365–6376.

Walløe, L. (2008). Medieval and modern bubonic plague: some clinical continuities. Med Hist Suppl 59–73.

Weening, E.H., Cathelyn, J.S., Kaufman, G., Lawrenz, M.B., Price, P., Goldman, W.E., and Miller, V.L. (2011). The dependence of the *Yersinia pestis* capsule on pathogenesis is influenced by the mouse background. Infect Immun *79*, 644–652.

Weiner, Z.P., and Glomski, I.J. (2012). Updating perspectives on the initiation of *Bacillus anthracis* growth and dissemination through its host. Infect Immun *80*, 1626–1633.

WHO (2004). Human plague in 2002 and 2003. Wkly Epidemiol Rec *79*, 301–306.

Wimsatt, J., and Biggins, D.E. (2009). A review of plague persistence with special emphasis on fleas. Journal of Vector Borne Diseases *46*, 85–99.

Wong, D., Wild, M.A., Walburger, M.A., Higgins, C.L., Callahan, M., Czarnecki, L.A., Lawaczeck, E.W., Levy, C.E., Patterson, J.G., Sunenshine, R., et al. (2009). Primary pneumonic plague contracted from a mountain lion carcass. Clin Infect Dis *49*, e33–e38.

Zav'yalov, V.P., Abramov, V.M., Cherepanov, P.G., Spirina, G.V., Chernovskaya, T.V., Vasiliev, A.M., and Zav'yalova, G.A. (1996). pH6 antigen (PsaA protein) of

*Yersinia pestis*, a novel bacterial Fc-receptor. FEMS Immunol Med Microbiol *14*, 53–57.

Zhang, P., Skurnik, M., Zhang, S.-S., Schwartz, O., Kalyanasundaram, R., Bulgheresi, S., He, J.J., Klena, J.D., Hinnebusch, B.J., and Chen, T. (2008). Human dendritic cell-specific intercellular adhesion molecule-grabbing nonintegrin (CD209) is a receptor for *Yersinia pestis* that promotes phagocytosis by dendritic cells. Infect Immun *76*, 2070–2079.

Zhou, D., and Yang, R. (2009). Molecular Darwinian evolution of virulence in *Yersinia pestis*. Infect Immun *77*, 2242–2250.

Zhou, D., Han, Y., and Yang, R. (2006). Molecular and physiological insights into plague transmission, virulence and etiology. Microbes Infect *8*, 273–284.

Zietz, B.P., and Dunkelberg, H. (2004). The history of the plague and the research on the causative agent *Yersinia pestis*. International Journal of Hygiene and Environmental Health *207*, 165–178.

# CHAPTER 2: BIOLUMINESCENCE IMAGING TO TRACK BACTERIAL DISSEMINATION OF *Yersinia pestis* USING DIFFERENT ROUTES OF INFECTION IN MICE

## 2.1. Overview

**Introduction**: Plague is caused by *Yersinia pestis*, a bacterium that disseminates inside of the host at remarkably high rates. Plague bacilli disrupt normal immune responses in the host allowing for systematic spread that is fatal if left untreated. How *Y. pestis* disseminates from the site of infection to deeper tissues is unknown. Dissemination studies for plague are typically performed in mice by determining the bacterial burden in specific organs at various time points.

**Methods:** To follow bacterial dissemination during plague infections in mice we tested the possibility of using bioluminescence imaging (BLI), an alternative non-invasive approach. Fully virulent *Y. pestis* was transformed with a plasmid containing the *luxCDABE* genes, making it able to produce light; this *lux*-expressing strain was used to infect mice by subcutaneous, intradermal or intranasal inoculation.

**Results:** We successfully obtained images from infected animals and were able to follow bacterial dissemination over time for each of the three different routes of inoculation. We also compared the radiance signal from animals infected with a wild type strain and a Δ*caf1*Δ*psaA* mutant that we previously showed to be

attenuated in colonization of the lymph node and systemic dissemination. Radiance signals from mice infected with the wild type strain were larger than values obtained from mice infected with the mutant strain (linear regression of normalized values, $P < 0.05$).

**Conclusions:** We demonstrate that BLI is useful for monitoring dissemination from multiple inoculation sites, and for characterization of mutants with defects in colonization or dissemination.

## 2.2. Introduction

*Yersinia pestis* is a highly virulent Gram-negative bacterial species that infects mammals and causes plague. Plague is a lethal disease known for its important role in history, mainly as the cause of the Black Death (Perry and Fetherston, 1997; Zhou and Yang, 2009; Zietz and Dunkelberg, 2004) . Due to the emergence of antibiotics (Anisimov and Amoako, 2006) , plague no longer poses the same threat to public health as it did in the past. However, the disease is still present in almost every continent (Gage and Kosoy, 2005) causing fatalities that, during the last two decades, have fluctuated between several hundred to several thousand deaths per year (Stenseth et al., 2008) . Plague is maintained in sylvatic animal reservoirs, and human populations that are in close contact with these reservoirs are at high risk (Bitam et al., 2010) . Chemotherapy is efficacious only if administered early after infection and untreated individuals succumb to plague in less than a week. Furthermore, public health concerns have been raised because of reports of drug resistant strains in endemic foci (Galimand et al., 2006) .

The disease manifests after inhalation of bacteria suspended in aerosols (pneumonic plague) or through contact with broken skin (bubonic and septicemic plague) (Prentice and Rahalison, 2007; Smiley, 2008). While pneumonic plague is the most virulent form of the disease, bubonic plague is the most prevalent perhaps due to its dynamics of transmission, for which a flea vector is essential (Wimsatt and Biggins, 2009) . Little is known about how *Y. pestis* disseminates within the host after infection. It is known, however, that at some point after infection, *Y. pestis* expresses a set of genes that impair host immune responses (DeLeo and Hinnebusch, 2005; Marketon et al., 2005; Matsumoto and Young, 2009) . These factors are thought to be essential for bacterial dissemination. Dissemination during bubonic plague traditionally has been studied through experiments where different organs from infected mice are harvested at various time points post inoculation. Harvested organs are then homogenized and plated to obtain bacterial burden. These experiments have suggested that *Y. pestis* travels from the site of infection to draining lymph nodes (LN) prior to disseminating throughout the rest of the body (Guinet et al., 2008; Sebbane et al., 2005) . Bacterial burden data from these experiments give a snapshot of a very narrow window (a specific organ at a specific time) through the course of infection. Furthermore, the approach is invasive, requires a large number of animals, and animals must be sacrificed at each time point making it impossible to keep track of the progression of infection on the same group of individuals.

*In vivo* bioluminescence imaging (BLI) is an approach that has been used to detect light-emitting cells inside of small mammals (Massoud and Gambhir, 2003) .

Using BLI, researchers have described and studied dissemination of viral, parasitic and bacterial pathogens within a host in a non-invasive manner (Hutchens and Luker, 2007; Hyland et al., 2008; Kong et al., 2009; Zincarelli et al., 2008) . Thus, the same group of animals can be imaged for as long as desired over the course of infection. The system requires that the pathogen produce luminescence, and infected animals are then imaged with a high-sensitivity camera that detects very small amounts of light. Non-luminescent bacteria can be genetically modified to express the *lux* genes (*luxCDABE*), which encode a bacterial luciferase and other enzymes which are necessary to generate luciferin (Contag and Bachmann, 2002). In the presence of oxygen, luciferin is converted into oxyluciferin in a reaction catalyzed by luciferase and of which light is a byproduct (Hastings, 1996) . We transformed *Y. pestis* CO92 with plasmid pGEN-*luxCDABE* that contains the *luxCDABE* genes (Lane et al., 2007) . Using this strain of *Y. pestis* expressing the *lux* genes we determined that it is suitable for in vivo BLI after subcutaneous, intradermal and intranasal inoculation. In addition, we determined that BLI is suitable for the study of mutant strains that are attenuated or defective in dissemination or colonization during infection. This extends the findings of a recent report demonstrating the suitability of BLI to study *Y. pestis* infections by the subcutaneous route of inoculation (Nham et al., 2012) .

BLI technology offers a new perspective to study the spread of *Y. pestis* in the host. This technology could be adopted in the future as an alternative to experiments that measured bacterial burdens in specific organs, facilitating the discovery and study of genes that are important in pathogenesis.

## 2.3. Methods

### *2.3.1. Bacterial strains and cultures*

*Y. pestis* CO92 and *Y. pestis* CO92 Δ*caf1*Δ*psaA* were transformed with pGEN-*luxCDABE* (Lane et al., 2007) . This plasmid contains the Hok/Sok toxin/antitoxin system enabling plasmid maintenance in vivo without antibiotic selection. Throughout the rest of the document we will refer to *Y. pestis* CO92 transformed with the pGEN-*luxCDABE* plasmid as Yp*lux*$^+$, to *Y. pestis* CO92 Δ*caf1*Δ*psaA* transformed with the same plasmid as YpΔ*caf1*Δ*psaA lux*$^+$ or simply as "double mutant" and to the pGEN-*luxCDABE* plasmid itself as pGEN-*lux*. Bacteria transformed with pGEN-*lux* were cultured in the presence of carbenicillin at 100 μg/mL, unless BHI alone is stated as growth medium. Bacteria were plated on brain heart infusion (BHI) agar (BD Biosciences, Bedford, MA) plates and incubated for 48 h at 26°C. For intranasal inoculations, liquid cultures were incubated at 37°C in the presence of 2.5 mM $CaCl_2$ as previously described (Lathem et al., 2005) . For subcutaneous and intradermal inoculations, liquid cultures were incubated at 26°C for 15 h. All strains (Yp*lux*$^+$, YpΔ*caf1*Δ*psaA lux*$^+$ and *Y. pestis* lacking pGEN-*lux*) showed comparable optical density ($OD_{600}$) values after culturing in liquid broth. To obtain the final inocula for all infections, liquid cultures were serial diluted in phosphate buffered saline (PBS). All procedures involving *Y. pestis* were conducted under strict biosafety level three conditions.

### *2.3.2. Animal infections and tissues*

Five-to-ten-week old female C57BL/6J or B6(Cg)-*Tyrc-2J*/J mice (Jackson Laboratory, Bar Harbor, ME) were subjected to subcutaneous (SC), intranasal (IN)

or intradermal (ID) inoculation after providing anesthesia (2% isoflurane for SC and ketamine/xylazine for IN and ID). For SC inoculations, a volume of 100 µL was injected in the subcutaneous space at an anterior cervical site. The ear pinna was injected with a volume of 10 µL for ID inoculations. A volume of 20 µL was delivered into the left nostril of the animal for IN inoculations. The inoculum for the SC and ID inoculations was ~200 CFU, and ~$10^4$ CFU for the IN inoculation.

For the determination of plasmid stability and strain characterization experiments, superficial cervical lymph nodes, spleens and lungs were removed from SC-infected mice after sacrificing the animals by injection of sodium pentobarbital. Plasmid stability was assessed by comparing bacterial counts after plating on BHI alone and BHI with carbenicillin. Strain characterization was determined by comparing bacterial counts of Yp*lux*$^+$ against *Y. pestis* lacking the plasmid.

All procedures involving animals were approved by the University of North Carolina and Duke University Animal Care and Use Committees, protocols 11-128 and A185-11-07, respectively.

*2.3.3. In vivo Imaging*

To enhance signal detection, the fur was shaved from the ventral and cervical regions of the mice with an electric razor two days before inoculation. Animals were anesthetized with 2% isoflurane during the entire imaging process, except for the time point 0 h post inoculation (hpi) for IN and ID, where the animals were still under the sedation from the ketamine/xylazine treatment. Prior to imaging, mice were placed in an animal isolation chamber (Caliper) to maintain containment of *Y.*

*pestis* outside the biosafety cabinet. We used four mice per group, as this is the maximum number of mice that can be placed in the isolation chamber to be imaged at one time. Mice were imaged with an IVIS Spectrum instrument (Caliper) at 0, 6, 24, 48, 72 and 96 hpi, unless animals died or had to be sacrificed because of advanced signs of plague. The same group of mice was imaged at each time point. Every image was taken after placing the mice in the isolation chamber in the same order relative to one another. After imaging the last time point, mice were sacrificed with an overdose of isoflurane and one animal per group was dissected. The dissected individual was imaged to identify luminescence from specific organs. Organs were then removed from the animal and imaged individually to confirm the origin of signal. The remaining animals were sacrificed and their organs (LN, spleens or lungs) were removed, macerated and plated to compare bacterial load with previous reports for each model and to confirm plasmid stability as described above. Radiance signal was measured in photons/sec/$cm^2$/steradian and analyzed using Living Image Software V.4.2 (Caliper). Radiance signal from a specific site (site of inoculation or abdomen) was quantified by defining a region of interest (ROI), which was drawn and measured using the Living Image Software (Caliper). Radiance background levels were obtained by measuring radiance from a ROI (from either site of inoculation or abdomen) of all animals imaged at 0 hours after inoculation. When signal was detected from one site (e.g. the neck) and not from a second site (e.g. the abdomen), the light emitting site from which signal was detected was covered with black opaque paper to increase image sensitivity. A specific site was considered to be negative (lacking signal) if no signal was

observed after covering all other irradiating sites or if quantification of signal was below background levels. Radiance values from each ROI were transformed into log values to normalize their distribution. Linear regression analysis of these values was performed in STATA 12 (Stata Corp, College Station, TX) to test differences in average radiance between groups. A two sided P value <0.05 was set to determine statistical significance.

## 2.4. Results

### *2.4.1. The pGEN-luxCDABE vector is stable in Y. pestis during infection*

Bacteria carrying a reporter plasmid could potentially lose it at a specific site or time point during infection. A subpopulation lacking the plasmid could result in false negatives or decreases in signal detection that are not necessarily related to lower numbers of bacteria. To determine if pGEN-*luxCDABE* (pGEN-*lux*) was maintained during *Y. pestis* infections, we performed a kinetic study with mice infected with CO92 carrying pGEN-*lux*. Mice were inoculated subcutaneously (SC) and LN harvested at 24 hours post inoculation (hpi), LN and spleens harvested at 48 and 72 hpi, and LN, spleens and lungs harvested at 96 hpi. Homogenates of each organ were plated on BHI and BHI with carbenicillin. Bacterial enumeration showed no differences between the two growth conditions, indicating that pGEN-*lux* is stable in vivo up to 96 hpi in all organs tested (Figure 2.1). Additionally, organs from all animals imaged in this study were also plated on BHI and BHI with carbenicillin (after last imaging time point). We observed the same levels of plasmid stability that we report in Figure 1 (data not shown).

Another important control experiment was to determine if pGEN-*lux* impacted the virulence of *Y. pestis*. Mice were inoculated with either *Y. pestis* alone or *Y. pestis* carrying pGEN-*lux*. Both groups of mice displayed signs of plague infection and mortality at similar times. However, the bacterial burden in tissues from mice infected with *Y. pestis* carrying pGEN-*lux* was lower in comparison to tissues from mice infected with *Y. pestis* without the plasmid (Figure 2.2). While bacterial counts suggest that pGEN-*lux* might cause a slight delay in the progression of infection, overt signs of plague were observed in all mice infected with either strain at comparable times. Additionally, all mice infected during our BLI experiments died at times expected from infections with a wild type strain. Since all strains used for BLI will carry the same plasmid, relative virulence attributes will be comparable despite the slight attenuation caused by pGEN-*lux*.

*2.4.2. BLI of Y. pestis after subcutaneous infection*

In order to determine if BLI would be a suitable method for following dissemination or colonization of *Y. pestis* in vivo, we turned to the well-characterized subcutaneous model of infection (Cathelyn et al., 2006) . C57BL/6J mice were inoculated SC with Yp*lux*$^{+}$, and the mice imaged at 0, 6, 24, 48, 72 and 96 hpi. Although the radiance levels were initially low, all animals had signal at the site of infection (neck) at 6 hpi, and the signal appeared to increase during the course of infection (Figure 2.3A). At 72 hpi, the region of radiance appeared to have two separate high intensity spots. The localization of these spots coincides with the approximate location of the superficial cervical LNs to which the site of infection is predicted to drain. Signal was also detected from the abdomen at 72

hpi. However, because of its low intensity, this signal is not evident in Figure 3A. All images in Figure 3A are standardized to the same radiance scale, thus low intensity spots are not visible. Low intensity spots, however, are visible when high intensity spots are covered. After covering high intensity spots from the neck with black opaque paper, we could visualize signal from the abdomen at 72 hpi (Figure 2.3B). Signal from the abdomen was not visualized before 72 hpi but quantification above background levels was obtained at 48 hpi (Figure 2.6C). At 96 hpi, radiance in the abdominal region increased in intensity (Figure 2.3A and B). From this and previous experiments, we observed that the presence and intensity of this signal tends to be variable among individuals. Also, from previous experiments where we imaged mice beyond 96 hpi, we determined that the presence of this signal, especially when high in intensity and spread in size, can be used as a predictor of death within the following 24 h. At time points subsequent to detection of light from the abdomen, signal was evident at sites where the skin was not covered by fur, such as the tail (data not shown). This might be the result of early stages of septicemia, where light from bacteria circulating in blood is only detectible from superficial vascularized tissue, such as the skin. At the latter stages of infection (>96 hpi), septicemia is evident as signal that can be detected from the entire animal.

Experiments in which bacterial load was measured showed that the LN are the first organs to be colonized, followed by deeper tissues (e.g. spleens and livers) (Sebbane et al., 2005) . The resolution provided by the BLI system, however, does not allow us to be certain that signal from the neck and abdomen comes from these

organs. Therefore, mice were dissected to determine that signal indeed originated from LN, spleens and livers. These organs, along with the patch of skin where bacteria were inoculated, also were imaged individually at 96 hpi and found to emit light (Figure 2.3C). Thus, origin of light in specific organs is consistent with previous data measuring bacterial burden by plating macerated tissues.

### *2.4.3. Dynamics of bacterial dissemination after intradermal infection in the ear pinna*

Having established that BLI is a useful method to monitor dissemination following a SC infection, we wanted to determine the dynamics of dissemination of plague bacilli after intradermal (ID) infection. This model is rarely used for plague studies despite the fact that it may mimic a fleabite more closely than a SC inoculation (Guinet and Carniel, 2003) . We employed the ear pinna as the site of infection to guarantee that no subcutaneous tissue is reached (Guinet and Carniel, 2003) . In this model, the draining LN is the superficial parotid LN [as identified from (Van den Broeck et al., 2006) ], which is distant from the site of infection. Thus, signal from the site of infection can be isolated from signal from the draining LN, a distinction not easily discerned in the SC model. Because the superficial parotid LNs are located deeper in the neck, we opted to infect B6(Cg)-*Tyrc-2J*/J mice. These mice differ from C57BL/6J in that pigment is absent from their skin. Using mice lacking skin pigments can increase light detection due to less absorption of light by the skin. Thus, the B6(Cg)-*Tyrc-2J*/J mice were a good alternative to maximize detection from small deeper tissues (i.e. superficial parotid

LNs) without compromising our well characterized C57BL/6J model for bubonic plague.

The ear pinna was inoculated with ~200 CFU and animals were imaged at different time points (Figure 2.4A). Low levels of signal from the site of infection could be detected in some animals at 6 hpi (data not shown). However, at 24 hpi, strong signal was consistently detected in the ear. In addition, some of the mice had detectible signal in the right side of the neck, approximately where the superficial parotid LN is located. At 48 hpi light signal from the site of infection appeared to increase considerably. At this same time point, signal from the parotid LN increased dramatically, and light was detected in the abdomen and rest of the body in some animals, indicating systemic dissemination. At 72 hpi only one mouse had survived and it showed high levels of signal from the whole body, indicating advanced stages of septicemic dissemination. The right superficial parotid LN was confirmed as the highest source of radiance from the neck after dissection of this mouse (Figure 2.4B). As previously reported for latter stages of infection (Sebbane et al., 2005) , the LN that drains the site of infection was not the only LN that appeared to be colonized. However, the superficial parotid LN that drains the site of infection (white asterisk, Figure 2.4B) appeared to emit higher levels of radiance in comparison to other LNs. Isolated spleens and livers were imaged to confirm them as the source of signal from the abdominal area (Figure 2.4B).

*2.4.4. Bacterial dissemination during pneumonic plague*

Pneumonic plague is less common but more fulminant than bubonic plague, and is the only form of the disease that can be transmitted directly from human to

human (does not require a flea vector). We used BLI to follow dissemination of *Y. pestis* after intranasal inoculation, a well-characterized model for pneumonic plague (Lathem et al., 2005) . Lung tissue is the primary tissue colonized by *Y. pestis* during pneumonic infections. Because the lungs reside in the thoracic cavity covered by other organs and bone, we again used B6(Cg)-*Tyrc*-*2J*/J mice to increase the probability of detecting signal from lung tissue.

In some isolated cases, radiance was detected from the abdomen and from feces at 6 hpi (data not shown). This signal was not detected at any latter time points and presence of abdominal or fecal signal did not appear to alter the course of infection in the animals where it was detected.

Very little light was detected in the mice at 24 hpi, at which time some mice showed signal from different regions in the neck or on the head (Figure 2.5A). At 48 hpi, light was detected in all animals, mainly from the mid and upper thorax (Figure 2.5B). Radiance spread and intensity increased considerably at 72 hpi, a time at which all mice showed pronounced signs of disease. Immediately after imaging at 72 hpi, one of the four mice in the group was sacrificed and dissected to determine the source of light. The lungs were determined to be the source of luminosity from the thorax, and light from this organ was confirmed to be unique to IN infections as animals infected using other routes (e.g. ID, Figure 2.5C) did not show signal from the lungs. Additionally, we observed that IN-inoculated animals showed signal from the tip of the nose (visible in Figure 2.5C) indicating that bacteria were present at the site of inoculation at 72 hpi. Upon dissection of the lungs, we noticed that part of the organ was necrotic in appearance; imaging of

isolated lungs showed that the necrotized tissue produced higher levels of signal (Figure 2.5D) in comparison to other areas of the lung. While Figures 2.5C and 2.5D show data from only one mouse, we performed this experiment multiple times and in all cases we made the same observations mentioned above (data not shown).

*2.4.5. BLI to identify mutants with defects in dissemination or colonization*

One of the goals of this study was to determine whether mutants with a defect in colonization and/or dissemination could be identified by BLI. As proof of concept, we compared radiance from mice infected with Yp*lux*$^{+}$ or Yp∆*caf1*∆*psaA lux*$^{+}$ mutant. Caf1 and PsaA previously were shown to play a role in dissemination and colonization in an additive manner (Weening et al., 2011) . The SC model of infection and C57BL/6J mice were chosen for this comparison because the colonization phenotype of the ∆*caf1*∆*psaA* strain was originally tested using this model. BLI revealed that the ∆*caf1*∆*psaA* strain was attenuated in dissemination or colonization to deeper tissues from the LN, in agreement with previous work (Weening et al., 2011) (Figure 2.6A and B). Radiance measurements allowed us to determine that signal intensity in the neck was lower in animals infected with the double mutant strain in comparison to those infected with Yp*lux*$^{+}$, indicating that colonization of the LN by the ∆*caf1*∆*psaA lux*$^{+}$ mutant also was impaired compared to wild type, in agreement with previous work (Weening et al., 2011) (Figure 2.6C). Differences of radiance values from mice infected with Yp*lux*$^{+}$ against ∆*caf1*∆*psaAlux*$^{+}$ attained statistical significance at 24, 48, 72 and 96 hpi (linear regression analysis of normalized values, $P < 0.05$).

Mice infected with the Δ*caf1*Δ*psaA* strain never displayed detectible signal from the abdomen at any time point (Figure 2.6A). The radiance values from the abdomen of these mice were below background levels at each time point examined. These radiance values were subjected to regression analysis and determined to be significantly different from the values obtained from mice infected with Yp*lux*$^{+}$ at 48, 72 and 96 hpi. To determine if the absence of signal in YpΔ*caf1*Δ*psaA lux*$^{+}$-infected mice was due to extremely low levels that were blocked by skin or other tissue, we dissected the mice and imaged isolated spleens and livers at 96 hpi. No signal was detected from the individual organs (Figure 2.6B). In addition, all animals infected with the Δ*caf1*Δ*psaA* mutant survived past 96 hpi and never showed any signs of disease. We continued to image these animals up to 168 hpi, and found that the signal from the neck never disappeared and that bacteria appeared to be contained at this site (data not shown). Overall, imaging from mice infected with YpΔ*caf1*Δ*psaA lux*$^{+}$ confirmed previous findings in C57BL/6J where bacteria were detected in LN, but at lower numbers in comparison to mice infected with a wild type strain, and never or rarely were detected in spleens (Weening et al., 2011) .

## 2.5. Discussion

Plague is a disease with devastating effects on the host that are fatal if left untreated. These effects are the result of the ability that *Y. pestis* displays to suppress host immune responses and to promote systemic dissemination at remarkably high rates. Numerous studies have described many virulence factors that are essential to suppress host immune responses (Price et al., 2012; Zhou and

Yang, 2009) . The direct contributions of these virulence factors to bacterial dissemination, however, are still unclear. The study of dissemination per se is a field that is lagging behind in plague research. BLI is a tool that allows for the visualization of a pathogen in a host during infection and a very promising alternative to better understand *Y. pestis* dissemination. A recent report described the use of BLI in a subcutaneous (SC) model of bubonic plague (Nham et al., 2012) . In this report, the pGEN-*luxCDABE* plasmid was described to have no effect on the virulence of *Y. pestis* and to be suitable for BLI as luminosity correlated with bacterial counts in vivo; our results confirmed and expanded upon these findings. Our goal was to determine whether BLI could be used to follow dissemination and colonization of *Y. pestis* in mice after using different routes of inoculation that closely mimic bubonic and pneumonic plague. Moreover, we tested whether BLI could be used to detect mutants with defects in colonization or dissemination.

After inoculation with a strain of *Y. pestis* that contains pGEN-*luxCDABE*, we showed that animals can be imaged through the course of infection in such a way that bacterial spread could be followed over time for three different models of infection. Our results from the SC inoculation model support the previous notion that, during bubonic plague, *Y. pestis* travels from the site of inoculation to the proximal lymph node prior to dissemination to deeper tissues (Sebbane et al., 2005) . We observed that bacteria were maintained at the site of inoculation during the course of infection, as previously reported for ear intradermal (ID) infections (Guinet et al., 2008) . For both, the SC and ID models, the bacterial population at

the site of inoculation appeared not only to be maintained, but also to expand. However, while we quantified signal from the site of infection in the SC-inoculated animals, we cannot conclude such signal comes from the skin alone. In our SC model, the patch of inoculated skin is located in an anatomical position on top of the superficial cervical LNs and thus, both, skin and LNs, are imaged as a single source of radiance. We could determine that signal was coming partly from the site of inoculation after removing the patch of skin and imaging it individually. This complication is minimized in the ID model, where the site of inoculation (ear pinna) is distant from the draining LN (superficial parotid LN). While an increase over time in signal intensity from the ear was observed, we were not able to quantify the signal, as it was difficult to place the ears of all mice at the same position inside of the animal isolation chamber.

Images taken during the first hours following intranasal (IN) infections suggested that, in isolated cases, at least part of the inoculum can go to the stomach. The IN route requires delivering small drops of inoculum into one of the nostrils (total volume of 20 µL), and some of this inoculum could be swallowed rather than inhaled. Signal from the stomach never seemed to last beyond the 6 hpi time point, suggesting that gastric infections with *Y. pestis* in these mice are cleared quickly. We also observed that the feces of half of the mice produced detectible signal, indicating that *Y. pestis* was being shed. This was only observed at very early time points (6 hpi), indicating that bacteria were fully shed from the gastrointestinal tract by 24 hpi. In humans, it has been shown that transmission can occur after ingestion of contaminated food (Arbaji et al., 2005) . While mice are

coprophagous, it is not know whether a fecal-oral route could be a mechanism for *Y. pestis* to disperse or infect other individuals. Detecting signal from the tip of the nose also opens the question whether bacteria could be transmitted to other individuals with whom food and water are shared. We do not know whether signal from the stomach or the tip of the nose would still be present after an aerosol infection, a route that pneumonic plague is assumed to be transmitted in nature. All mice, independent of the presence of signal from the stomach or feces, showed the same progression of infection with comparable levels of signal from the thorax. More importantly, all animals showed signs of disease and mortality at very similar times. This observation suggests that the fraction of the inoculum that may go to the gastrointestinal tract has no effect on the overall pneumonic infection. The low number of mice used during BLI is one of its more important advantages. However, it can also be a disadvantage because of the variability in bacterial load for a specific organ from animal to animal and sudden death, both inherent aspects of plague infections. The differences in the levels of significance from time point to time point when comparing radiance values between the wild type and double mutant infected animals are due to this high variability of bacterial load and death. Despite these challenges, we found that BLI is a suitable method for studying dissemination/colonization of *Y. pestis* in three separate models of plague, and that significant differences in radiance could be detected between wild type and a mutant of modest attenuation using relatively few mice.

## 2.6. Figure and Tables

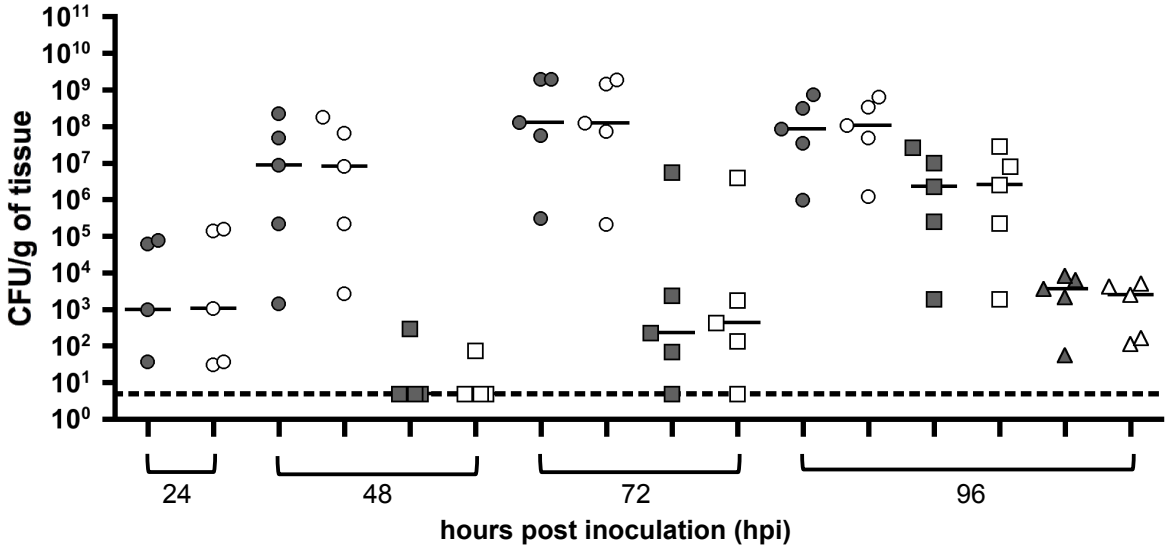


**Figure 2.1. Bacterial loads in C57Bl/6J mice infected subcutaneously with pGEN-luxCDABE-carrying *Y. pestis*.**
Animals were infected with ~200 CFU at a cervical site. Organs were harvested and plated for bacterial counts at the indicated hours post inoculation on BHI alone (gray symbols) and BHI + carbenicillin (white symbols). Bacterial numbers are reported in CFU/g of tissue. Each mark represents a value from a single organ and the horizontal lines represent the median of the group. Superficial cervical lymph nodes are represented as circles, spleens as squares, and lungs as triangles. A dotted line represents the limit of detection. Data shown from a single experiment.

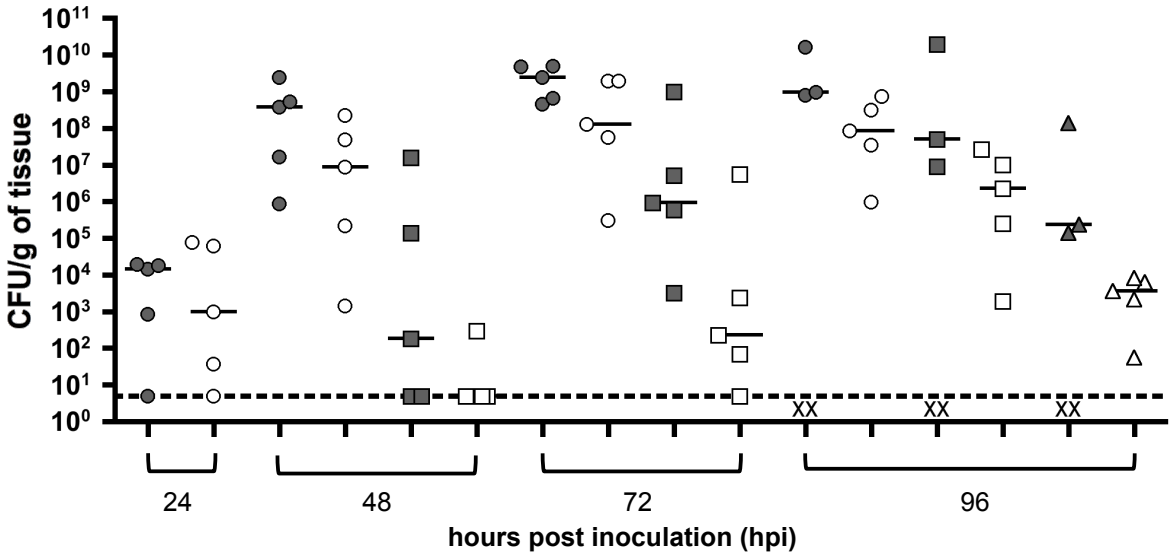


**Figure 2.2. Bacterial loads in C57Bl/6J mice infected subcutaneously with either wild type or pGEN-luxCDABE-carrying *Y. pestis*.**
Animals were infected with ~200 CFU at a cervical site. Organs were harvested and plated for bacterial counts at the indicated hours post inoculation. Bacterial numbers are reported in CFU/g of tissue. Gray and white symbols represent organs from animals infected with *Y. pestis* and *Y. pestis* carrying pGEN-*luxCDABE*, respectively. Each mark represents a value from a single organ and the horizontal lines represent the median of the group. Superficial cervical lymph nodes are represented as circles, spleens as squares, and lungs as triangles. A dotted line represents the limit of detection and an x letter represents missing values of a specific tissue due to the death of an animal. Data shown from a single experiment.

**A**

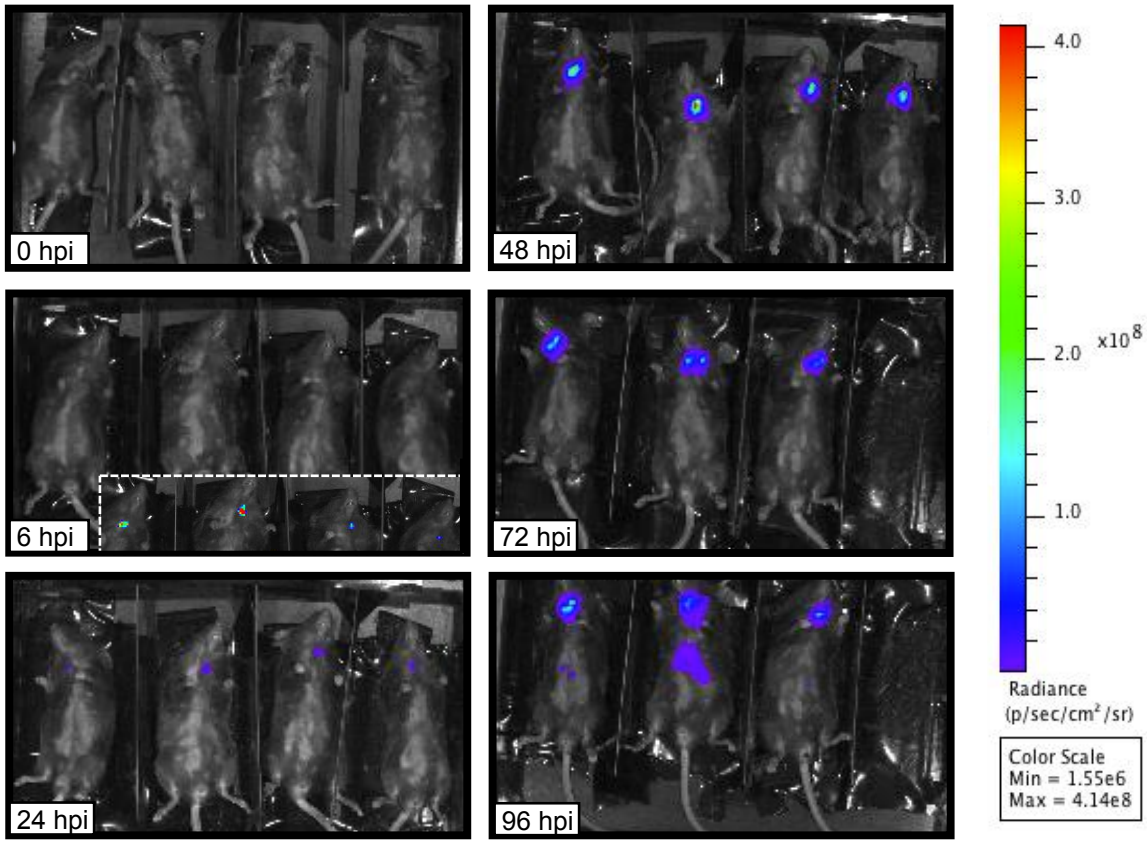
0 hpi
48 hpi
6 hpi
72 hpi
24 hpi
96 hpi
4.0
3.0
2.0
1.0
x10^8
Radiance
(p/sec/cm²/sr)
Color Scale
Min = 1.55e6
Max = 4.14e8

**B**

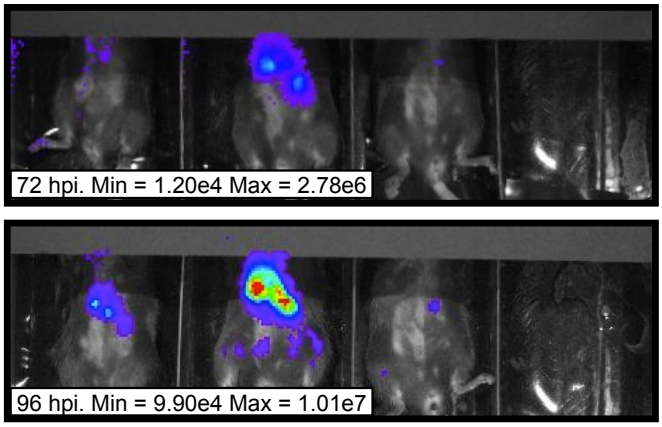
72 hpi. Min = 1.20e4 Max = 2.78e6
96 hpi. Min = 9.90e4 Max = 1.01e7

**C**

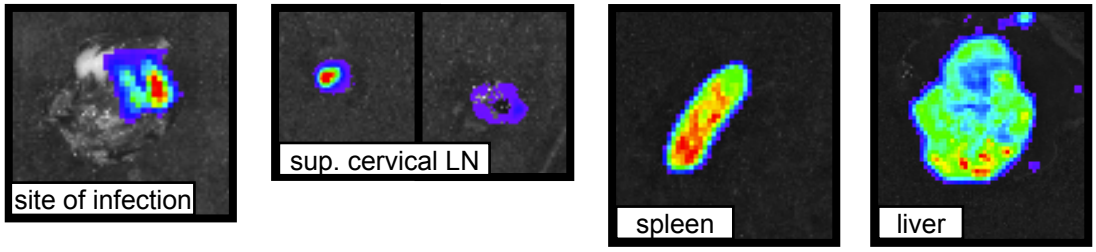


**Figure 2.3. BLI of C57BL/6J mice infected subcutaneously with Yp*lux*$^{+}$ at a cervical site.**
(A) Animals were inoculated with ~200 CFU and imaged at the indicated hours post inoculation (hpi). Luminescence signal is reported as radiance (p/sec/cm$^2$/sr) in a scale paired with a color bar shown next to the images. For 6 hpi, the image in the window is shown using an individual color scale with radiance of Min = 8.53e3 and Max = 3.97e4. (B) Images of the abdomen at 72 and 96 hpi (same mice shown in panel A) under an individual radiance scale (Max and Min values are shown). (C) Site of inoculation [skin (inner side)], superficial cervical lymph nodes, spleen and liver (from one of the mice shown in A) imaged individually after dissection. Individual scales of radiance were used due to variability in signal (site of infection and liver, Min = 1.57e5 Max = 3.74e6; lymph nodes, Min = 2.10e6 Max = 2.28e8; spleen, Min = 1.73e5 Max = 1.38e7). Shown is a representative experiment.

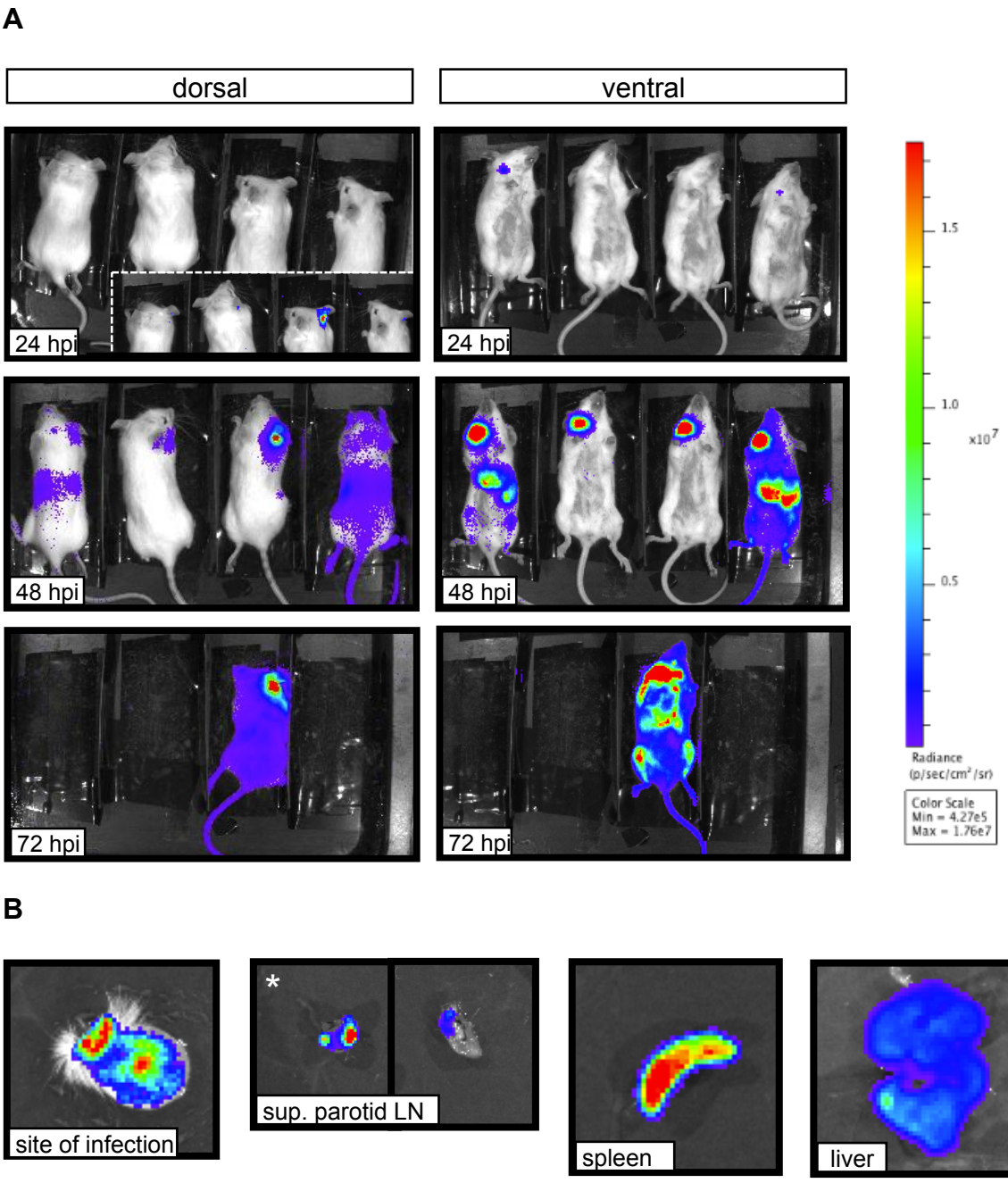


**Figure 2.4. BLI of B6(Cg)-*Tyrc-2J*/J mice infected intradermally with Yp*lux*$^{+}$ in the ear pinna.**

(A) Mice were inoculated with ~200 CFU and were imaged (ventral and dorsal sides) at the indicated hours post inoculation (hpi). Luminescence signal is reported as radiance (p/sec/cm$^2$/sr) in a scale paired with a color bar shown next to the images. For 24 hpi (dorsal view), the window shows an image with signal at an individual radiance color scale with of Min = 1.11e4 and Max = 1.43e5. (B) Site of infection (right ear), superficial parotid right and left lymph nodes, spleen and liver (from one of the mice shown in A) imaged individually after dissection. An

asterisk denotes the LN that drains the site of infection. Individual scales of radiance were used due to variability in signal (site of infection, Min = 1.89e4 Max = 8.97e4; lymph nodes, Min = 1.89e6 Max = 8.97e7; spleen and liver, Min = 5.25e5 Max = 2.34e7). Shown is a representative experiment.

**A**

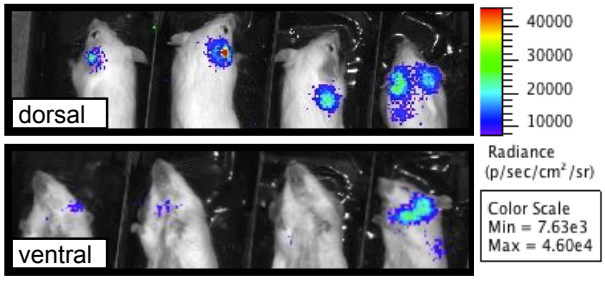
dorsal
ventral
40000
30000
20000
10000
Radiance
(p/sec/cm²/sr)
Color Scale
Min = 7.63e3
Max = 4.60e4

**B**

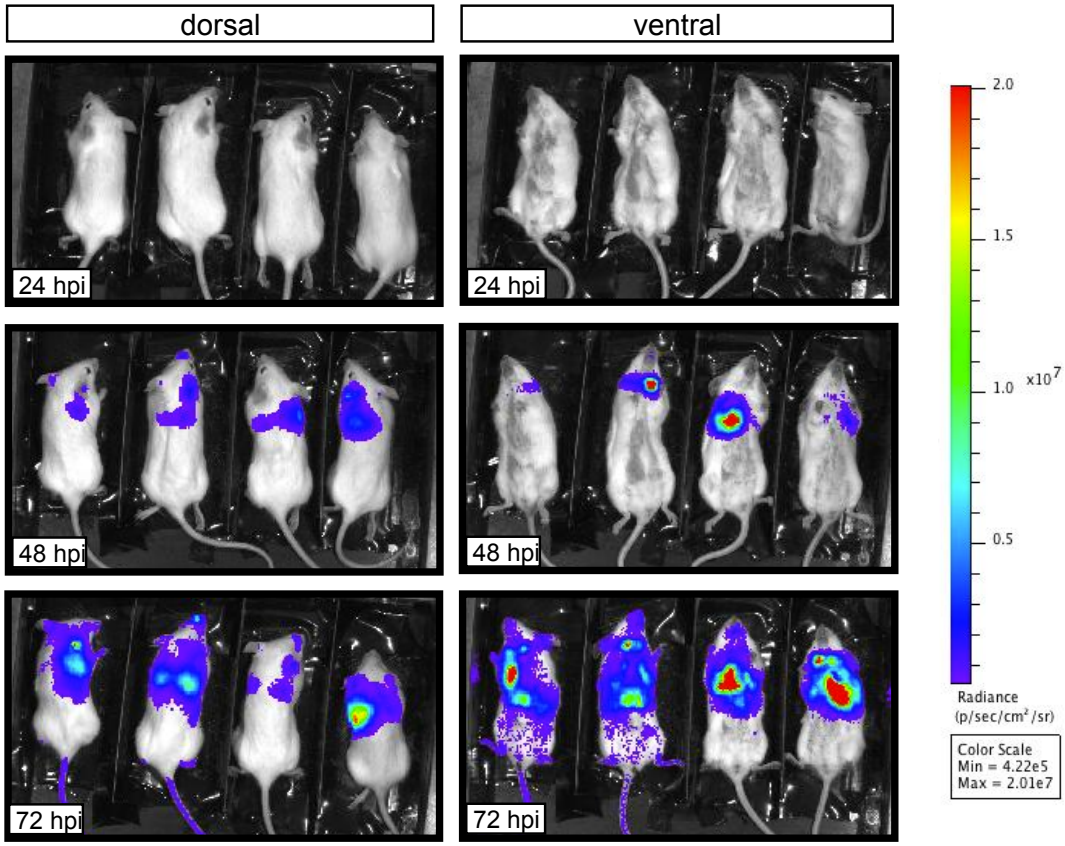
dorsal
ventral
24 hpi
24 hpi
48 hpi
48 hpi
72 hpi
72 hpi
2.0
1.5
1.0
x10⁷
0.5
Radiance
(p/sec/cm²/sr)
Color Scale
Min = 4.22e5
Max = 2.01e7

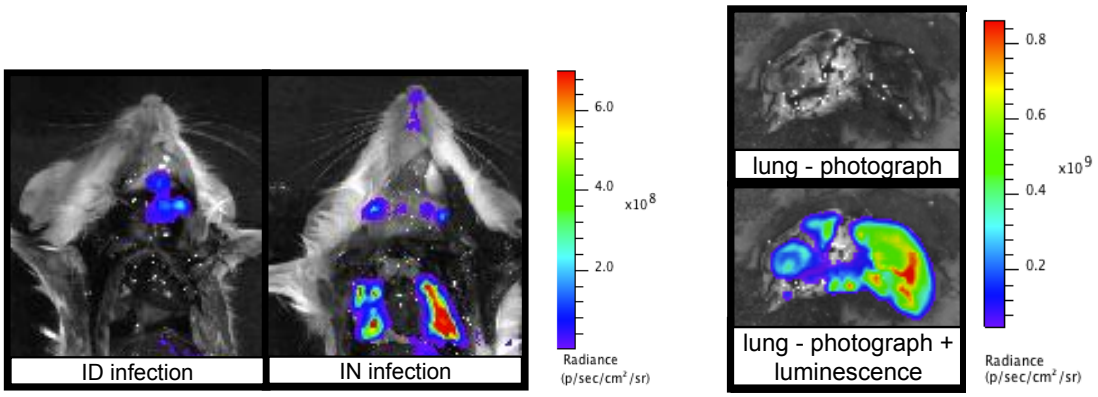


**Figure 2.5. BLI after Yp*lux*$^+$ intranasal inoculation in the left nostril of B6(Cg)-*Tyrc-2J*/J mice.**

(A) Mice were inoculated IN with ~$10^4$ CFU. Images of the neck and head (dorsal and ventral) at 24 hpi under an individual radiance scale. The color bars serve as reference for radiance intensity (p/sec/cm$^2$/sr; Min and Max values are shown) from each spot in the mouse from which signal was detected. (B) Images of the dorsal and ventral sides of the animals at different time points (shown in hpi). (C) Signal from the lungs after dissection in an animal infected ID in comparison to an animal infected IN (Min = 5.02e7 and Max = 8.62e8). (D) Isolated lungs showing a necrotic spot (photograph) and how highest levels of radiance (photograph + luminescence) originated from this spot (Min = 4.42e6 and Max = 7.02e8). Color bars serve as reference for radiance values. Shown is a representative experiment.

**A**

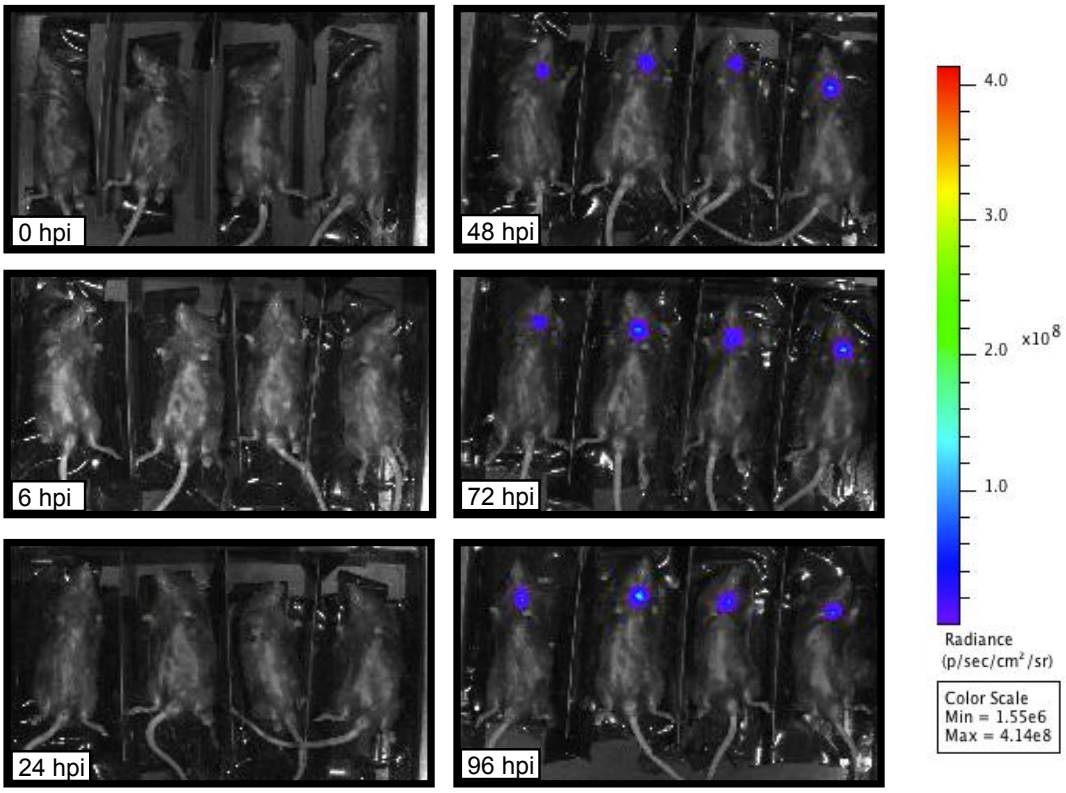
0 hpi
48 hpi
6 hpi
72 hpi
24 hpi
96 hpi
4.0
3.0
2.0
x10^8
1.0
Radiance
(p/sec/cm²/sr)
Color Scale
Min = 1.55e6
Max = 4.14e8

**B**

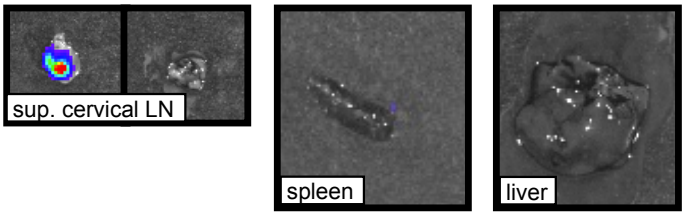
sup. cervical LN
spleen
liver

**C**

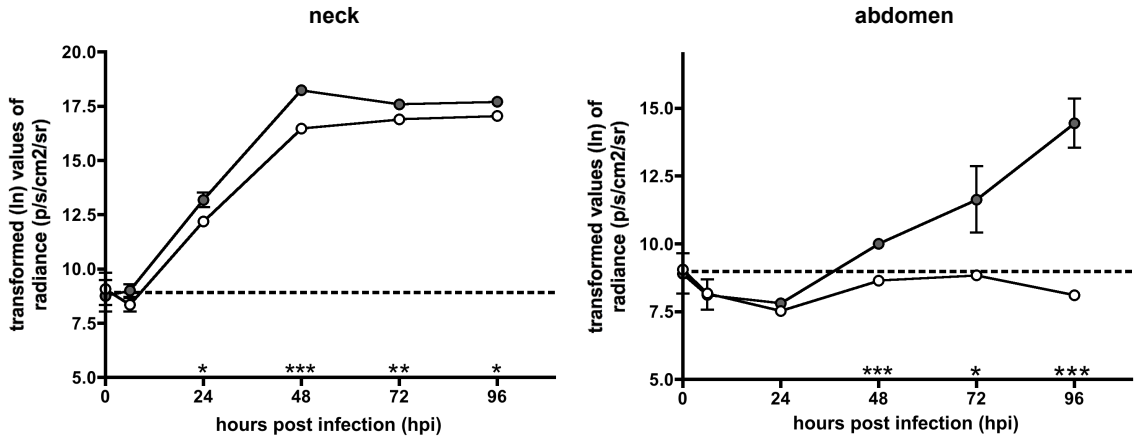


**Figure 2.6. BLI of C57BL/6J mice infected subcutaneously with Δ*caf1*Δ*psaA* *Y. pestis* carrying the pGEN-*luxCDABE* vector.**

(A) Mice were inoculated with ~200 CFU of the double mutant. Images correspond to infected animals at different time points post inoculation (shown in hpi). A color bar serves as a reference for the radiance scale (p/sec/cm$^2$/sr) used to standardize all images. (B) Images of superficial cervical lymph nodes, spleen and liver (from one of the mice shown in A) imaged individually after dissection. Luminescence was detected only from lymph nodes, imaged in an individual scale of radiance with a Min = 2.28e6 and Max = 4.27e7. (C) Transformed values (ln) of the mean radiance per group from the neck (left) and abdomen (right) from animals infected with Yp*lux*$^+$ (gray circles) and YpΔ*caf1*Δ*psaA lux*$^+$ (white circles), as determined by measurements from regions of interest (ROI) of images from two independent experiments. A dotted line depicts background radiance levels. Asterisks denote statistical significance in differences between the two means compared in a time point, as determined by linear regression analysis of transformed values (*, $P < 0.05$; **, $P < 0.005$; ***, $P < 0.0005$). Error bars represent the standard error of the mean (SEM). Shown is a representative experiment.

## REFERENCES


Anisimov, A.P., and Amoako, K.K. (2006). Treatment of plague: promising alternatives to antibiotics. J Med Micro *55*, 1461–1475.

Arbaji, A., Kharabsheh, S., Al-Azab, S., Al-Kayed, M., Amr, Z.S., Abu Baker, M., and Chu, M.C. (2005). A 12-case outbreak of pharyngeal plague following the consumption of camel meat, in north-eastern Jordan. Ann Trop Med Parasitol *99*, 789–793.

Bitam, I., Dittmar, K., Parola, P., Whiting, M.F., and Raoult, D. (2010). Fleas and flea-borne diseases. Int J Infect Dis *14*, e667–e676.

Cathelyn, J.S., Crosby, S.D., Lathem, W.W., Goldman, W.E., and Miller, V.L. (2006). RovA, a global regulator of Yersinia pestis, specifically required for bubonic plague. Proc Natl Acad Sci USA *103*, 13514–13519.

Contag, C.H., and Bachmann, M.H. (2002). Advances in *in vivo* bioluminescence imaging of gene expression. Annu Rev Biomed Eng *4*, 235–260.

DeLeo, F.R., and Hinnebusch, B.J. (2005). A plague upon the phagocytes. Nat Med *11*, 927–928.

Gage, K.L., and Kosoy, M.Y. (2005). Natural history of plague: perspectives from more than a century of research. Annu Rev Entomol *50*, 505–528.

Galimand, M., Carniel, E., and Courvalin, P. (2006). Resistance of *Yersinia pestis* to antimicrobial agents. Antimicrob Agents Chemother *50*, 3233–3236.

Guinet, F., and Carniel, E. (2003). A technique of intradermal injection of *Yersinia* to study *Y. pestis* physiopathology. Adv Exp Med Biol *529*, 73–78.

Guinet, F., Avé, P., Jones, L., Huerre, M., and Carniel, E. (2008). Defective innate cell response and lymph node infiltration specify *Yersinia pestis* infection. PLoS ONE *3*, e1688.

Hastings, J.W. (1996). Chemistries and colors of bioluminescent reactions: a review. Gene *173*, 5–11.

Hutchens, M., and Luker, G.D. (2007). Applications of bioluminescence imaging to the study of infectious diseases. Cell Microbiol *9*, 2315–2322.

Hyland, K.V., Asfaw, S.H., Olson, C.L., Daniels, M.D., and Engman, D.M. (2008). Bioluminescent imaging of *Trypanosoma cruzi* infection. International Journal for Parasitology *38*, 1391–1400.

Kong, Y., Subbian, S., Cirillo, S.L.G., and Cirillo, J.D. (2009). Application of optical imaging to study of extrapulmonary spread by tuberculosis. Tuberculosis (Edinb) *89*, S15–S17.

Lane, M.C., Alteri, C.J., Smith, S.N., and Mobley, H.L.T. (2007). Expression of flagella is coincident with uropathogenic *Escherichia coli* ascension to the upper urinary tract. Proc Natl Acad Sci USA *104*, 16669–16674.

Lathem, W.W., Crosby, S.D., Miller, V.L., and Goldman, W.E. (2005). Progression of primary pneumonic plague: a mouse model of infection, pathology, and bacterial transcriptional activity. Proc Natl Acad Sci USA *102*, 17786–17791.

Marketon, M.M., DePaolo, R.W., DeBord, K.L., Jabri, B., and Schneewind, O. (2005). Plague bacteria target immune cells during infection. Science *309*, 1739–1741.

Massoud, T.F., and Gambhir, S.S. (2003). Molecular imaging in living subjects: seeing fundamental biological processes in a new light. Genes Dev *17*, 545–580.

Matsumoto, H., and Young, G.M. (2009). Translocated effectors of *Yersinia*. Curr Opin Microbiol *12*, 94–100.

Nham, T., Filali, S., Danne, C., Derbise, A., and Carniel, E. (2012). Imaging of bubonic plague dynamics by in vivo tracking of bioluminescent *Yersinia pestis*. PLoS ONE *7*, e34714.

Perry, R.D., and Fetherston, J.D. (1997). *Yersinia pestis*--etiologic agent of plague. Clin. Microbiol. Rev. *10*, 35–66.

Prentice, M.B., and Rahalison, L. (2007). Plague. Lancet *369*, 1196–1207.

Price, P.A., Jin, J., and Goldman, W.E. (2012). Pulmonary infection by *Yersinia pestis* rapidly establishes a permissive environment for microbial proliferation. Proc Natl Acad Sci USA *109*, 3083–3088.

Sebbane, F., Gardner, D., Long, D., Gowen, B.B., and Hinnebusch, B.J. (2005). Kinetics of disease progression and host response in a rat model of bubonic plague. Am J Pathol *166*, 1427–1439.

Smiley, S.T. (2008). Immune defense against pneumonic plague. Immunol Rev *225*, 256–271.

Stenseth, N.C., Atshabar, B.B., Begon, M., Belmain, S.R., Bertherat, E., Carniel, E., Gage, K.L., Leirs, H., and Rahalison, L. (2008). Plague: past, present, and future. PLoS Med *5*, e3.

Van den Broeck, W., Derore, A., and Simoens, P. (2006). Anatomy and nomenclature of murine lymph nodes: Descriptive study and nomenclatory standardization in BALB/cAnNCrl mice. Journal of Immunological Methods *312*, 12–19.

Weening, E.H., Cathelyn, J.S., Kaufman, G., Lawrenz, M.B., Price, P., Goldman, W.E., and Miller, V.L. (2011). The dependence of the *Yersinia pestis* capsule on pathogenesis is influenced by the mouse background. Infect Immun *79*, 644–652.

Wimsatt, J., and Biggins, D.E. (2009). A review of plague persistence with special emphasis on fleas. Journal of Vector Borne Diseases *46*, 85–99.

Zhou, D., and Yang, R. (2009). Molecular Darwinian evolution of virulence in *Yersinia pestis*. Infect Immun *77*, 2242–2250.

Zietz, B.P., and Dunkelberg, H. (2004). The history of the plague and the research on the causative agent *Yersinia pestis*. International Journal of Hygiene and Environmental Health *207*, 165–178.

Zincarelli, C., Soltys, S., Rengo, G., and Rabinowitz, J.E. (2008). Analysis of AAV serotypes 1-9 mediated gene expression and tropism in mice after systemic injection. Mol Ther *16*, 1073–1080.

# CHAPTER 3: BOTTLENECK FORMATION AND HOST EFFORTS TO CONTROL BUBONIC PLAGUE

## 3.1. Overview

**Introduction**: Host-pathogen interactions are complex and difficult to study because biologically relevant observations can be made only if all the components of infection are taken into account. We studied host-pathogen interactions *in vivo* during dissemination of the causative agent of bubonic plague, *Yersinia pestis*.

**Methods:** We used an intradermal murine model of bubonic plague and assess the presence of bottlenecks during dissemination. Oligonucleotide-tagged *Y. pestis* were inoculated in the dermis and tracked to different organs throughout infection. In addition, we used confocal microscopy to study bacterial interactions with the host at a cellular level during different stages of infection. Moreover, cell depletions were used to determine if neutrophils play a role during infection.

**Results:** Only a fraction of the tagged strains that were inoculated survived in the lymph nodes and in spleens. The majority of the strains were found in the dermis throughout infection. After depletion of neutrophils, bacterial numbers were significantly higher in the skin in comparison with mice whose neutrophils were not depleted. Neutrophils, platelets, and bacteria appeared to interact in blood vessels during systemic stages.

**Conclusions:** We identified a bottleneck that restricts bacterial trafficking from the skin to the draining lymph node and defines the population that colonizes the host. We also found that neutrophils likely restrict colonization of the skin.

### 3.2. Introduction

Most pathogens disseminate from the initial site of contact with the host (site of inoculation, SI) to distant tissues. Dissemination allows a pathogen to reach sites where nutrients are more abundant or the probability of being transmitted to other hosts is higher. A pathogen uses an intricate arsenal to invade new tissues, to which the host responds by eliciting immune responses in an effort to eliminate infection. The battle between pathogen survival/dissemination and the host immune response is critical in defining the outcome of infection and the severity of disease. Thus, determining how host and pathogen interact during infection is key to understanding disease and to design strategies to control it. For most infectious diseases, however, there is a lack of in-depth knowledge about host-pathogen interactions *in vivo*.

A particularly challenging question is whether dissemination of highly virulent pathogens is affected by immune responses. If so, a second challenge is understanding when and where these barriers occur. A bottleneck is an example of such a barrier, as it restricts the number of individual pathogenic clones that can traffic to or colonize a tissue. Bottlenecks have only recently been explored in animal models but have been reported in viral (Lancaster and Pfeiffer, 2010), parasitic (Mackinnon et al., 2005; Oberle et al., 2010), and bacterial (Lowe et al., 2013; Melton-Witt et al., 2012; Plaut et al., 2012; Troy et al., 2013) infections. The

identification and characterization of bottlenecks is remarkably relevant because they (a) mark a stage of infection when an immune response is elicited and when a pathogen is susceptible to it, and (b) provide valuable information regarding the order in which tissues are colonized through dissemination, and (c) can potentially define the final pathogen population that will be transmitted to a new host. This latter point has major implications for pathogen evolution.

*Yersinia pestis* is the causative agent of bubonic plague, a severe bacterial disease characterized by aggressive dissemination within the host and that can be lethal if untreated. The bacteria first disseminate from the SI into the draining lymph node (LN) after inoculation in the skin (Sebbane et al., 2005). Colonization of LNs is then followed by bacterial escape into the bloodstream, resulting in septic shock and death (Brubaker, 2006). The ability of *Y. pestis* to disseminate at high rates makes it an unparalleled model to study bacterial dissemination *in vivo* and to understand how the host responds to the threat of severe infection. Successful colonization of the host depends on the expression of bacterial virulence factors (e.g. type III secretion system, pH6 antigen, F1 antigen) that are upregulated at 37°C and prevent phagocytosis (Brubaker, 2006; Prentice and Rahalison, 2007; Trosky et al., 2008; Zhou et al., 2006)These antiphagocytic factors are predicted to be expressed at low levels during the first hours of infection, a notion that gave rise to the hypothesis that an intracellular stage facilitates transport from skin to LN (Pujol and Bliska, 2005; Titball et al., 2003). This is partially supported by *in vitro* experiments showing bacterial survival in macrophages (Pujol and Bliska, 2003). However, recent studies report that *in vivo*, neutrophils might be the most relevant

lineage of cells that interacts with *Y. pestis* upon inoculation (Bosio et al., 2012; Shannon et al., 2013).

Neutrophils are prominent components of the immune response and are well known for their role in controlling infection at multiple levels (Appelberg, 2007; Kobayashi et al., 2005; McDonald et al., 2012). As with most studies addressing bubonic plague, many reports describing *Y. pestis* interactions with neutrophils have been conducted *in vitro* and/or with attenuated bacterial strains. For this reason, questions such as whether neutrophils play a role during infection have been difficult to answer.

The goal of this study was to identify the major events that occur during bubonic plague and the key mechanisms that define the outcome of infection. Moreover, we aimed to obtain a high-resolution picture of the host-pathogen interactions that take place after inoculation of *Y. pestis* into the skin of mice. We used tagged, virulent *Y. pestis* to address the presence of bottlenecks during dissemination and confocal microscopy to track the bacterium during dissemination.

## 3.3. Methods

### *3.3.1. Bacterial strains and culture conditions.*

Fully virulent Y. pestis CO92 (Parkhill et al., 2001) was used in all experiments. For the DA Y. pestis was tagged with 10 variants of an oligonucleotide signature tag (Walters et al., 2012). The oligonucleotide tag, along with a kanamycin resistance cassette, was inserted at the Tn7 att site in the bacterial chromosome (Choi et al., 2005). Each tag contains a unique sequence of

~80 bp flanked by invariant sequences that were used for amplification. The10 tagged Y. pestis CO92 strains were tested in our animal models to ensure each had retained the same virulence characteristics of the parent strain. For the DA tagged strains were cultured in brain and heart infusion broth (BHI, BD Biosciences, Bedford MA) with kanamycin and incubated at 26°C unless otherwise stated. Standardized liquid cultures (based on optical density at 600 nm) were mixed in a single tube and the mix was serial diluted in phosphate buffer solution (PBS) to obtain the desired inoculum. Methods for detection of the tagged strains are described in supplemental experimental procedures. For the double inoculation experiments, the carbenicillin resistant strain also expressed rfp (for easy detection). A mix of the tagged strains was used as the kanamycin resistant strain. For the experiments with bacteria grown at 37°C, liquid cultures were grown in BHI with 2.5 mM $CaCl_2$ for 6 h at 26°C and then shifted to 37°C for 12.5 h (Lathem et al., 2005). Where needed, kanamycin was added at 25 μg/ml and carbenicillin at 100 μg/ml.

*3.3.2. Animal infections.*

Six-to-eight week-old female C57BL/6J mice (Jackson Laboratory, Bar Harbor, ME) were inoculated under anesthesia (ketamine/xylazine). ID inoculations were done in the dorsal side of the ear pinna or the upper side of the foot. A volume of 2 μL was inoculated with the aid of a Pump11 Elite syringe pump (Harvard Apparatus, Holliston, MA) and a SURFLO winged infusion set with a 27-gauge needle (Terumo, Lakewood, CO). Animals were sacrificed by injection with sodium pentobarbital. Organs were harvested at different time points and homogenized in

1xPBS with a bead beater. Homogenates were serial diluted and plated on BHI agar and incubated at 26°C for 48 hours to obtain bacterial counts. Mann Whitney or Wilcoxon matched pairs signed rank tests were used for statistical analysis, establishing statistical significance at $p < 0.05$ using GraphPad Prism version 4.0c (GraphPad Software, La Jolla, CA). All animal studies were approved by the University of North Carolina Office of Animal Care and Use, protocol 11-128. For experiments with phagocyte depletion see supplemental experimental procedures.

*2.3.3. Whole ear imaging*

Mice were inoculated with *gfp*- or *rfp*-expressing *Y. pestis* (Hoopes et al., 2012; Price et al., 2012) following the procedures described above. After the mice were sacrificed, their ears were separated from the head, gently punctured with scissors (to facilitate fixative diffusion), and submerged in 10% buffered formalin for 24 hours. The dermis of the dorsal leaflet was exposed by separating both leaflets and removing the layer of cartilage that separates them. Ears were mounted on glass slides with ProLong Gold antifade reagent with 4',6-diamidino-2-phenylindole (DAPI; Molecular Probes, Eugene, OR). Neutrophils and platelets were stained by tail-vein injection of fluorescently labeled antibodies against Ly6G (BD, Franklin Lakes, NJ) and GPIX clone Xia.B4 (Emfret Analytics, Eibelstadt, Germany), respectively. Lymphatic vessels were stained by ID injection of fluorescently labeled podoplanin antibody clone 8.1.1 (BioLegend, San Diego, CA) and LYVE1 antibody (Fitzgerald, Acton, MA) (Hoopes et al., 2012; Schindelin et al., 2012). For all antibodies, 5 ng of antibody was used per mouse. Images were taken with an Olympus FV1000 MPE SIM laser scanning confocal microscope and analyzed with

the Fiji software package (Chtanova et al., 2008; Daley et al., 2007; Schindelin et al., 2012). The same procedures were used to image LNs and the lymphatic vessels that connect ears and LNs. These vessels were also visualized by injection of 10% Evan's blue in the ear.

*3.3.4. Detection of oligonucleotide-tagged strains*

Bacteria that grew on agar plates from undiluted homogenized organs were mixed with 1 mL of PBS using a bacterial cell spreader until a homogeneous suspension was formed. A volume of 20 µL of this suspension was added to BHI broth with kanamycin and incubated at 26°C in a roller drum for 14 h. When less than 15 colonies were present on a plate, individual colonies were picked with a wooden stick and grown under the same conditions described. DNA was extracted from liquid cultures using a Wizard Genomic Purification Kit (Promega, Madison, WI). DNA concentrations were measured and standardized at 100 ng/µL. The oligonucleotide tag sequence was amplified by PCR using primers P2 (5'-TAC CTA CAA CCT CAA GCT-3') and P4 (5'-TAC CCA TTC TAA CCA AGC-3'), which hybridize to the invariable region of all oligonucleotide tags. PCR reactions were prepared under standard conditions except for (a) the use of a mix of dideoxynucleotides (ddNTPs) with a ddATP:ddCTP:ddGTP:ddTTP ratio of 5:1:5:5 and (b) ddCTP labeled with $P^{32}$ was incorporated into the reaction. PCR reactions were cleaned using a MiniElute kit (Promega, Madison, WI). Southern dot blot assays were conducted using the obtained amplicon as probe. The probe was hybridized to positively charged nylon membranes (Roche, Manheim, Germany) with 200 ng of crosslinked plasmid DNA. The DNA crosslinked to the nylon

membrane was arranged in 10 separate spots, each one containing DNA of each of the unique oligonucleotide tags used in the study. Because 10 of the oligonucleotides were used in the membranes and 9 were used to inoculate the mice, one of the oligonucleotides spotted on the membranes served as negative control.

*3.3.5. Phagocyte depletion*

$Ly6G^+$ cells were depleted after tail vein injection of 100 µL (0.2 mg/mL) of low endotoxin Ly6G antibody clone 1A8 (BioLegend, San Diego, CA) (Chtanova et al., 2008; Daley et al., 2007). Monocytes and monocyte-derived cells were depleted by injecting 0.45 mg/mouse of clodronate-encapsulated liposomes (Encapsula Nano Sciences, Nashville, TN) (Eidsmo et al., 2009; Kataru et al., 2009; Price et al., 2012; Ward et al., 2011). Both, Ly6G antibody and clodronate-encapsulated liposomes, were injected 24 hours before inoculation of bacteria. Depletion of targeted cells was assessed by flow cytometry defining neutrophils as $Ly6G^+$ cells; monocytes as $F4/80^-$, $CD11b^+$, $Ly6G^-$ cells; macrophages as $F4/80^+$ cells; and dendritic cells as $F4/80^-$, $CD11b^+$ cells.

## 3.4. Results

*3.4.1. Y. pestis passes through a bottleneck during dissemination to the LN that drains the skin*

Conventional approaches to assess dissemination *in vivo* include quantifying bacterial burden in tissues at different time points. We wanted to learn about *Y. pestis* dissemination at a population level by determining whether all the members

of the inoculum population could be found beyond the SI. Thus a dissemination assay (DA) was developed based on the use of 10 oligonucleotide-tagged *Y. pestis* strains. These strains (hereafter referred to as “tagged strains” or simply “strains”) were generated by inserting a unique oligonucleotide tag at a neutral site in the bacterial chromosome (Walters et al., 2012). Each tagged strain was tested and found to possess the same levels of virulence and growth as un-tagged *Y. pestis* (data not shown). A mix of 9 tagged strains served as the inoculum in a murine intradermal (ID) model of infection [the tenth strain (A6) served as a negative control]. In this model, ~200 colony forming units (CFU) are injected in the ear pinna in a 2 µl volume to avoid confounding effects derived from tissue damage caused by larger volumes. DNA extracted from bacteria recovered at desired time points post-inoculation was subjected to Southern Blot analysis to determine which strains disseminated from the SI. DNA from the inoculum and from un-tagged *Y. pestis* was used as positive and negative controls, respectively.

At early time points, 12 hours post inoculation (hpi), the number of tagged strains in the LN ranged from one to five (average 2.2 Figure 3.1A). At 48 hpi, colonization of the LN was well established, systemic dissemination has occurred, and mice were close to succumbing to disease. The number of tagged strains present in the LN at 48 hpi ranged from one to five (average 2.8, Figure 3.1B). We then increased the inoculum 10-fold (~2000 CFU) to test if increasing the numbers of each tagged strain (~222 CFU per tagged strain) would alter the number of strains reaching the LN. This inoculum far exceeds the reported average inoculated in mouse skin by a flea (636 CFU, median 82 CFU) (Lorange et al., 2005). Out of

eight mice, four had all 9 tagged strains, one had 8, one had 7, and two had 6 (data not shown). Overall, these data indicate *Y. pestis* passes through a strong bottleneck after inoculation into the ear. Our data also suggests this bottleneck occurs during the first 12 hours of infection, before systemic dissemination takes place.

### *3.4.2. The bottleneck defines the population that colonizes the host and is abrogated after subcutaneous inoculation*

While it is currently thought that *Y. pestis* follows a SI-LN-blood route for systemic colonization (Gonzalez et al., 2012; Sebbane et al., 2005), it is possible that some bacteria escape from the SI directly into blood. We repeated our DA and included spleens, an organ used to assess systemic dissemination. All but one mouse (n=8) had the exact same strain population in spleens and in LNs (Figure 3.1C). The mouse that was the exception to this, had strains A3, A4, A5, and B2 in the LN but only A5 and B2 in the spleen. Repetitions of this experiment showed the same trend: either the exact same strains in both organs (majority of cases), or spleens lacking one or more strains that were present in LNs. We have never observed a strain present in the spleen that was not present in the LN. This is in agreement with the notion of *Y. pestis* disseminating from SI to LN and then to the rest of the body. More importantly, this suggests that the bottleneck defines the population that is responsible for systemic colonization of the host and that will be (potentially) transmitted to a naïve flea.

We next wanted to test if the bottleneck was an ear-specific phenomenon or if it could be replicated from a different anatomical site. We performed a DA

comparing mice inoculated in the ear (superficial parotid LN) with mice inoculated in the foot (popliteal LN). A limited number of tagged strains were observed in the LN (median of 3) and spleens (median of 2) of mice that were inoculated in the foot, indicating that this bottleneck is not an infection-site specific phenomenon (data not shown).

To determine if the dermis influenced the bottleneck, we repeated the DA with a subcutaneous (SC) route of infection. We used a well-established SC model that has been used extensively in our laboratory, inoculating on the ventral side of the neck (Cathelyn et al., 2006). The number of tagged strains in LNs from mice inoculated SC increased significantly over those inoculated ID (median value of 8.5, Figure 3.1D). This suggests the bottleneck can be abrogated if bacteria are deposited in a site other than the dermis and that its formation is linked to this specific layer of the skin.

### *3.4.3. The bacteria that do not pass through the bottleneck are confined to the site of inoculation*

We hypothesized that the source of the bottleneck was bacterial killing in the ear (SI). If this were true, the population of tagged strains in the ear should match that found in the LN. To test this, we performed a DA and compared the tagged strains in the ears with the respective LNs at 12 and 48 hpi. As opposed to what was observed in LN and spleens, the ear contained a majority of tagged strains, ranging from four to nine strains (median of seven and six at 12 and 48 hpi, respectively; Figure 3.2A). These data indicate survival of *Y. pestis* in the ear and formation of bottleneck are separate events. These data also indicate the

bottleneck between the SI and draining LN is established early and is maintained throughout infection.

We hypothesized that, after being in the skin for some time, bacteria could elicit a change in the microenvironment of the skin, altering their ability to move to the LN. To test this, we inoculated mice in the ear with a *Y. pestis* strain that is resistant to carbenicillin (~650 CFU) and, 24 hpi, we inoculated the same animals at the exact same spot with a *Y. pestis* strain that is resistant to kanamycin (~450 CFU). The inocula were intentionally different to make any effect more evident. LNs were harvested 48h after the first inoculation and plated on media with either carbenicillin or kanamycin. Bacterial loads in LNs were compared to those from a group of mice that were injected with PBS at the first inoculation time. We found lower bacterial loads of kanamycin resistant bacteria in LN of mice whose ears were previously exposed to bacteria in comparison with those that were exposed to PBS (Figure 3.2B). This reduction of bacterial loads could be very pronounced (no bacteria in LNs,), or moderate (data not shown) but was always found to be statistically significant when compared to the control group. These data indicate that the skin develops growth restrictive properties after being exposed to *Y. pestis*. These properties affect the movement of newly inoculated bacteria into the LN.

*3.4.4. Visualization of bacteria at the injection site, LNs, and lymphatic vessels that connect both tissues*

*Y. pestis* survives in multiple tissues during infection. This has been shown extensively through experiments where tissues of infected animals are harvested to obtain bacterial burdens. However, such an approach makes it impossible to make

qualitative observations of direct interactions with the host. We used microscopy to study in more detail how *Y. pestis* interacts with the host during dissemination from the ear. After ID inoculation with *Y. pestis* expressing *rfp* (RFP-*Y. pestis*) or *gfp* (GFP-*Y. pestis*), whole tissues were fixed and imaged using confocal microscopy. This approach was chosen as opposed to histological sections to obtain images of bacteria in tissues whose architecture was minimally disrupted. To improve visualization of bacteria, however, the cartilage was removed to expose the dermal layer of the ear pinna after fixation. Bacteria were localized exclusively at two specific sites in the ear. One was the injection site, defined by the small and transient wheal (bubble) that forms in the skin during inoculation. Bacteria at this site were found mostly in large clumps or as small groupings of cells (Figure 3.3A and B). The second site where bacteria were found was at the base of the ear in the shape of tube like structures, noted at 24 hpi. The presence of these tubes was infrequent but when seen, signal was so strong that it could be seen easily at lower magnifications without separating the ear leaflets (Figure 3.3C). As opposed to blood vessels, which look red under bright field microscopy, the tubes were only visible using fluorescence microscopy (Figure 3.3D). Bacteria were distributed unevenly in these tubes and appeared as individual or very tight clumps of bacteria (Figure 3.3 E, F, and G). Staining with DAPI revealed the presence of host cells in very close proximity to bacteria inside of these tubes (Figure 3.3H).

To determine if bacteria could be detected in the lymphatic vessels that connect ear and LN, we removed and fixed the infected ear pinna along with as much adjacent tissue as possible up to the cervical region (Figure 3.4A), including

the draining LN and the lymphatic vessels that connect both tissues. In LNs at 24 hpi, *Y. pestis* appeared to be in discrete microcolonies and inside afferent lymphatic vessels (Figure 3.4Ai, Aii, and Aiii). At 48 hpi, very strong signal was detected from these sites (Figure 3.4B). Bacteria inside the afferent lymphatic vessels were found either as single cells and small groups or formed tight clumps (Figure 3.4C, D, and E). There also were numerous bacterial associations with host cells, as revealed by DAPI stain (Figure 3.4F). Lastly, bacteria were detected in the lymphatic vessels that connect the LN and the ear pinna (Figure 3.4G, H, I, and J). These data provide direct evidence that *Y. pestis* travels to the lymph node in the lymphatic vessels rather than through blood. These data also indicate for the first time that many bacteria in the lymphatics are not associated with host cells.

*3.4.5. Neutrophils control Y. pestis expansion in the dermis.*

To gain insights into what role neutrophils play during infection, we tracked these cells by microscopy imaging. Because our model of infection causes very little disruption to the dermis, observations of the skin at very high resolution and with high levels of accuracy can be made. We used fluorescently labeled anti-Ly6G, an antibody that binds to neutrophils (Daley et al., 2007) to track these cells during infection. At 30 minutes post inoculation, very few isolated clusters of neutrophils were observed in the skin, and none were associated with *Y. pestis* (Figure 3.5A). Between 4 and 8 hpi, many bacteria were in close proximity to neutrophils or inside them (as determined by confocal microscopy). At 24 hpi a prominent increase in neutrophils was observed in comparison to previous time points. Neutrophils were highly concentrated at the injection site, forming very

dense clusters. However, very few bacteria seemed to be associated with neutrophils at this time point. Similar to previous time points, neutrophils were present in vascular tissue at very low numbers/densities. At 48 hpi, systemic infection was evidenced by bacteria observed inside blood vessels. In the vascular tissue, large numbers of neutrophils were observed, and bacteria were associated with some neutrophils. These neutrophils with associated bacteria appeared to be circulating (one or two bacteria with very few neutrophils, (Figure 3.5B, 48 hpi, i), or in tight aggregates that localized to the walls of blood vessels, filling the entire lumen of the vessel in some instances (Figure 3.5B, 48 hpi, ii). Staining with fluorescently labeled anti-GPIX, an antibody that binds to platelets, revealed clusters of neutrophils that appeared to be connected by platelets. This was especially true for the tight neutrophil aggregates that localized to the walls of the blood vessels (Figure 3.5B, 48 hpi, iii). We collected ears from mice that were found dead (0-12 hours after death) in hopes of seeing what infection looked like at the moment of death. These images revealed a striking increase in bacterial numbers in blood vessels, with dense bacterial clusters localized to the walls of blood vessels and filled capillaries. Some vessels had a “bacterial plug” surrounded by neutrophils that stretched across the transversal plane of the vessel (Figure 3.5B, mouse found dead, iii-vi).

Bacterial numbers in the skin at the injection site did not seem to increase over time, but did not decrease either. We hypothesized that neutrophils control bacterial burden in the skin, but are unable to clear the infection. We and others have speculated that neutrophils could have an effect on bacterial trafficking to LNs

(Shannon et al., 2013) and bottleneck formation. Depletion of neutrophils using the Ly6G antibody had no impact on bacterial trafficking (Figure 3.6A) or bottleneck formation as determined using the DA (data not shown), indicating that neutrophils do not contribute to these processes. However, mice depleted for neutrophils showed a highly significant increase in the number of bacteria in the skin (ear) compared to mock treated mice (Figure 3.6B). In addition, nearly all anti-Ly6G-treated mice retained all nine tagged strains at the SI (data not shown). We noted that an increase in bacterial burden at the SI only occurs in the absence of neutrophils. Because this observation conflicts with previous reports describing bacterial growth in the ear (Bosio et al., 2012; Guinet and Carniel, 2003; Shannon et al., 2013), we speculated that differences in the ID models of infection could contribute to these divergent results. In our model, a 2 µl volume is used to deliver the inoculum, whereas others have used 10 µl (Belkaid et al., 1998; Gonzalez et al., 2012; Guinet and Carniel, 2003; Lin et al., 2012; Shannon et al., 2013; Thackray and Field, 2000). We compared bacterial burden in the ear of mice after inoculation of 2 and 10 µL, keeping the inoculum CFU constant for both groups. Mice inoculated with the larger volume showed a statistically significant increase in the number of bacteria recovered from the ear in comparison with mice inoculated with the smaller volume (data not shown). Overall, these experiments suggest *Y. pestis* interacts with neutrophils in the dermis and that these interactions restrict colonization of the skin. In addition, these data show that bacteria that circulate systemically interact with neutrophils and other cell types such as platelets.

*3.4.6. Dissemination of Y. pestis with the flow of lymph*

It has been suggested that for *Y. pestis* to move into LNs, an intracellular stage must exist (Pujol and Bliska, 2005; Titball et al., 2003). Results presented here and another recent study (Shannon et al., 2013), suggest neutrophils are not important for bacterial movement to LN. Shannon, et al. also concluded that the interactions of *Y. pestis* with dendritic cells *in vivo* are minimal and unlikely to be significant for bacterial dissemination. To gain insight on how *Y. pestis* travels to draining LNs, we explored the notion that it could be transported by the flow of lymph as opposed to being associated with phagocytes. *In vivo* models of bubonic plague infections use *Y. pestis* grown at 26°C, the temperature consistent with delivery from a flea. At 26°C, the antiphagocytic factors that are crucial for *Y. pestis* survival in the host are predicted to be weakly expressed. Studies with cell lines and primary cells found that *Y. pestis* is significantly less susceptible to phagocytosis by macrophages, dendritic cells, and to a lesser extent by neutrophils, when grown at 37°C than when grown at 26°C (Charnetzky and Shuford, 1985; Spinner et al., 2008; 2013; Zhang et al., 2008). Because it has been predicted that *Y. pestis* travels from the skin to LNs inside of phagocytes, we hypothesized that bacteria grown at 37°C would not disseminate efficiently to LNs. Surprisingly, we found that mice inoculated with comparable numbers of bacteria grown either at 26°C or 37°C showed no difference in bacterial loads in LNs, spleens, or ears (Figure 3.7). These data suggest that association with phagocytes might not be necessary for *Y. pestis* to disseminate from the skin to the draining LN.

### 3.5. Discussion

Pathogen dissemination in the host is a crucial and understudied process of infection. Although many studies have addressed bacterial-host interactions of *Y. pestis* (and other highly virulent pathogens), most of them are limited by the use of *in vitro* approaches and/or the use of attenuated strains. While many noteworthy observations have derived from these studies, we believe that a complete picture of infection can only be achieved by using fully virulent strains in an *in vivo* context. Herein, we looked at dissemination of fully virulent *Y. pestis* in mice. We used (1) an ID model of infection with minimal disruption to the skin, (2) an assay (DA) that allowed us to follow dissemination at a population level, and (3) microscopic imaging of the skin and underlying tissue to observe host-pathogen interactions at a cellular level. The combination of these strategies gave us a high-resolution picture of infection that allowed us to make biologically relevant observations of a bacterial-host system.

Upon ID injection, the dissemination assay revealed that a bottleneck accounts for a previously unrecognized barrier for *Y. pestis* dissemination from the SI. The bottleneck has strong evolutionary implications for *Y. pestis*. This is because it defines the population of bacteria that have the potential to be acquired by a naïve flea and thus be transmitted to a new host. Interestingly, the bottleneck is abrogated when bacteria are delivered in the SC space beyond the dermis. This is relevant, as it is very likely that fleas deliver *Y. pestis* into the dermis and not the SC space (Hinnebusch, 2005; Sebbane et al., 2006). The dermis is particularly proficient in triggering immune responses against invaders. Differences in

immunogenicity between layers of the skin have also been shown to exist in cancer research. Adenocarcinoma cells in rats develop into tumors only after SC but not ID injections (Bonnotte et al., 2003). The SC layer of the skin, on the other hand, is less immunologically competent and this might facilitate the passage of more tagged strains into the LN (Combadiere and Liard, 2011). This might occur due to delayed influx of immune cells from blood therefor allowing for more local bacterial replication prior to dissemination. Our research is currently focusing on what is unique in the dermis that makes it an optimal site for bottleneck formation. We propose that the bottleneck originates from multiple factors that work in an additive manner and that derive from both the pathogen and host. We found that factors that we hypothesized affect bacterial movement to LNs such as injection volume play no role in bottleneck formation. Preliminary studies testing the role of other potential factors in bottleneck formation (iNOS, coagulation, mast cells) indicate these factors have no effect either (unpublished results).

Even under conditions when most mice succumb to plague, bottleneck formation could be highly efficient in some individuals. Nearly 10% of our mice showed no bacteria in the LN. This was not due to ineffective inoculation as we confirmed that 100% of the mice had bacteria in the inoculated ear. This suggests that efficient bottlenecks form in a fraction of more immunocompetent individuals, perhaps as a result of inherent variability in the immune responses of a population. It is not known how the immune response varies during a natural flea inoculation (vs. needle inoculation) and how this would affect bottleneck formation. However, in *Leishmania major* infections, more robust and prevalent infiltration of neutrophils

is observed during sand fly versus needle inoculations (Peters et al., 2009). If a *Y. pestis* inoculating fleabite also results in augmented immune responses, one would expect that the rate of successful infections from fleabites would be low, due to the bottleneck. In agreement with this, studies using fleas have estimated the rate of successful plague infections in mice by fleabites to be less than 50% (Lorange et al., 2005).

Very few studies have used imaging to probe host-pathogen interactions during cutaneous infections *in vivo* (Chong et al., 2013). We used an ID model with little disruption to the dermis and fluorescence confocal microscopy of unsectioned tissues to track *Y. pestis* throughout infection. This provided us with high-resolution observations to reveal bacterial localization and associations in the host without requiring the use of attenuated strains. Microscopy imaging provides qualitative information to understand interactions with the host that is impossible to collect by traditional approaches using bacterial counts from harvested organs. The use of microscopy imaging, in combination with the use of depleting antibodies, allowed us to reveal a role of neutrophils during infection of the dermis. Recent research suggested bacteria could evade a strong neutrophil response in the skin (Bosio et al., 2012; Shannon et al., 2013). Our observations are in agreement with these reports, as we did not observe bacterial clearance in the skin. However, we also found that neutrophils severely restrict bacterial colonization of the skin, and thus, established a function for neutrophils *in vivo*. The bacterial restrictive properties of the skin (largely driven by neutrophils) are likely to be absent at the onset of infection. However, once present, they affect the bacteria in the skin in such a way

that movement of newly inoculated bacteria into LNs is restricted, as shown by our double inoculation experiment. Altering the skin environment by injecting higher volumes appears to abrogate these restrictive properties of the dermis. Higher volumes might “dilute” components of the initial immune response in the dermis, preventing direct contact of bacteria with neutrophils, or delaying detection of bacteria.

In addition to the role played by neutrophils, we also found numerous platelet associations with these cells during systemic infection. Platelets associate with neutrophils during sepsis and play a role in the formation of neutrophil extracellular traps (NETs) (McDonald et al., 2012). Although it has been suggested that *Y. pestis* inhibits platelet aggregation (Leung et al., 1990), we observed robust accumulation of these cells associated with neutrophils in blood vessels. Whether the platelet-neutrophil associations we observed result in efficient formation of NETs or affect disease progression in any way is unknown.

How pathogens disseminate from the SI into deeper tissues is one of the most relevant questions in microbial pathogenesis and one that is very difficult to address using direct approaches. For many pathogens, including *Y. pestis*, an intracellular stage to reach distant tissues has been proposed (Pujol and Bliska, 2005; Titball et al., 2003). In this study, our data suggest that association with host cells does might not be necessary for *Y. pestis* to travel to LNs. Similar claims have been made for the highly virulent pathogen *Bacillus anthracis* (Weiner and Glomski, 2012) and for *Salmonella abortusovis*. In the latter case, 80% of the bacteria traveling to LN were found to be free in lymphatic vessels during the first

90 minutes of infection (Bonneau et al., 2006). While our data suggest *Y. pestis* flows freely in lymph fluid, we cannot discard the possibility that bacteria travel to LNs in multiple ways. Movement with the flow of lymph (free bacteria) and trafficking with host cells (intracellularly or attached to their surface) might occur simultaneously.

In conclusion, our observations suggest that upon inoculation most bacteria remain in the skin and few escape to lymphatic vessels, in part carried along by the flow of lymph. For the bacteria that remain in the skin, an equilibrium state develops where bacteria are neither cleared nor able to proliferate. These bacteria have no means to move to the LN and do not contribute to disease. By the time these processes occur, the few bacteria that escaped via lymphatic vessels have likely already reached the LN, and subsequently move into blood vessels. Expression of specific genes might be necessary for *Y. pestis* to adapt to these very different immunological environments, where new threats (such as NETs) are encountered. Most likely, however, once in the lymph node, *Y. pestis* is favored over the host and the outcome of infection is already defined.

## 3.6. Figures and Tables

**A**

| mouse (n=8) | CFU | LN 12 hpi | # of strains |
|---|---|---|---|
| 1 | 47 | 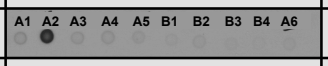 | 1 |
| 2 | 0 | no bacteria present | 0 |
| 3 | 20 | 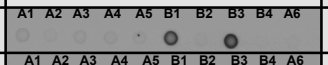 | 2 |
| 4 | 3 | 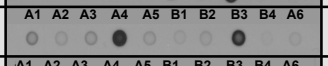 | 2 |
| 5 | 111 | 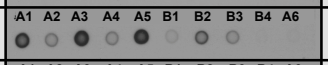 | 4 |
| 6 | 143 | 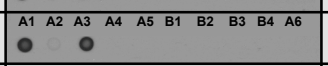 | 2 |
| 7 | 0 | no bacteria present | 0 |
| 8 | 0 | no bacteria present | 0 |

**B**

| mouse (n=7) | CFU | LN 48 hpi | # of strains |
|---|---|---|---|
| 1 | 0 | no bacteria present | 0 |
| 2 | 0 | no bacteria present | 0 |
| 3 | lawn | 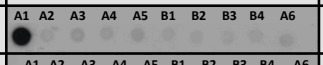 | 1 |
| 4 | lawn | 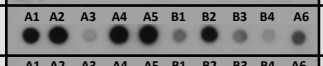 | 5 |
| 5 | lawn | 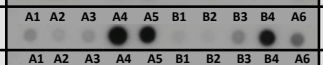 | 3 |
| 6 | lawn | 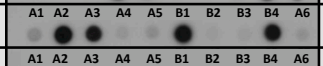 | 4 |
| 7 | 6 | 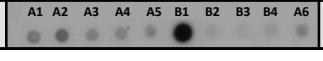 | 1 |

**C**

| mouse (n=8) | LN | spleen | # of strains LN/spleen |
|---|---|---|---|
| 1 | no bacteria present | no bacteria present | 0/0 |
| 2 | 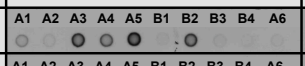 | 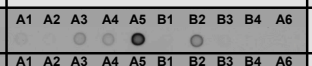 | 4/2 |
| 3 | 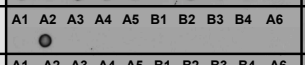 | 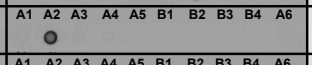 | 1/1 |
| 4 | 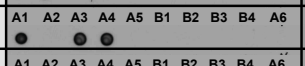 | 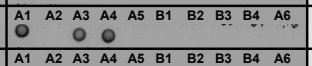 | 3/3 |
| 5 | 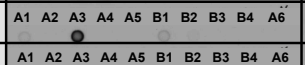 | 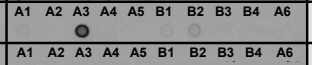 | 1/1 |
| 6 | 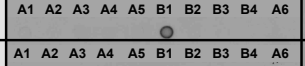 | 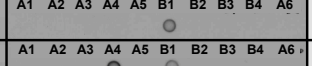 | 1/1 |
| 7 | 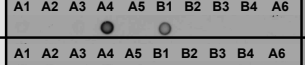 | 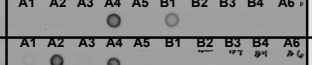 | 2/2 |
| 8 | 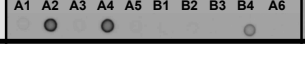 |  | 3/3 |

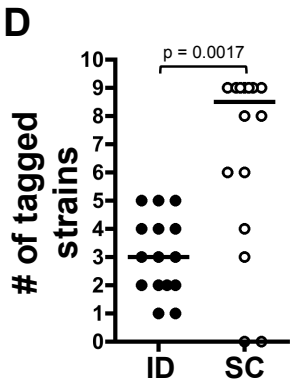


**Figure 3.1. A bottleneck limits dissemination of *Y. pestis* to the draining LN.** (A and B) Southern dot blot analysis of DNA from bacteria from LNs harvested at 12 hpi (A) and 48 hpi (B). Each row shows results from a single mouse (identified with a number). The number of CFU obtained from each tissue and from which DNA was extracted is also shown (CFU). (C) Southern dot blot analysis of DNA from bacteria from LNs and spleens belonging to the same mouse and harvested at 48 hpi. Each row shows results from a single mouse (identified with a number). "no bacteria present" identifies mice whose LN or spleen had no detectable bacteria. All mice had comparable numbers of bacteria in the ear (including the ones with negative LNs, not shown). The number of tagged strains present in each LN is also shown. At least 10 experiments were done and the blots shown belong to one representative experiment. (D) The number of tagged strains were quantified in LNs at 48 hpi of mice inoculated ID in the ear pinna (black circles) or subcutaneously (white circles) in the ventral side of the neck. Differences between groups were determined by the Mann-Whitney test and statistical significance was established at $p < 0.05$. Data from two combined experiments are shown. Each circle represents the number of tagged strains obtained from LNs from a single mouse. Horizontal bars represent the median value of the group.

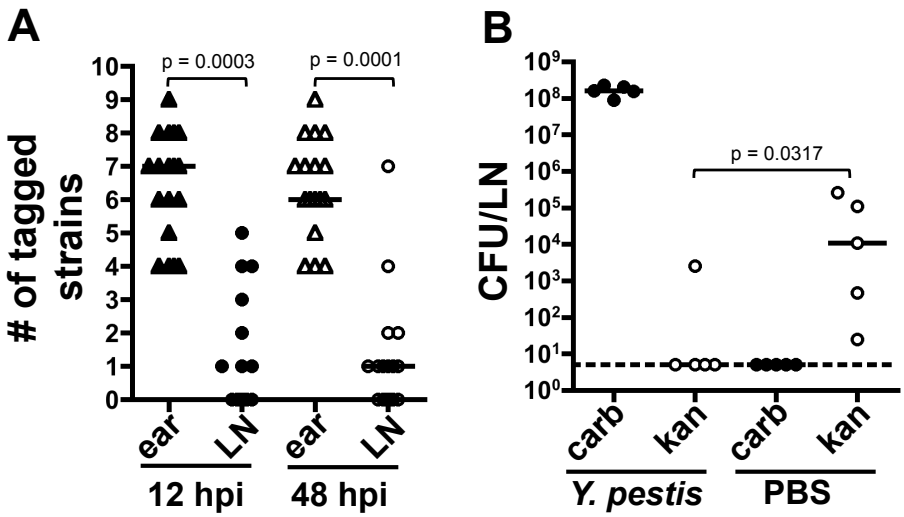


**Figure 3.2. Bacteria that do not pass through the bottleneck are confined to the site of inoculation.**

(A) Mice were inoculated ID in the ear pinna with ten tagged strains of *Y. pestis*. The number of tagged strains present in ears (triangles) and LNs (circles) at 12 hpi (black symbols) and 48 hpi (white symbols) is shown. Combined data from two independent experiments are shown. Differences between groups were determined by Wilcoxon matched pairs signed rank test, establishing statistical significance at $p < 0.05$. (B) Bacterial burden from LNs after two consecutive inoculations. Mice were inoculated with carbenicillin resistant *Y. pestis* (*Y. pestis*, carb) and, 24 hours after, were inoculated again at the same spot in the ear with kanamycin resistant *Y. pestis* (*Y. pestis*, kan). Another group of mice was mock inoculated with PBS and, 24 hours after, inoculated with kanamycin resistant *Y. pestis* (PBS, kan). The dotted line represents the limit of detection (values of one or zero CFU/plate are considered to be at the limit of detection). The experiment was repeated three times under similar conditions. Data from one representative experiment are shown. The experiment was repeated under similar conditions two more times. Differences between groups were determined by the Mann-Whitney test and statistical significance was established at $p < 0.05$. Each symbol (triangle or circle) represents the number of tagged strains (A) or CFU (B) obtained from a tissue from a single mouse. Horizontal bars represent the median value of the group.

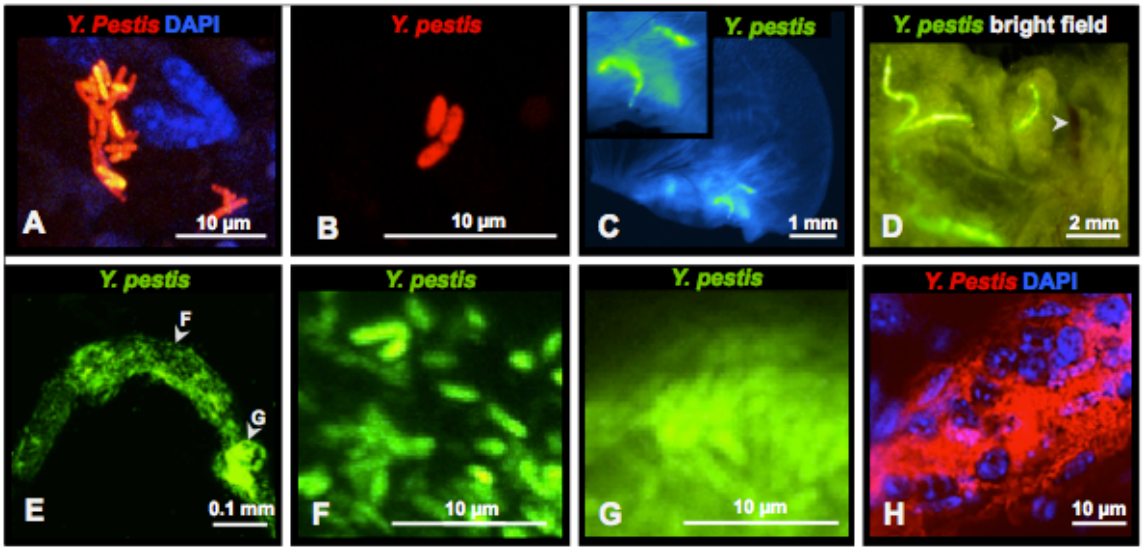


**Figure 3.3. Bacteria are visualized at the injection site and in tubes at the base of the ear pinna.**
GFP or RFP-*Y. pestis* were inoculated ID in the ear pinna and this tissue was imaged using confocal microscopy to determine bacterial distribution in this tissue. (A and B) RFP-*Y. pestis* in clumps (A) or small groups (B) at the injection site minutes after inoculation. (C-G) GFP-*Y. pestis* in tubes located at the base of the ear (C). The tubes are not blood vessels (arrowhead), as the latter appear dark red under bright field microscopy (D). (E-G) Bacteria are in these tubes are dispersed (F) or in tight aggregates (G). (H) RFP-*Y. pestis* are associated with host cells inside of the tubes. Except for C and D (taken with a dissecting stereomicroscope), the images show maximum intensity projections from z-stacks. The white bar is shown as reference for scale.

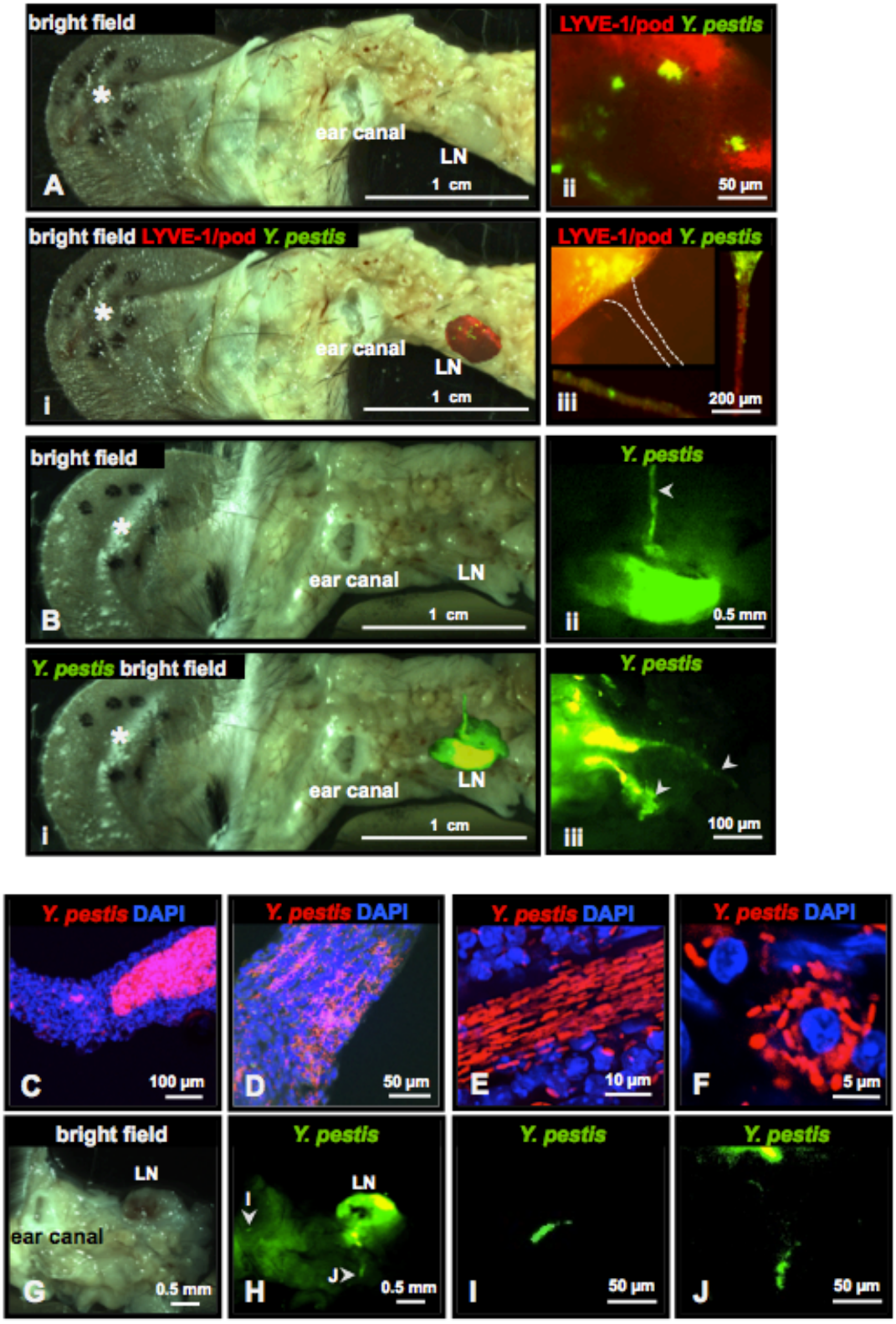


**Figure 3.4. Bacteria are visualized in LNs and in the lymphatic vessels that connect these compartments with the ear.**

Mice were inoculated with RFP-*Y. pestis* and the ear pinna was removed along with surrounding tissue, including draining LNs. (A and B) Ears were injected with fluorescently labeled podoplanin and LYVE-1 antibody (red) and tissues were removed at 24 (A) and 48 (B) hpi. Site of injection (asterisk), ear canal, and LN are shown. LNs show few microcolonies (green) at 24 hpi (Aii shows the LN in Ai at higher magnification). An afferent tube connected to LN is shown (Aiii). In the same panel, two sections of an afferent tube (red) with bacteria (green) are shown. Tissues removed at 48 hpi show strong signal from LN (B). Bii shows the LN in Bi at higher magnification. Lymphatic vessels (arrowheads) attached to LN and filled with bacteria (green) are shown in Bii and Biii. (C-D) Lymphatic vessels attached to LNs with dissociated bacteria (red) or bacteria arranged in clumps (C and D). Section of a lymphatic vessel with bacteria arranged with their long axis running along the long axis of the tube (E). Bacteria associated with host cells inside lymphatic vessels (F). (G-J) Bacteria (green) in tubes (arrowhead, I and J) in the space in between the ear and LN. In A, B, and H-J, bacteria were false-colored. The white bar is shown as reference for scale.

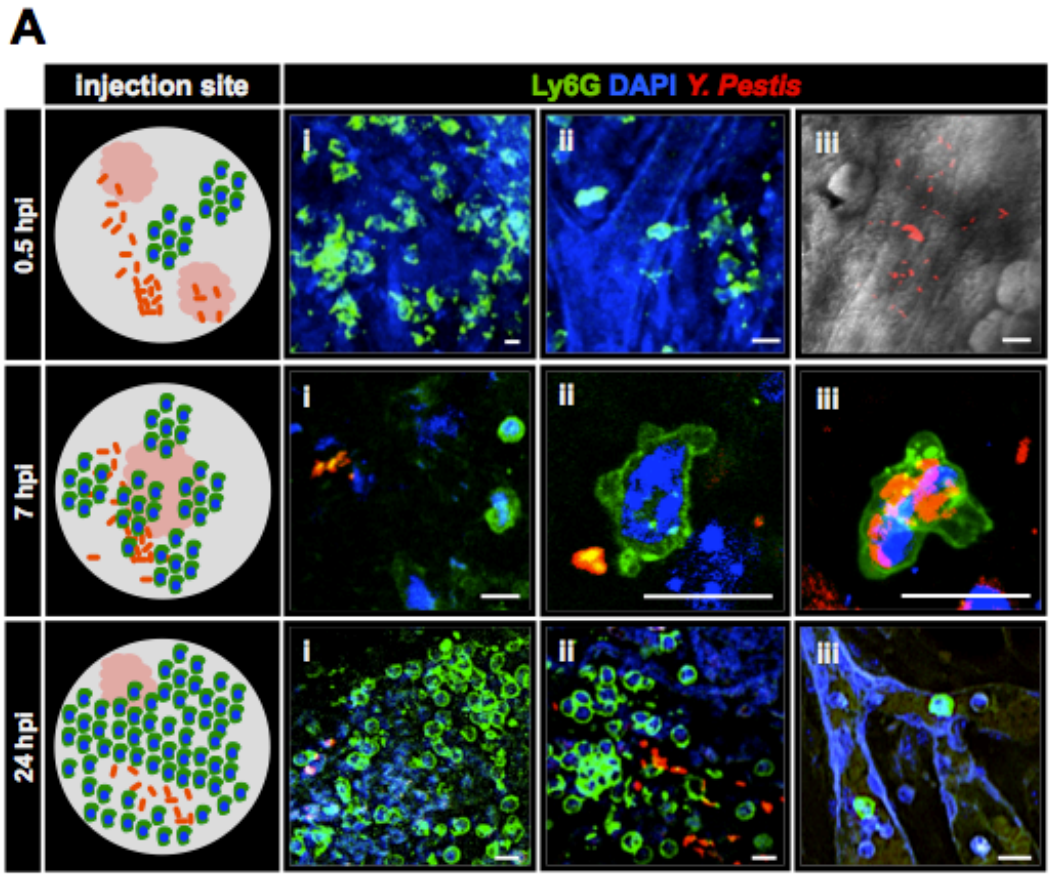

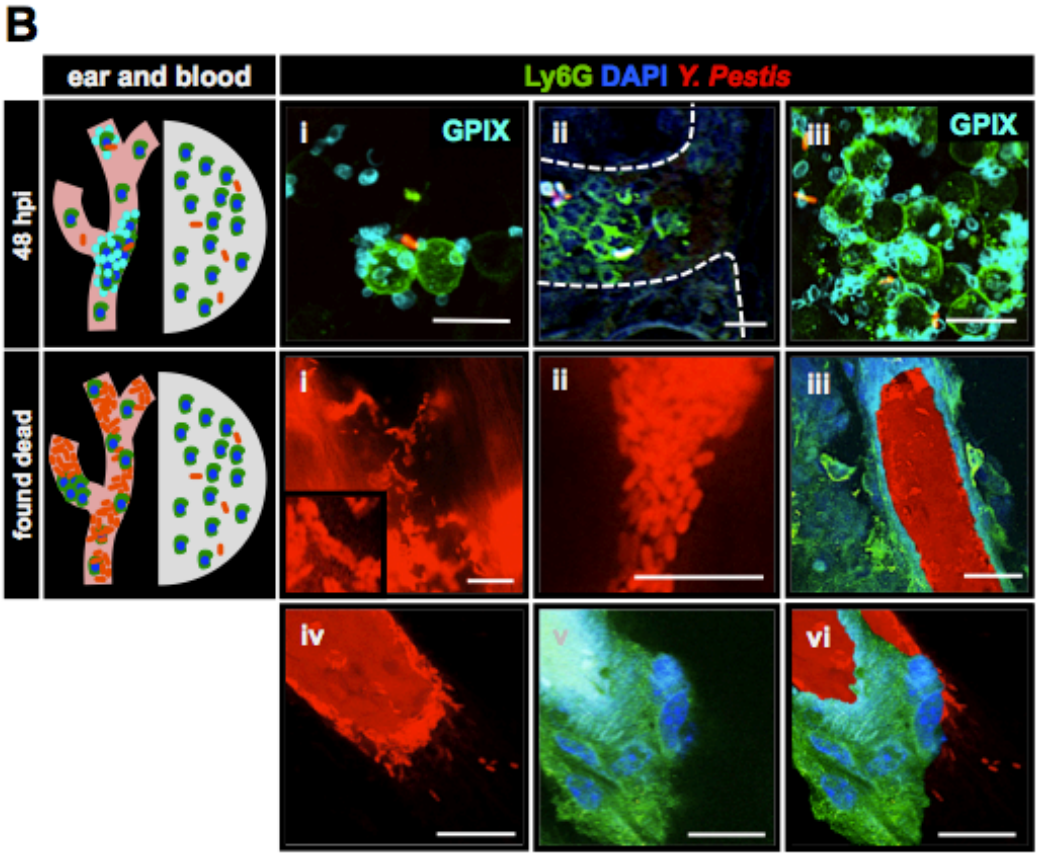


**Figure 3.5. Bacterial interactions with neutrophils throughout infection.**
Mice were inoculated ID in the ear pinna with RFP-*Y. pestis* prior to intravenous injection with fluorescently labeled Ly6G antibody to visualize neutrophils (green). Ears were removed for confocal microscopy imaging. Diagrams of the major observations per time point (from a representative ear) are shown (left). Blood from injection is represented with a pink irregular mark, bacteria as small red rods, neutrophils as green blebs with a blue nuclei, and platelets as small cyan circles. At least four ears per time point were analyzed to determine the major observations that are reported. The images show maximum intensity projections from z-stacks. The scale bar represents 10 μm.
(A) Ears were removed before systemic dissemination at 0.5, 7 and 24 hpi and the site of injection was imaged. For 0.5 hpi, i and ii, illustrate clouds of neutrophils and iii illustrates isolated bacteria. For 7 hpi, i, and ii, illustrate bacteria distant and close to neutrophils. iii illustrates bacteria inside of a neutrophil. For 24 hpi, i illustrates dense aggregates of neutrophils in the skin; ii illustrates bacteria in close proximity to neutrophil aggregates; iii illustrates neutrophils in blood vessels in the injection site.
(B) Ears were removed after systemic dissemination at 48 hpi and from mice that were found dead. Images shown belong to blood vessels outside the injection site. For 48 hpi, i illustrates bacterial associations with neutrophils and platelets (stained with fluorescently labeled GPIX, false-colored cyan); ii illustrates neutrophil aggregates filling the lumen of a blood vessel; iii illustrate large aggregates of

neutrophils with platelets in association with bacteria and localized to the wall of a blood vessel. For the mouse found dead i and ii illustrate bacteria in a large blood vessel and a capillary, respectively; iii illustrates a blood vessel with a “bacterial plug”; a similar vessel is illustrated in iv and neutrophils covering the plug are shown in v; vi shows an overlay of iv and v.

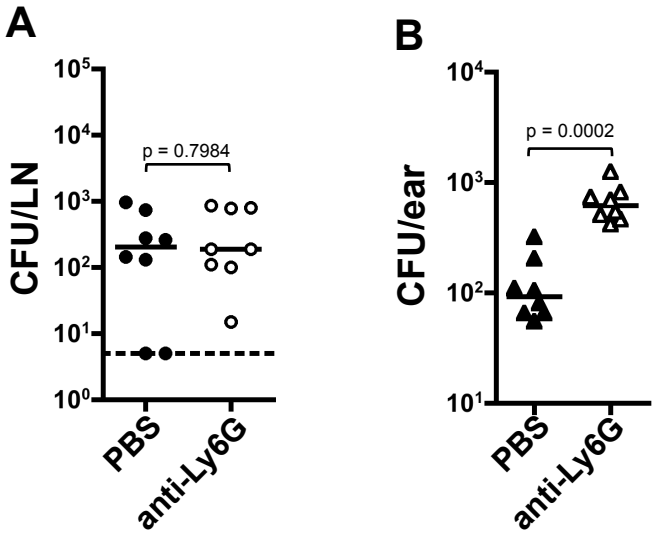


**Figure 3.6. *Y. pestis* colonization of the skin is restricted by neutrophils.**
Mice were injected intravenously with PBS (black symbols) or with an antibody (Ly6G) that depletes neutrophils (white symbols). At 12 hours after ID inoculation of *Y. pestis* in the ear pinna, LNs (A, circles) and ears (B, triangles) were harvested, homogenized and plated to obtain bacterial counts. Each symbol (triangle or circle) represents the number of CFU obtained from a tissue from a single mouse. Horizontal bars represent the median value of the group. The dotted line represents the limit of detection (values of one or zero CFU/plate are considered to be at the limit of detection). All values obtained from ears were higher than the limit of detection. The experiment was repeated two times under similar conditions. Data from one representative experiment are shown. Differences between groups were determined by the Mann-Whitney test and statistical significance was established at $p < 0.05$.

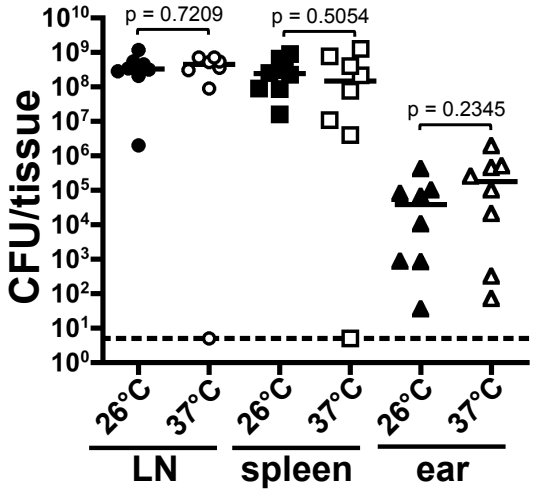


**Figure 3.7. Bacterial dissemination from the ear to the draining LN.**
Mice were inoculated ID in the ear pinna with *Y. pestis* grown at 26°C (black symbols) or 37°C (white symbols) and colony forming units (CFU) per tissue from lymph nodes (circles), spleens (squares), and ears (triangles) were harvested at 48 hpi. Each symbol (circle, square, or triangle) represents the number of CFU obtained from a tissue from a single mouse. Horizontal bars represent the median value of the group. The dotted line represents the limit of detection (values of one or zero CFU/plate are considered to be at the limit of detection). The experiment was repeated two times. Data from one representative experiment are shown. Differences between groups were determined by the Mann-Whitney test and statistical significance was established at $p < 0.05$.

## REFERENCES


Appelberg, R. (2007). Neutrophils and intracellular pathogens: beyond phagocytosis and killing. Trends Microbiol *15*, 87–92.

Belkaid, Y., Kamhawi, S., Modi, G., Valenzuela, J., Noben-Trauth, N., Rowton, E., Ribeiro, J., and Sacks, D.L. (1998). Development of a natural model of cutaneous leishmaniasis: powerful effects of vector saliva and saliva preexposure on the long-term outcome of *Leishmania major* infection in the mouse ear dermis. J Exp Med *188*, 1941–1953.

Bonneau, M., Epardaud, M., Payot, F., Niborski, V., Thoulouze, M.-I., Bernex, F., Charley, B., Riffault, S., Guilloteau, L.A., and Schwartz-Cornil, I. (2006). Migratory monocytes and granulocytes are major lymphatic carriers of *Salmonella* from tissue to draining lymph node. J Leukoc Biol *79*, 268–276.

Bonnotte, B., Gough, M., Phan, V., Ahmed, A., Chong, H., Martin, F., and Vile, R.G. (2003). Intradermal injection, as opposed to subcutaneous injection, enhances immunogenicity and suppresses tumorigenicity of tumor cells. Cancer Research *63*, 2145–2149.

Bosio, C.F., Jarrett, C.O., Gardner, D., and Hinnebusch, B.J. (2012). Kinetics of innate immune response to *Yersinia pestis* after intradermal infection in a mouse model. Infect Immun *80*, 4034–4045.

Brubaker, R. (2006). *Yersinia pestis* and bubonic plague. Prokaryotes *6*, 399–442.

Cathelyn, J.S., Crosby, S.D., Lathem, W.W., Goldman, W.E., and Miller, V.L. (2006). RovA, a global regulator of *Yersinia pestis*, specifically required for bubonic plague. Proc Natl Acad Sci USA *103*, 13514–13519.

Charnetzky, W.T., and Shuford, W.W. (1985). Survival and growth of Yersinia pestis within macrophages and an effect of the loss of the 47-megadalton plasmid on growth in macrophages. Infect Immun *47*, 234–241.

Choi, K.-H., Gaynor, J.B., White, K.G., Lopez, C., Bosio, C.M., Karkhoff-Schweizer, R.R., and Schweizer, H.P. (2005). A Tn7-based broad-range bacterial cloning and expression system. Nat. Methods *2*, 443–448.

Chong, S.Z., Evrard, M., and Ng, L.G. (2013). Lights, Camera, and Action: Vertebrate Skin Sets the Stage for Immune Cell Interaction with Arthropod-Vectored Pathogens. Front Immunol *4*, 286.

Chtanova, T., Schaeffer, M., Han, S.-J., van Dooren, G.G., Nollmann, M., Herzmark, P., Chan, S.W., Satija, H., Camfield, K., Aaron, H., et al. (2008). Dynamics of neutrophil migration in lymph nodes during infection. Immunity *29*, 487–496.

Combadiere, B., and Liard, C. (2011). Transcutaneous and intradermal vaccination. Hum Vaccin *7*, 811–827.

Daley, J.M., Thomay, A.A., Connolly, M.D., Reichner, J.S., and Albina, J.E. (2007). Use of Ly6G-specific monoclonal antibody to deplete neutrophils in mice. J Leukoc Biol *83*, 64–70.

Eidsmo, L., Allan, R., Caminschi, I., van Rooijen, N., Heath, W.R., and Carbone, F.R. (2009). Differential migration of epidermal and dermal dendritic cells during skin infection. The Journal of Immunology *182*, 3165–3172.

Gonzalez, R.J., Weening, E.H., Frothingham, R., Sempowski, G.D., and Miller, V.L. (2012). Bioluminescence imaging to track bacterial dissemination of *Yersinia pestis* using different routes of infection in mice. BMC Microbiol *12*, 147.

Guinet, F., and Carniel, E. (2003). A technique of intradermal injection of *Yersinia* to study *Y. pestis* physiopathology. Adv Exp Med Biol *529*, 73–78.

Hinnebusch, B.J. (2005). The evolution of flea-borne transmission in *Yersinia pestis*. Current Issues in Molecular Biology *7*, 197–212.

Hoopes, S.L., Willcockson, H.H., and Caron, K.M. (2012). Characteristics of multi-organ lymphangiectasia resulting from temporal deletion of calcitonin receptor-like receptor in adult mice. PLoS ONE *7*, e45261.

Kataru, R.P., Jung, K., Jang, C., Yang, H., Schwendener, R.A., Baik, J.E., Han, S.H., Alitalo, K., and Koh, G.Y. (2009). Critical role of CD11b+ macrophages and VEGF in inflammatory lymphangiogenesis, antigen clearance, and inflammation resolution. Blood *113*, 5650–5659.

Kobayashi, S.D., Voyich, J.M., Burlak, C., and DeLeo, F.R. (2005). Neutrophils in the innate immune response. Arch. Immunol. Ther. Exp. (Warsz.) *53*, 505–517.

Lancaster, K.Z., and Pfeiffer, J.K. (2010). Limited trafficking of a neurotropic virus through inefficient retrograde axonal transport and the type I interferon response. PLoS Pathog *6*, e1000791.

Lathem, W.W., Crosby, S.D., Miller, V.L., and Goldman, W.E. (2005). Progression of primary pneumonic plague: a mouse model of infection, pathology, and bacterial transcriptional activity. Proc Natl Acad Sci USA *102*, 17786–17791.

Leung, K.Y., Reisner, B.S., and Straley, S.C. (1990). YopM inhibits platelet aggregation and is necessary for virulence of *Yersinia pestis* in mice. Infect Immun *58*, 3262–3271.

Lin, L.C.W., Smith, S.A., and Tscharke, D.C. (2012). An intradermal model for vaccinia virus pathogenesis in mice. Methods Mol Biol *890*, 147–159.

Lorange, E.A., Race, B.L., Sebbane, F., and Hinnebusch, B.J. (2005). Poor vector competence of fleas and the evolution of hypervirulence in *Yersinia pestis*. J Infect Dis *191*, 1907–1912.

Lowe, D.E., Ernst, S.M.C., Zito, C., Ya, J., and Glomski, I.J. (2013). Bacillus anthracis has two independent bottlenecks that are dependent on the portal of entry in an intranasal model of inhalational infection. Infect Immun *81*, 4408–4420.

Mackinnon, M.J., Bell, A., and Read, A.F. (2005). The effects of mosquito transmission and population bottlenecking on virulence, multiplication rate and rosetting in rodent malaria. International Journal for Parasitology *35*, 145–153.

McDonald, B., Urrutia, R., Yipp, B.G., Jenne, C.N., and Kubes, P. (2012). Intravascular neutrophil extracellular traps capture bacteria from the bloodstream during sepsis. Cell Host Microbe *12*, 324–333.

Melton-Witt, J.A., Rafelski, S.M., Portnoy, D.A., and Bakardjiev, A.I. (2012). Oral infection with signature-tagged Listeria monocytogenes reveals organ-specific growth and dissemination routes in guinea pigs. Infect Immun *80*, 720–732.

Oberle, M., Balmer, O., Brun, R., and Roditi, I. (2010). Bottlenecks and the maintenance of minor genotypes during the life cycle of *Trypanosoma brucei*. PLoS Pathog *6*, e1001023.

Parkhill, J., Wren, B.W., Thomson, N.R., Titball, R.W., Holden, M.T., Prentice, M.B., Sebaihia, M., James, K.D., Churcher, C., Mungall, K.L., et al. (2001). Genome sequence of *Yersinia pestis*, the causative agent of plague. Nature *413*, 523–527.

Peters, N.C., Kimblin, N., Secundino, N., Kamhawi, S., Lawyer, P., and Sacks, D.L. (2009). Vector transmission of leishmania abrogates vaccine-induced protective immunity. PLoS Pathog *5*, e1000484.

Plaut, R.D., Kelly, V.K., Lee, G.M., Stibitz, S., and Merkel, T.J. (2012). Dissemination bottleneck in a murine model of inhalational anthrax. Infect Immun *80*, 3189–3193.

Prentice, M.B., and Rahalison, L. (2007). Plague. Lancet *369*, 1196–1207.

Price, P.A., Jin, J., and Goldman, W.E. (2012). Pulmonary infection by *Yersinia pestis* rapidly establishes a permissive environment for microbial proliferation. Proc Natl Acad Sci USA *109*, 3083–3088.

Pujol, C., and Bliska, J.B. (2003). The ability to replicate in macrophages is conserved between *Yersinia pestis* and *Yersinia pseudotuberculosis*. Infect Immun *71*, 5892–5899.

Pujol, C., and Bliska, J.B. (2005). Turning *Yersinia* pathogenesis outside in: subversion of macrophage function by intracellular yersiniae. Clin Immunol *114*, 216–226.

Schindelin, J., Arganda-Carreras, I., Frise, E., Kaynig, V., Longair, M., Pietzsch, T., Preibisch, S., Rueden, C., Saalfeld, S., Schmid, B., et al. (2012). Fiji: an open-source platform for biological-image analysis. Nat Methods *9*, 676–682.

Sebbane, F., Gardner, D., Long, D., Gowen, B.B., and Hinnebusch, B.J. (2005). Kinetics of disease progression and host response in a rat model of bubonic plague. Am J Pathol *166*, 1427–1439.

Sebbane, F., Jarrett, C.O., Gardner, D., Long, D., and Hinnebusch, B.J. (2006). Role of the *Yersinia pestis* plasminogen activator in the incidence of distinct septicemic and bubonic forms of flea-borne plague. Proc Natl Acad Sci USA *103*, 5526–5530.

Shannon, J.G., Hasenkrug, A.M., Dorward, D.W., Nair, V., Carmody, A.B., and Hinnebusch, B.J. (2013). *Yersinia pestis* subverts the dermal neutrophil response in a mouse model of bubonic plague. MBio *4*, e00170–13.

Spinner, J.L., Cundiff, J.A., and Kobayashi, S.D. (2008). *Yersinia pestis* type III secretion system-dependent inhibition of human polymorphonuclear leukocyte function. Infect Immun *76*, 3754–3760.

Spinner, J.L., Winfree, S., Starr, T., Shannon, J.G., Nair, V., Steele-Mortimer, O., and Hinnebusch, B.J. (2013). *Yersinia pestis* survival and replication within human neutrophil phagosomes and uptake of infected neutrophils by macrophages. J Leukoc Biol.

Thackray, A.M., and Field, H.J. (2000). Persistence of infectious herpes simplex virus type 2 in the nervous system in mice after antiviral chemotherapy. Antimicrob Agents Chemother *44*, 97–102.

Titball, R.W., Hill, J., Lawton, D.G., and Brown, K.A. (2003). *Yersinia pestis* and plague. Biochem Soc Trans. *31*, 104–107.

Trosky, J.E., Liverman, A.D.B., and Orth, K. (2008). *Yersinia* outer proteins: Yops. Cell Microbiol *10*, 557–565.

Troy, E.B., Lin, T., Gao, L., Lazinski, D.W., Camilli, A., Norris, S.J., and Hu, L.T. (2013). Understanding barriers to *Borrelia burgdorferi* dissemination during Infection using massively parallel sequencing. Infect Immun *81*, 2347–2357.

Walters, M.S., Lane, M.C., Vigil, P.D., Smith, S.N., Walk, S.T., and Mobley, H.L.T. (2012). Kinetics of uropathogenic *Escherichia coli* metapopulation movement during urinary tract infection. MBio *3*.

Ward, N.L., Loyd, C.M., Wolfram, J.A., Diaconu, D., Michaels, C.M., and McCormick, T.S. (2011). Depletion of antigen-presenting cells by clodronate liposomes reverses the psoriatic skin phenotype in KC-Tie2 mice. Br. J. Dermatol. *164*, 750–758.

Weiner, Z.P., and Glomski, I.J. (2012). Updating perspectives on the initiation of *Bacillus anthracis* growth and dissemination through its host. Infect Immun *80*, 1626–1633.

Zhang, P., Skurnik, M., Zhang, S.-S., Schwartz, O., Kalyanasundaram, R., Bulgheresi, S., He, J.J., Klena, J.D., Hinnebusch, B.J., and Chen, T. (2008). Human dendritic cell-specific intercellular adhesion molecule-grabbing nonintegrin (CD209) is a receptor for *Yersinia pestis* that promotes phagocytosis by dendritic cells. Infect Immun *76*, 2070–2079.

Zhou, D., Han, Y., and Yang, R. (2006). Molecular and physiological insights into plague transmission, virulence and etiology. Microbes Infect *8*, 273–284.

# CHAPTER 4: AN INTRADERMAL ROUTE OF BUBONIC PLAGUE REVEALS UNIQUE PATHOGEN ADAPTATIONS TO THE DERMIS

## 4.1. Overview

**Introduction**: Arthropods transmitting infectious diseases most likely inoculate pathogens in the dermis of mammals. Despite this, subcutaneous models of infection are broadly used in many fields, including *Yersinia pestis* pathogenesis. We compared an intradermal with a subcutaneous model of *Y. pestis* during bubonic plague in mice to determine if the route of inoculation affects disease progression.

**Methods:** We inoculated mice using each route, assessed survival, and obtained bacterial burden in different tissues to assess the kinetics of infection. In addition, attenuation of a deletion mutant of *yapH* was tested to determine phenotype changes with each model.

**Results:** We found that the size of the inoculum influenced mouse survival after intradermal inoculation but not after subcutaneous inoculation. In addition, intradermal inoculation resulted in faster kinetics of infection. Moreover, the *yapH* deletion mutant we tested was attenuated in the intradermal but not subcutaneous model of infection.

**Conclusions:** Our data indicate that the more biologically relevant intradermal model of bubonic plague shows important differences in multiple aspects of infection when compared with a subcutaneous model. We believe our findings

might have important implications for the study of vector-borne pathogens, skin immunology, and vaccine development.

### 4.2. Introduction

As a pathogen disseminates inside a host, it must travel through multiple tissues to reach distant sites. These tissues are in themselves microenvironments with defined immunological characteristics that serve as barriers to prevent spread. Epithelial tissues, such as the skin, are the first barriers an invader has to break in order to penetrate into deeper organs. The skin epithelium is an active immune site that can elicit an effective immune response against many invaders. However, some pathogens can overcome these immune responses and are able to disseminate to deeper tissues and cause disease.

Based on its histological architecture, the skin can be divided into three main layers: epidermis, dermis, and subcutaneous space (also known as hypodermis) (Teunissen et al., 2012). Each layer encompasses unique immunological characteristics that we are just beginning to understand (Nestle et al., 2009). The epidermis is the outermost layer and constitutes a physical barrier that pathogens must cross to enter the body. This barrier can be surpassed by the mechanical action of a bite from a blood feeding arthropod (Frischknecht, 2007). Arthropods that carry a pathogen and that can actively transmit it to a host are termed vectors.

The dermis is generally the starting site for natural infections with vector-borne pathogens (Belkaid et al., 1998; Chong et al., 2013; Choumet et al., 2012; Sebbane et al., 2006). These pathogens must adapt quickly and abrogate the immune responses of the dermis for infection to be established. Whether vector-

borne pathogens have special adaptations that define their interactions with the host in this specific layer of the skin is unknown.

*Yersinia pestis* is a Gram-negative bacterium and the causative agent of plague. This highly virulent pathogen was responsible for major pandemics in history such as The Black Death (Bos et al., 2011). *Y. pestis* survives in animal reservoirs in many parts of the world, including the United States (Butler, 2013). Human populations that live in close proximity to plague foci are at high risk of infection. Bubonic plague is the most prevalent form of the disease and occurs after bacterial inoculation into the skin, typically by a flea vector (Wimsatt and Biggins, 2009). From the skin, *Y. pestis* disseminates to draining lymph nodes (LNs) via lymphatic vessels (see Chapter 3) and then to deeper organs through the bloodstream (Sebbane et al., 2005). Systemic dissemination results in severe organ failure, septicemia, and death.

Models of infection that target the subcutaneous (SC) space are broadly used in plague research (Abu Khweek et al., 2010; Demeure et al., 2012; Lenz et al., 2011; Oyston et al., 2000) as this is a fairly easy tissue to target. However, the dermis is strongly suggested to be the layer of the skin probed by fleas during transmission (Hinnebusch, 2005; Sebbane et al., 2006). In comparison with SC models, ID inoculations require more dexterity and can be more challenging to implement in biosafety level three facilities, which are mandatory when handling fully virulent strains of *Y. pestis*. In this study, we followed the progression of infection after ID and SC inoculation to determine if inoculation site impacted the infection. We found important differences in the disease progression of wild type

(WT) *Y. pestis*. In addition, we also found a mutant strain that is attenuated following ID inoculation, but not after SC inoculation. These findings are relevant for the understanding of *Y. pestis* pathogenesis and host responses to different inoculation routes. In addition, this study sheds light into processes regarding antigen delivery to LNs. For this reason, our findings might be relevant to the implementation of new vaccine strategies.

## 4.3. Methods

### *4.3.1. Bacterial cultures and strains*

Fully virulent *Y. pestis* CO92 was used in all the experiments of this study (Doll et al., 1994; Parkhill et al., 2001). Bacteria were streaked on brain and heart infusion (BHI, BD Biosciences, Bedford MA) agar plates from frozen stocks and incubated at 26°C for 48 h. Liquid cultures in BHI broth were incubated for 15 h at 26°C with aeration. The procedures employed to construct the isogenic set of tagged strains used in the dissemination assays are described elsewhere (see Chapter 3)(Walters et al., 2012). Briefly, *Y. pestis* was tagged with an oligonucleotide signature tag (along with a kanamycin resistant cassette), which was inserted in a neutral site in the bacterial chromosome at the Tn7 *att* site (Choi et al., 2005). We generated 10 *Y. pestis* tagged strains, which have similar growth and virulence characteristics compared to those of un-tagged bacteria. For the dose dependent survival assays (DDSA) an un-tagged strain was used. The Δ*yapH* strain has an in-frame deletion and was constructed with the λ Red recombination system, as described somewhere else (Datsenko and Wanner, 2000; Lathem et al., 2007). Briefly, Briefly, the upstream flanking region of *yapH*

was amplified with primers DNA134/DNA135 (5'- GCA TGA TTA CAG CCA ATC CCA CA-3' and 5'-GAA GCA GCT CCA GCC TAC ACC ATA TAT AGC CTT AAC AAA TTT TTA ATT TGT CAA TTA AGT TG-3', respectively) and the downstream flanking region was amplified with DNA136/DNA137 (5'-GGT CGA CGG ATC CCC GGA ATA ATT TTA TCG TCA GGT AAT TAA CCA CTA ACG ACA-3' and 5'-CGC TTC TTT GGC GTA TCA CAT-3', respectively). The primers DNA135 and DNA136 add recognition sites for FLP recombinase to their respective PCR products. These flanking regions were then joined with a kanamycin resistance cassette ($Kan^R$) by overlap extension PCR to obtain the resulting *yapH*5'-FRT-$Kan^R$-FRT-*yapH*3' product. Wild type *Y. pestis* expressing the λ Red recombinase gene (from pWL204) was transformed with this fragment. $Kan^R$ colonies were streaked on BHI with 10% sucrose to cure pWL204. The $Kan^R$ was removed with the FRT recombinase (from pLH29). Deletion of *yapH* was confirmed by PCR.

*4.3.2. Animal inoculations*

Female C57BL/6J mice (six-to-eight week-old, Jackson Laboratory, Bar Harbor, ME) were inoculated with *Y. pestis* after injection of a ketamine/xylazine mix. Intradermal (ID) inoculations are described elsewhere (see Chapter 3). Briefly, ~200 colony forming units (CFU) in 2 µL were injected into the dorsal leaflet of the ear pinna with the aid of a Pump11 Elite syringe pump (Harvard Apparatus, Holliston, MA). The same procedure was used for the subcutaneous (SC) inoculations except that mice were injected in the ventral cervical region (2 µL were also used for this route). Organs were harvested at different time points, homogenized, diluted and plated on BHI agar to enumerate bacteria in each organ.

For the ID inoculations, the superficial parotid lymph nodes were harvested (Van den Broeck et al., 2006). For the SC inoculations, the superficial cervical lymph nodes were harvested.

For the assay to determine the presence of a bottleneck, 9 of the 10 tagged strains were grown in BHI broth with 25 μg/mL kanamycin. After standardizing all cultures based on optical density at 600 nm ($OD_{600}$), equal amounts of each culture were mixed in a tube. The mix was serially diluted in PBS to obtain an inoculum equivalent to ~200 CFU. The tenth tagged strain was omitted from the mix so it could be used as a negative control. Recovered bacteria were used for DNA extraction and this DNA was then used as a probe for Southern dot blot (see Chapter 3). Statistical analysis was performed using a Mann Whitney test calculated by GraphPad Prism version 4.0c for Macintosh (GraphPad Software, La Jolla, CA). We established statistical significance at $p < 0.05$.

## 4.4. Results

### *4.4.1. The ID inoculations result in faster kinetics but lower mortality rates when compared with SC inoculations*

We recently reported the presence of a bottleneck during ID but not SC inoculations of *Y. pestis* in mice (see Chapter 3). We hypothesized that inoculations into these layers of the skin would also affect disease progression. To test this, mice were inoculated ID or SC, and bacterial loads in LNs and spleens at 48 hours post infection (hpi) were compared (Figure 4.1A). The median value of bacterial burden in LNs of mice inoculated ID was ~100-fold higher than the median value of bacterial burden in LNs of mice inoculated SC. This difference was

determined to be statistically significant (Mann-Whitney test, p = 0.0002). Bacteria burdens in the spleen, an organ used to assess systemic dissemination, showed an even larger difference between groups. The median value of bacterial burden in spleens from mice inoculated ID was ~$10^6$-fold higher than in mice inoculated SC. This difference also was determined to be statistically significant (Mann-Whitney test, p = 0.0001). From this, we predicted that the inoculation route would also impact survival. A dose dependent survival assay (DDSA) was used to determine differences in survival times for each of the inoculation routes. A DDSA can also reveal how these differences are influenced by the size of the inocula. Mice were inoculated ID with a low [~7 colony forming units (CFU)], medium (~71 CFU) or high (~710 CFU) inoculum and survival was monitored during the following 14 days. The survival percentage of the mice inoculated with the low inoculum was 67% (Figure 4.1B). Survival rates of mice inoculated with the medium and high inocula were 25% and 0%, respectively. For the whole group, death was first observed at day 2. Most mice died between days two and four, with the exception of one mouse from the low inoculum group, which died on day 11. For inoculation by the SC route, the low, medium, and high inocula were ~24 CFU, ~240 CFU, and ~2400 CFU, respectively. No mice inoculated SC survived (Figure 4.1C). With the exception of one mouse in the high inoculum group that died at day 3.5, all mice died between days 4.5 and 7. These data indicate that the route of inoculation has an effect on the kinetics of infection. In addition, they suggest that *Y. pestis* survival is less compromised in response to ID inoculations in comparison with SC

inoculations. However, mouse survival after ID inoculation, but not after SC inoculation, appeared to be strictly linked to inoculum size.

*4.4.2. A deletion mutant lacking a putative autotransporter protein is attenuated when inoculated ID but not SC*

YapH is a 3705-amino acid putative autotransporter protein located in a pathogenicity island of *Y. pestis* (Deng et al., 2002; Yen et al., 2007). It has 21% identity in sequence with a gene that encodes an adhesin autotransporter of *Haemophilus influenzae* (Yen et al., 2007), but its function in *Y. pestis* is unknown. The expression of *yapH* is upregulated *in vivo* during bubonic and pneumonic plague (Lenz et al., 2011), a measure that is often interpreted as indicating a role during infection. Thus, we predicted YapH to be important for *Y. pestis* pathogenesis during bubonic plague. To test this, we inoculated mice with wild type (WT) or a *yapH* deletion mutant (Δ*yapH*) strain using a SC route of inoculation. We compared bacterial loads in LNs and spleens from mice inoculated with each strain at 36, 60, and 72 hpi. This allowed us to evaluate early and late stages of infection based on the kinetics for our SC model of inoculation (Lane et al., 2013; Weening et al., 2011). None of the tissues showed a significant difference in bacterial loads between mice inoculated with WT or Δ*yapH* strains, suggesting YapH does not play a critical role during bubonic plague (Figure 4.2A). Because we noted that the formation of a bottleneck to dissemination of *Y. pestis* to the LN was only observed following *Y. pestis* inoculation into the dermis (see Chapter 3), we decided to test whether the Δ*yapH* strain would show the same phenotype when inoculated ID. We used time points relevant to the kinetics for this route (24 and 48 hpi) and, in

addition to LNs and spleens, we also harvested ears (site of inoculation). At 24 hpi, LNs from Δ*yapH*-inoculated mice showed a slightly lower median than WT-inoculated mice, but this difference was not statistically significant (Figure 4.2B). However, at 48 hpi, a statistically significant difference was observed: lower burdens were observed in LNs, spleens and ears of mice inoculated with Δ*yapH* in comparison to mice inoculated with the WT strain (Figure 4.2C). Overall, these data suggest that the inoculation route can affect the dissemination or colonization of a deletion mutant (in this case Δ*yapH*) revealing attenuation in one route (ID) but not in the other (SC).

### *4.4.3. A SC route of inoculation reveals a bottleneck in bacterial dissemination from LN to blood*

The use of oligonucleotide-tagged strains was used in our laboratory to identify a bottleneck to draining LNs following ID inoculation (see Chapter 3). We found that only a fraction of the tagged strains were present in LNs suggesting the bottleneck impacted bacterial dissemination from skin to LN. We also found that this bottleneck was less prevalent after SC inoculations, as most of the tagged strains were found in LNs when using this route. Because LNs of mice inoculated SC show most of the tagged strains (Figure 4.3A) we have enough tagged strains in that tissue to determine whether or not a bottleneck exists further downstream in the dissemination from LN to blood. Mice were inoculated SC with the nine tagged strains and LNs and spleens were harvested at 48 hpi. Seven out of eight mice had bacteria in the spleen, and six of these mice had fewer tagged strains in the spleens than in the LNs (Figure 4.3B). The number of strains present in the LN but

absent in the spleen ranged from one to seven. Interestingly, we observed two mice with tagged strains in the spleen that were not present in the LN. One of these had no detectible bacteria in the LN, but had two tagged strains present in the spleen. The second mouse had one strain in the spleen that was absent in the LN. Overall, these data indicate the existence of a bottleneck in the dissemination of *Y. pestis* from the LN into the bloodstream following a SC inoculation.

### 4.5. Discussion

Only in recent years have we begun to understand the significance of the differences of *in vivo* over *in vitro* approaches to study host-pathogen interactions. This has resulted in the development of new animal models with a goal of mimicking natural infections as closely as possible. However, a big limitation of implementing animal models is how little it is known about what aspects of a natural infection truly affect disease progression. In this study, we report important differences in progression of bubonic plague when comparing the common SC route and the more biologically relevant ID route.

We observed that bacteria are able to colonize the host more efficiently after ID than after SC inoculations. This might be due to differences in the density and the anatomy of lymphatic vessels in each layer of the skin. The dermis is rich in terminal lymphatic vessels (O'Mahony et al., 2004). These vessels, absent in the epidermis and SC space, readily take up lymph and antigen due to their high permeability resulting from the lack of smooth muscle cells and a basal membrane (Shayan et al., 2006). The anatomy of terminal lymphatic vessels can explain why, in comparison to SC injections, dyes to map lymphatic vessels for tumor detection

are detected faster in LNs after ID injections (Kersey et al., 2001). In addition to lymphatic vessel physiology, it has also been suggested that the dermis is subject to high fluid pressures (O'Mahony et al., 2004). High pressures are important to drain fluid from the dermis to prevent edema and could also contribute to more efficient movement of *Y. pestis* to the LNs. This is especially true if, as we have previously suggested, *Y. pestis* travels to LNs freely with the flow of lymph (see Chapter 3). As opposed to terminal lymphatic vessels, collecting lymphatics possess circumferential smooth muscle cells and a basement membrane (Shayan et al., 2006). These two elements restrict the access of particles into the lumen and make them less efficient in antigen uptake. Interestingly, collecting lymphatics are found in the SC layer of the skin and not in the dermis. Thus, this suggests that *Y. pestis* cannot access LNs through lymphatic vessels when deposited in the SC space as easily as when deposited into the dermis.

Intriguingly, we found that while the kinetics of infection are faster when *Y. pestis* is delivered into the dermis, some mice survive after ID inoculation but none after SC inoculation. This is more evident when low inocula are used. Most mice survived after inoculation of 7 CFU in the dermis and none after inoculation of a very similar dose (24 CFU) in the SC space. We recently reported the formation of a bottleneck during ID inoculation of *Y. pestis* and its abrogation during SC inoculation (see Chapter 3). We reported in the same study that a small percentage of ID inoculated mice did not show any bacteria in LNs and spleens, and we interpreted this as an indication of a highly efficient bottleneck. It would be expected that the effects of a barrier (i.e. bottleneck) that limits dissemination to

LNs are stronger when few bacteria are inoculated, and weaker when larger numbers of bacteria are used. Consequently, all mice inoculated ID with the higher inoculum (~710 CFU) died and most of the mice inoculated with the lowest inoculum (~7 CFU) survived. As opposed to the dermis, the SC layer of the skin possesses a very limited number of resident cells of the immune response (Combadiere and Liard, 2011). In addition, the SC space is less vascularized than the dermis and, thus, access to it by infiltrating immune cells might be less efficient (Combadiere and Liard, 2011; Teunissen et al., 2012). We speculated that a less efficient immune response might account for abrogation of the bottleneck after SC inoculation (see Chapter 3). A less efficient immune response could allow for local bacterial replication in the SC space, resulting in more bacteria moving to the LNs.

Another observation we made is the attenuation of a deletion mutant after ID but not SC inoculation. We believe this might be due to a role of YapH in bacterial adaptation to the immune response of the dermis, where different insults than those found in the SC space are faced. While many aspects of the anatomy and physiology of the different layers of the skin are understood, their effects on the immune response to pathogens are not clear. However, studies in the cancer and vaccine development fields have shed some light on this. Bonnotte and collaborators found that injection of a tumorigenic cell line results in tumor formation after SC but not ID injection in rats (Bonnotte et al., 2003). In another study, injection of a virus like particle to test its immunogenicity found more LN involvement and cellular response after ID injections when compared with SC delivery (Cubas et al., 2009). In addition, results favoring the use of ID, and not SC,

inoculation have been reported in experiments using an HIV1 antigen in vaccine development against this virus (Liard et al., 2011). Much less work has been done comparing routes of inoculation during cutaneous infections caused by vector-borne pathogens. One exception is the work done with *Leishmania* parasites where the use of an ID route was strongly suggested to recreate disease progression more accurately than a SC route (Belkaid et al., 1998). These studies indicate that the different layers of the skin vary considerably in the immune responses they can elicit. Differences in the immune response might account for the different phenotypes the Δ*yapH* strain showed after inoculation in each layer of the skin. In addition to insights into the function of *yapH*, our experiments might have important implications for other studies in bacterial pathogenesis. Our experiments suggest that when testing mutants, unless using the appropriate model, not observing a phenotype might simply be the result of confounding effects of the model itself.

Lastly, while we support the use of an ID model of inoculation, we believe the SC model should be considered as a tool to help reveal the function of a bacterial gene or of a specific component of the immune response. An example of an advantage of using the SC model as a tool is the observation of a bottleneck in bacterial dissemination from LN to blood. In the presence of a strong bottleneck after ID inoculation, only a few tagged strains survive in the LN. Consequently it is difficult to determine if a bottleneck occurs in the dissemination from LN to blood because very few strains are present in the LN. The SC inoculation route allowed us to have a higher number of tagged strains in the LN. This made it possible to assess whether some of these tagged strains were lost as disease progresses into

the bloodstream. A caveat is that we do not know with certainty how many bacteria of each tagged strain inoculated SC reach the LNs. Regardless, we know that many of the strains that reach the LN compartment are not found systemically. We believe this is enough evidence to support the existence of a bottleneck from LN to blood. Because the strains that were absent in the spleens were present in the LNs, the bottleneck is not caused by elimination of strains in the LN. Most likely, the bottleneck is caused by restricted movement of bacteria from LN into the bloodstream. Interestingly, and contrary to what we observed during ID-induced bottleneck in previous studies (see Chapter 3), some strains were found systemically and not in LNs. This could be due to (1) direct movement of bacteria from the SC site of inoculation into blood, or (2) killing of the remaining members of these strains in the lymph node after a fraction of them escaped to the bloodstream. More experiments would be needed to clarify this aspect of the SC model.

Overall, we believe that studies that explore the skin in an infection context are extremely valuable for fields as diverse as vector borne pathogenesis, cutaneous immunology, and vaccine development. For vector borne infections, including bubonic plague, well-established models might need to be revisited and new models might need to be considered. Findings that derive from well-established models that have not been appropriately tested might reflect confounding effects of the model rather than biologically relevant observations.

## 4.6. Figure and Tables

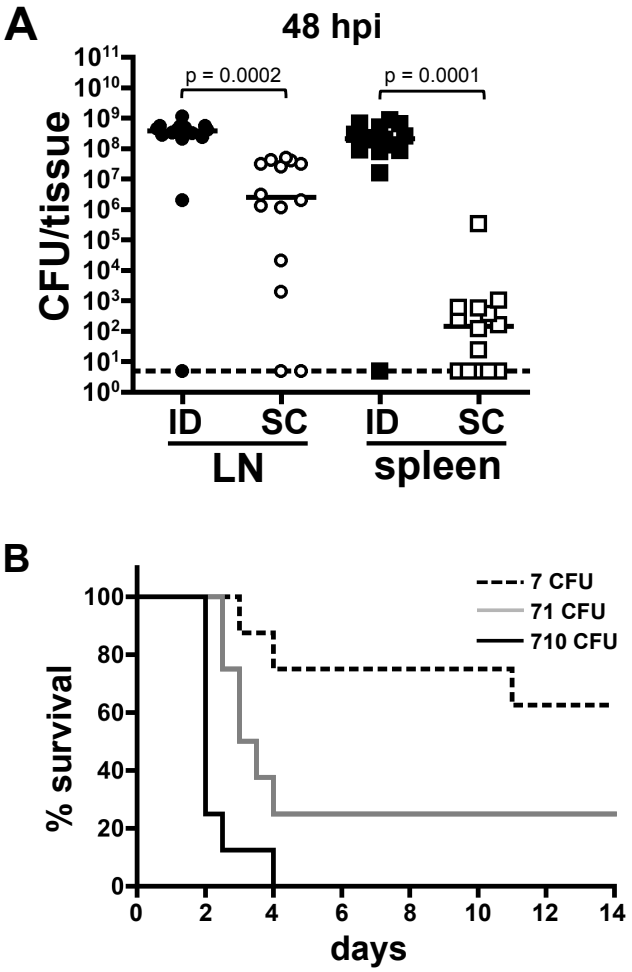

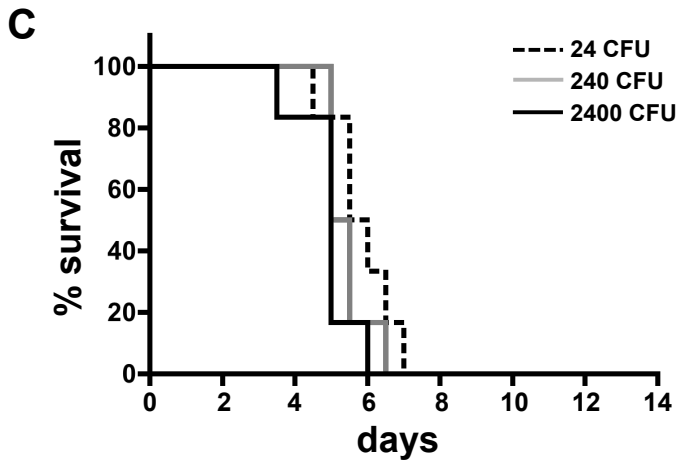


**Figure 4.1. Kinetics of infection and survival in mice inoculated ID and SC.** (A) CFU from LNs (circles) and spleens (squares) harvested 48 hours after ID (black symbols) or SC (white symbols) inoculation. Each symbol represents the number of CFU obtained from a tissue. The horizontal lines depict the median of the group. Statistically significant differences between groups were determined by a Mann-Whitney test, establishing significance at $p < 0.05$. The dotted line shows the limit of detection. (B and C) DDSA of mice inoculated ID (B) or SC (C) using three different inocula. A low inoculum is represented with a dotted line, a medium inoculum with a gray continuous line, and a high inoculum with a black continuous line. Each line depicts the percentage of mice surviving in a group (n=8 per inoculum for ID, n=6 per inoculum for SC) at different time points (in days).

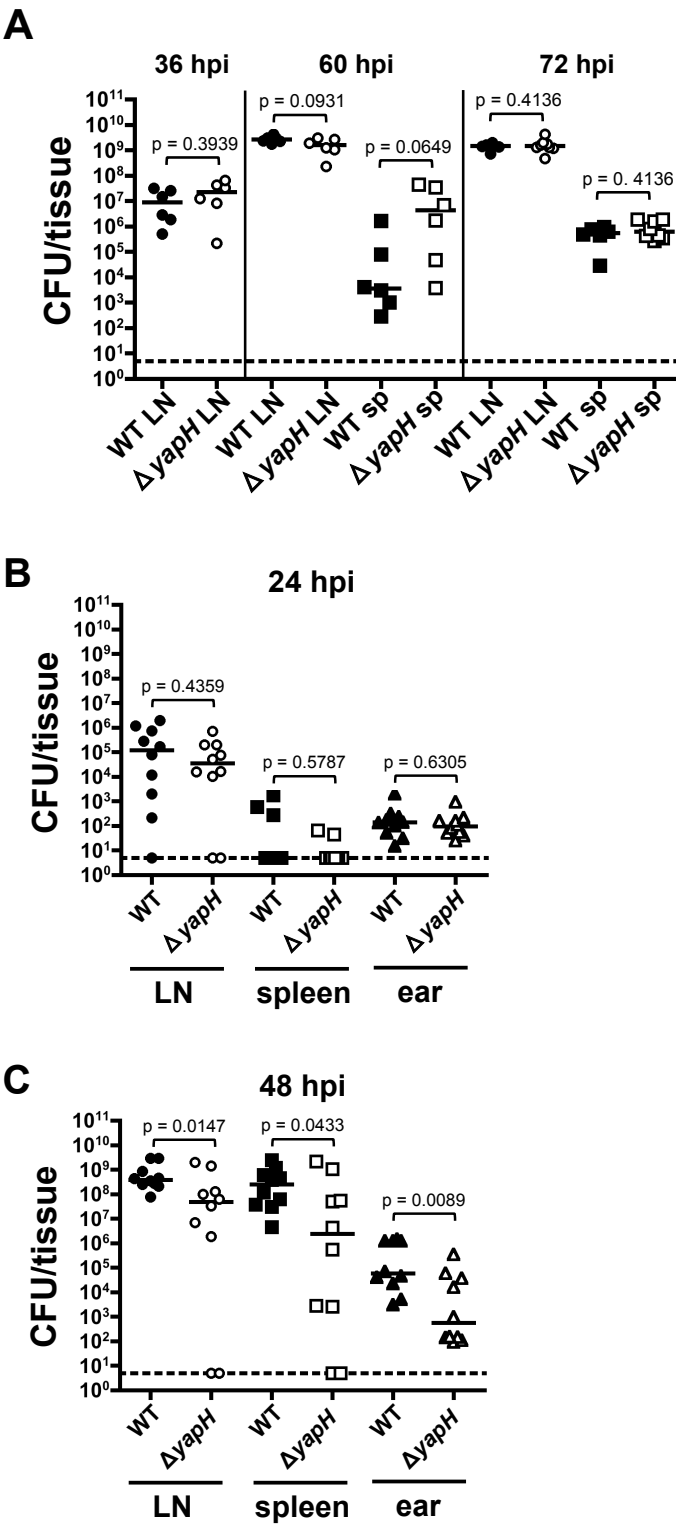


**Figure 4.2. Kinetics of infection of a deletion mutant (*ΔyapH*) after ID and SC inoculation.**

(A) CFU from LNs (circles) and spleens (squares) harvested at 36, 60, and 72 hours after SC inoculation with WT (black symbols) or Δ*yapH* (white symbols) *Y.*

*pestis*. (B and C) CFU from LNs (circles), spleens (squares), and ears (triangles) harvested at 24 (B) and 48 (C) hours after ID inoculation with WT (black symbols) or Δ*yapH* (white symbols) *Y. pestis*. Each symbol represents the number of CFU obtained from a tissue. The horizontal lines depict the median of the group. Statistically significant differences between groups were determined by a Mann-Whitney test, establishing significance at $p < 0.05$. The dotted line shows the limit of detection.

**A**

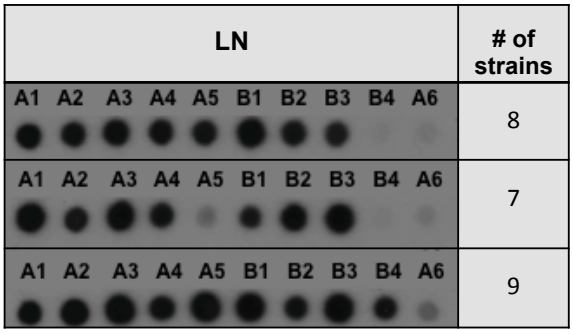


**B**

| | LN | | | | | | | | | | spleen | | | | | | | | | |
|---|---|---|---|---|---|---|---|---|---|---|---|---|---|---|---|---|---|---|---|---|
| mouse (n=8) | A1 | A2 | A3 | A4 | A5 | B1 | B2 | B3 | B4 | A6 | A1 | A2 | A3 | A4 | A5 | B1 | B2 | B3 | B4 | A6 |
| 1 | ■ | ■ | ■ | ■ | ■ | ■ | ■ | ■ | ■ | | ■ | ■ | ■ | ■ | ■ | ■ | ■ | ■ | ■ | |
| 2 | | | X | | X | | | | | | | | ■ | | ■ | | | | | |
| 3 | ■ | ■ | ■ | ■ | ■ | ■ | | ■ | ■ | | + | + | + | + | ■ | + | | + | + | |
| 4 | | ■ | ■ | ■ | | X | ■ | ■ | ■ | | | ■ | ■ | ■ | | ■ | + | ■ | + | |
| 5 | ■ | ■ | ■ | ■ | ■ | ■ | ■ | ■ | ■ | | ■ | ■ | ■ | ■ | ■ | + | + | + | + | |
| 6 | ■ | ■ | ■ | ■ | ■ | ■ | | ■ | ■ | | ■ | + | + | ■ | + | ■ | | ■ | + | |
| 7 | ■ | | ■ | ■ | ■ | | ■ | ■ | | | + | | + | + | + | | + | + | | |
| 8 | ■ | ■ | ■ | ■ | ■ | ■ | ■ | ■ | ■ | | ■ | ■ | ■ | ■ | ■ | ■ | ■ | ■ | + | |

**Figure 4.3. A bottleneck from LN to spleen revealed after SC inoculation.**
(A) Southern dot blot of bacterial DNA obtained from the LNs of mice inoculated SC with nine oligonucleotide tagged strains of *Y. pestis*. Each row depicts the results from a single mouse. Each strain is identified (A1 to 5 and B1 to 4; A6 was used as a negative control). (B) Results of Southern dot blots analogous to those shown in (A) are represented pictorially. Tagged strains are shown as present (gray) or absent (white). The "+" symbol represents tagged strains present in LNs that are absent in spleens. The "X" symbol represents tagged strains absent in LNs and present in spleens.

## REFERENCES


Abu Khweek, A., Fetherston, J.D., and Perry, R.D. (2010). Analysis of HmsH and its role in plague biofilm formation. Microbiology (Reading, Engl) *156*, 1424–1438.

Belkaid, Y., Kamhawi, S., Modi, G., Valenzuela, J., Noben-Trauth, N., Rowton, E., Ribeiro, J., and Sacks, D.L. (1998). Development of a natural model of cutaneous leishmaniasis: powerful effects of vector saliva and saliva preexposure on the long-term outcome of *Leishmania major* infection in the mouse ear dermis. J Exp Med *188*, 1941–1953.

Bonnotte, B., Gough, M., Phan, V., Ahmed, A., Chong, H., Martin, F., and Vile, R.G. (2003). Intradermal injection, as opposed to subcutaneous injection, enhances immunogenicity and suppresses tumorigenicity of tumor cells. Cancer Research *63*, 2145–2149.

Bos, K.I., Schuenemann, V.J., Golding, G.B., Burbano, H.A., Waglechner, N., Coombes, B.K., McPhee, J.B., DeWitte, S.N., Meyer, M., Schmedes, S., et al. (2011). A draft genome of *Yersinia pestis* from victims of the Black Death. Nature *478*, 506–510.

Butler, T. (2013). Plague Gives Surprises in the First Decade of the 21st Century in the United States and Worldwide. American Journal of Tropical Medicine and Hygiene *89*, 788–793.

Choi, K.-H., Gaynor, J.B., White, K.G., Lopez, C., Bosio, C.M., Karkhoff-Schweizer, R.R., and Schweizer, H.P. (2005). A Tn7-based broad-range bacterial cloning and expression system. Nat. Methods *2*, 443–448.

Chong, S.Z., Evrard, M., and Ng, L.G. (2013). Lights, camera, and action: vertebrate skin sets the stage for immune cell interaction with arthropod-vectored pathogens. Front Immunol *4*, 286.

Choumet, V., Attout, T., Chartier, L., Khun, H., Sautereau, J., Robbe-Vincent, A., Brey, P., Huerre, M., and Bain, O. (2012). Visualizing non infectious and infectious *Anopheles gambiae* blood feedings in naive and saliva-immunized mice. PLoS ONE *7*, e50464.

Combadiere, B., and Liard, C. (2011). Transcutaneous and intradermal vaccination. Hum Vaccin *7*, 811–827.

Cubas, R., Zhang, S., Kwon, S., Sevick-Muraca, E.M., Li, M., Chen, C., and Yao, Q. (2009). Virus-like particle (VLP) lymphatic trafficking and immune response generation after immunization by different routes. J. Immunother. *32*, 118–128.

Datsenko, K.A., and Wanner, B.L. (2000). One-step inactivation of chromosomal genes in *Escherichia coli* K-12 using PCR products. Proc Natl Acad Sci USA *97*, 6640–6645.

Demeure, C.E., Blanchet, C., Fitting, C., Fayolle, C., Khun, H., Szatanik, M., Milon, G., Panthier, J.-J., Jaubert, J., Montagutelli, X., et al. (2012). Early systemic bacterial dissemination and a rapid innate immune response characterize genetic resistance to plague of SEG mice. J Infect Dis *205*, 134–143.

Deng, W., Burland, V., Plunkett, G., Boutin, A., Mayhew, G.F., Liss, P., Perna, N.T., Rose, D.J., Mau, B., Zhou, S., et al. (2002). Genome sequence of *Yersinia pestis* KIM. J Bacteriol *184*, 4601–4611.

Doll, J.M., Zeitz, P.S., Ettestad, P., Bucholtz, A.L., Davis, T., and Gage, K. (1994). Cat-transmitted fatal pneumonic plague in a person who traveled from Colorado to Arizona. American Journal of Tropical Medicine and Hygiene *51*, 109–114.

Frischknecht, F. (2007). The skin as interface in the transmission of arthropod-borne pathogens. Cell Microbiol *9*, 1630–1640.

Hinnebusch, B.J. (2005). The evolution of flea-borne transmission in *Yersinia pestis*. Current Issues in Molecular Biology *7*, 197–212.

Kersey, T.W., Van Eyk, J., Lannin, D.R., Chua, A.N., and Tafra, L. (2001). Comparison of intradermal and subcutaneous injections in lymphatic mapping. J. Surg. Res. *96*, 255–259.

Lane, M.C., Lenz, J.D., and Miller, V.L. (2013). Proteolytic processing of the *Yersinia pestis* YapG autotransporter by the omptin protease Pla and the contribution of YapG to murine plague pathogenesis. Journal of Medical Microbiology *62*, 1124–1134.

Lathem, W.W., Price, P.A., Miller, V.L., and Goldman, W.E. (2007). A plasminogen-activating protease specifically controls the development of primary pneumonic plague. Science *315*, 509–513.

Lenz, J.D., Lawrenz, M.B., Cotter, D.G., Lane, M.C., Gonzalez, R.J., Palacios, M., and Miller, V.L. (2011). Expression during host infection and localization of *Yersinia pestis* autotransporter proteins. J Bacteriol *193*, 5936–5949.

Liard, C., Munier, S., Arias, M., Joulin-Giet, A., Bonduelle, O., Duffy, D., Shattock, R.J., Verrier, B., and Combadiere, B. (2011). Targeting of HIV-p24 particle-based vaccine into differential skin layers induces distinct arms of the immune responses. Vaccine *29*, 6379–6391.

Nestle, F.O., Di Meglio, P., Qin, J.-Z., and Nickoloff, B.J. (2009). Skin immune sentinels in health and disease. Nat Rev Immunol *9*, 679–691.

O'Mahony, S., Rose, S.L., Chilvers, A.J., Ballinger, J.R., Solanki, C.K., Barber, R.W., Mortimer, P.S., Purushotham, A.D., and Peters, A.M. (2004). Finding an optimal method for imaging lymphatic vessels of the upper limb. Eur. J. Nucl. Med. Mol. Imaging *31*, 555–563.

Oyston, P.C., Dorrell, N., Williams, K., Li, S.R., Green, M., Titball, R.W., and Wren, B.W. (2000). The response regulator PhoP is important for survival under conditions of macrophage-induced stress and virulence in *Yersinia pestis*. Infect Immun *68*, 3419–3425.

Parkhill, J., Wren, B.W., Thomson, N.R., Titball, R.W., Holden, M.T., Prentice, M.B., Sebaihia, M., James, K.D., Churcher, C., Mungall, K.L., et al. (2001). Genome sequence of *Yersinia pestis*, the causative agent of plague. Nature *413*, 523–527.

Sebbane, F., Gardner, D., Long, D., Gowen, B.B., and Hinnebusch, B.J. (2005). Kinetics of disease progression and host response in a rat model of bubonic plague. Am J Pathol *166*, 1427–1439.

Sebbane, F., Jarrett, C.O., Gardner, D., Long, D., and Hinnebusch, B.J. (2006). Role of the *Yersinia pestis* plasminogen activator in the incidence of distinct septicemic and bubonic forms of flea-borne plague. Proc Natl Acad Sci USA *103*, 5526–5530.

Shayan, R., Achen, M.G., and Stacker, S.A. (2006). Lymphatic vessels in cancer metastasis: bridging the gaps. Carcinogenesis *27*, 1729–1738.

Teunissen, M.B.M., Haniffa, M., and Collin, M.P. (2012). Insight into the immunobiology of human skin and functional specialization of skin dendritic cell subsets to innovate intradermal vaccination design. Curr Top Microbiol Immunol *351*, 25–76.

Van den Broeck, W., Derore, A., and Simoens, P. (2006). Anatomy and nomenclature of murine lymph nodes: Descriptive study and nomenclatory standardization in BALB/cAnNCrl mice. Journal of Immunological Methods *312*, 12–19.

Walters, M.S., Lane, M.C., Vigil, P.D., Smith, S.N., Walk, S.T., and Mobley, H.L.T. (2012). Kinetics of uropathogenic Escherichia coli metapopulation movement during urinary tract infection. MBio *3*.

Weening, E.H., Cathelyn, J.S., Kaufman, G., Lawrenz, M.B., Price, P., Goldman, W.E., and Miller, V.L. (2011). The dependence of the *Yersinia pestis* capsule on pathogenesis is influenced by the mouse background. Infect Immun *79*, 644–652.

Wimsatt, J., and Biggins, D.E. (2009). A review of plague persistence with special emphasis on fleas. Journal of Vector Borne Diseases *46*, 85–99.

Yen, Y.T., Karkal, A., Bhattacharya, M., Fernandez, R.C., and Stathopoulos, C. (2007). Identification and characterization of autotransporter proteins of Yersinia pestis KIM. Mol. Membr. Biol. *24*, 28–40.

# CHAPTER 5: DISCUSSION

## 5.1. Summary of main findings

The traditional approach to study *Y. pestis* dissemination includes harvesting organs from infected animals to establish bacterial burden at a determined time point. In Chapter 2, I described a non-invasive approach to track bacterial dissemination in mice. With this technique, mice are inoculated with bioluminescent *Y. pestis,* and the presence of the bacteria in multiple organs can be assessed by bioluminescence imaging technology. The non-invasive nature of this *in vivo* imaging approach allows for the use of the same group of mice over different time points. This results in accurate observations of the progression of infection and strong statistical power to analyze them. We showed that this technique works efficiently for intradermal and subcutaneous models of bubonic plague, as well as for an intranasal model for pneumonic plague. In addition, we showed that bioluminescent imaging technology is suitable for characterizing *Y. pestis* mutants with defects in dissemination or colonization (Gonzalez et al., 2012).

One large gap in the field is an understanding of how *Y. pestis* interacts with the host during dissemination. In Chapter 3, I described important events that occur upon inoculation and that have the potential to define the outcome of infection. These events include formation of a bottleneck that restricts the passage of bacteria as they disseminate form the skin to lymph nodes. I also described host-pathogen interactions of *Y. pestis* throughout infection, at a cellular level, by

microscopy imaging. This approach, along with neutrophil depletion, allowed us to uncover that neutrophils control bacterial growth in the skin. In addition, we showed bacterial interaction with both neutrophils and platelets in the bloodstream.

Finally, in Chapter 4 I described how the use of an intradermal model of infection might be more relevant for the study of bubonic plague than traditional subcutaneous models. In comparison with a subcutaneous model, an intradermal model resulted in faster progression of infection. In addition, a deletion mutant lacking a gene of unknown function was attenuated after inoculation using an intradermal route. This same mutant colonizes tissues equally when compared with wild type *Y. pestis* when inoculated using a subcutaneous route.

### 5.2. Implications for the study of bubonic plague

The study of host-pathogen interactions during bubonic plague has largely been conducted using *in vitro* approaches. The emphasis on *in vitro* studies is largely due to the availability of cell lines and also because of the complications that working with animal models entail. Another element that has characterized plague research is the use of attenuated strains. Work with fully virulent *Y. pestis* is restricted to biosafety level three laboratories, which are expensive to maintain and not available at most institutions. As a consequence, most of the ideas we have about *Y. pestis* host-pathogen interactions derive from models that are missing one or many key elements of infection.

Because we conducted all our experiments *in vivo* and using a fully virulent strain of *Y. pestis*, our observations are more biologically relevant, as the major elements of infection are taken into account. We identified many previously

unrecognized events that define bacterial dissemination and colonization of the host. These events include the formation of a bottleneck during *Y. pestis* dissemination as well as neutrophil-dependent restriction of bacterial growth in the skin. We also provided images of bacteria as they disseminate through multiple tissues. This provided new information on the nature of host-pathogen interactions, such as bacterial association with host cells in lymphatic vessels and with neutrophils and platelets in the bloodstream.

Besides the novel observations we report, we believe that the techniques that were developed to make these observations will be of relevance to the field for future studies. Our microscopy approach allows for direct qualitative observations of host-pathogen interactions without compromising the use of fully virulent strains. This method serves as a reliable approach that can be implemented for the study of specific mutants to gain insights into the function of specific bacterial genes.

Lastly, we modified a previously described murine intradermal model of infection to study bubonic plague (Guinet and Carniel, 2003). We provided information that revealed biologically relevant differences between this intradermal model and a more widely used subcutaneous approach. The observed differences strongly suggest that an intradermal model should be considered over subcutaneous models to study bubonic plague.

We believe that the use of the aforementioned approaches provide valuable new tools to improve our understanding of *Y. pestis* interactions with the host.

### 5.3. Caveats of our intradermal model of infection

Our intradermal model of infection is based on the injection of a very small volume into the dermis of the mouse ear. Previously reported models use considerably larger volumes, which result in significant disruption of the dermis (Guinet and Carniel, 2003; Spinner et al., 2013). One of the advantages of the use of smaller volumes is that it allowed for accurate observations by microscopy imaging. The use of larger volumes causes major disruption of the skin, which can result in confounding effects when assessing bacterial interactions with the host in this tissue. More importantly, the use of smaller volumes eliminated confounding effects related to bacterial growth that derived from disruption of the dermis (Shannon et al., 2013). While we are confident that our approach very closely mimics an infectious fleabite, we believe that many modifications should still be explored.

Models where needles are used to deliver bacteria instead of a fleabite are unavoidable because it is impossible to control the number of bacteria inoculated when using flea models. While the caveats of needle delivery are many, we think two of them are of major importance. The first caveat is related to the disruption of dermal tissue an injection causes in comparison with a fleabite. Disruption to the dermis by the volume injected by a fleabite might be minimal, if not negligible. While we inject a very small volume (2 μL), this still causes some damage to the dermis, in addition to mechanical damage derived from the needle itself. An alternative to minimize skin disruption could be to deposit the same inoculum (2 μL) on the tip of a needle and puncture the dermis with it. This would deliver bacteria

without forcing a volume of liquid to penetrate into the skin. Plating homogenized ears immediately after inoculation can easily be used to assess the accuracy of this method to deliver a desired inoculum. The second caveat is that saliva components and other molecules present in the mouthparts of the flea are absent during needle inoculations (Belkaid et al., 1998). Saliva components of arthropods have been shown to influence the progression of infection during vector borne diseases (Bizzarro et al., 2013; Leitner et al., 2013). For this reason, the absence of flea saliva might be the most important caveat of needle infections when attempting to mimic a fleabite. This caveat has been partially addressed in other fields with great success. Salivary glands of sand flies have been inoculated along with *Leishmania* parasites in a model that reproduced previously unattainable clinical signs of cutaneous leishmaniasis (Belkaid et al., 1998; Peters et al., 2009). Establishing similar approaches in the plague field would be important to determine whether the observations reported by us or other groups are a true recapitulation of flea-inoculated infections.

An additional limitation is the use of a single animal species. *Y. pestis* has multiple hosts and their role in maintenance of plague is not well established. Rodents have been shown to be relevant for bacterial maintenance in sylvatic plague and thus they make an ideal model for the study of *Y. pestis* (Gage and Kosoy, 2005). However, much genetic variability exists within this multispecies group of animals. The implications of this were shown in an study where deletion mutants were shown to behave differently when tested in different mouse backgrounds (Weening et al., 2011). A promising alternative is the use of mouse

systems that encompass variable genetic backgrounds (termed the Collaborative Cross) (Churchill et al., 2004). These systems might better reflect the diverse gene pool *Y. pestis* is exposed to in its different hosts.

Beyond the above-mentioned limitations, much can be learned from any *in vivo* model that is not limited by the use of attenuated strains. The use of animal models to study *Y. pestis* pathogenesis is extremely promising and there are still many aspects of these models that have not been explored. Murine models in particular provide a remarkable advantage in plague studies when compared to other fields. This advantage is that, along with rats, mice are natural hosts. This means that much of what is learned through murine models of infection should closely recapitulate many, if not all, of the important components present during a natural infection.

### 5.4. Understudied aspects of *Y. pestis* dissemination.

This body of work has provided new windows to take a direct look at fundamental aspects of dissemination and pathogenesis of *Y. pestis* that are currently understudied. Three aspects are worth mentioning and require urgent attention for the field to advance. The first aspect is bacterial colonization of the lymph node. We showed that bacterial growth is severely restricted in the ear most likely by the action of neutrophils. A striking change seems to occur once bacteria reach the lymph node as they grow profusely in this compartment. This could result from the absence of growth-restrictive immune responses in the lymph node, a component of lymph node tissue that triggers bacterial growth, or a combination of both. It is easy to propose that the bacterium must be equipped with specific genes

that allow for such a dramatic change in growth from one tissue to the next. Neither host nor bacterial components that could explain this phenomenon have been reported.

A second aspect that is understudied is bacterial migration from the lymph node into the bloodstream. Fatalities during plague infections are caused by the effects of bacteria in the bloodstream, and thus, most research efforts should be devoted to address this systemic stage of disease. It is currently unknown what mechanisms the bacteria use to escape the lymph node, an organ whose function is precisely to prevent pathogens from moving into the bloodstream. Escape could occur in a direct manner if *Y. pestis* is able to actively invade the high endothelial venules that enter lymph nodes and allow for easy access of leukocytes to this compartment. Because infected lymph nodes are enlarged and bloody, we believe that entrance to the high endothelial veins might occur as the bacteria disrupt the normal architecture of this compartment. An alternative mechanism could involve bacterial escape through efferent lymphatic vessels. These vessels collect the lymph that is filtered by a lymph node and conduct it to the thoracic duct. The thoracic duct drains into the left subclavian vein, which serves as a direct entry into systemic circulation. The disruption of the normal functions of the lymph node to prevent further bacterial dissemination is one of the most relevant abilities of *Y. pestis* to cause disease. For this reason, insights into the mechanisms that result in lymph node escape are imperative to fully understand *Y. pestis* pathogenesis.

Lastly, the study of *Y. pestis* during septicemic stages is the most neglected aspect of plague research and it is limited to a very modest number of studies

(Chauvaux et al., 2007; Zhou et al., 2013). This is contradictory to what would be expected since the presence of bacteria in the bloodstream is the actual cause of death for bubonic plague patients. Aspects of the septicemic stages of infection that need critical attention are (1) interactions with cells of the innate immune response, (2) bacteria-induced damage to endothelial tissue, and (3) bacterial mechanisms that elicit septic shock. We partially addressed some of these aspects by providing tools to visualize bacteria in the bloodstream. Even though we limited our studies to the observation of neutrophils and platelets, additional antibodies can be used to assess interactions with other host cells.

Many important aspects of the host-pathogen interactions that occur during *Y. pestis* infections are understudied. Addressing these understudied aspects of *Y. pestis* pathogenesis and providing mechanisms that explain them is the first step to proposing strategies to control disease.

### 5.4. Translational implications and impact to other fields

During these studies we followed multiple components of the host as it attempts to control bacterial spread during bubonic plague. We took a closer look at cutaneous immunity and showed the role of neutrophils in controlling bacterial growth in the skin. We also reported the presence of a bottleneck that limits bacterial spread from the skin into the lymph nodes and from lymph nodes into the bloodstream. These constitute efforts by the host to control *Y. pestis.* These efforts could be exploited in clinical settings to prevent disease progression in exposed individuals. More importantly, the microscopy approaches we implemented to study bacterial dissemination can easily be used to address questions relevant to

cutaneous immunology. This is not limited to *Y. pestis*, or even, bacterial infections but could be extended to other infectious diseases, autoimmune disorders or even cancer. Moreover, vaccine development could directly be influenced by our work. Cutaneous immunity, cutaneous physiology, antigen transport, and host-pathogen interactions in the skin, are aspects of our research with biologically relevant implications to vaccine development. Our work might be of importance not only for the improved understanding of bubonic plague, but could also contribute to efforts to prevent and control other infectious diseases that are relevant to public health.

### 5.4. Future experiments

The list bellow contains future directions that can serve as a guide to continue with this work.

1. Determine whether the bottlenecks are present after inoculation of other bacteria. A comparison between *Y. pestis* and species that are closely related to it (e.g. *Y. pesudotuberculosis*) and species that are not related (e.g. *Francisella tularensis*) can be made.
2. Determine whether the absence of a bottleneck after SC injection replicates from other anatomical sites in the mouse (e.g. back or leg).
3. Determine whether the neutrophils in the skin that interact with *Y. pestis* are targeted by the bacteria's type 3 secretion system apparatus.
4. Determine bacterial associations with host cells in the lymph node.
5. Establish whether bacteria can be found in afferent lymph vessels and the thoracic duct.

6. Determine whether the neutrophil-platelet-bacterial associations observed during bacteremia are *Y. pestis* specific or if they can occur with other bacteria as well.
7. Establish the role of neutrophils and platelets during bacteremia.
8. Establish if there is tissue damage during bacteremia (e.g. endothelium) and if it is bacteria or host dependent.
9. Assess the role of other cells of the immune response through microscopy imaging of mice with fluorescently labeled immune cells.

## REFERENCES


Belkaid, Y., Kamhawi, S., Modi, G., Valenzuela, J., Noben-Trauth, N., Rowton, E., Ribeiro, J., and Sacks, D.L. (1998). Development of a natural model of cutaneous leishmaniasis: powerful effects of vector saliva and saliva preexposure on the long-term outcome of *Leishmania major* infection in the mouse ear dermis. J Exp Med *188*, 1941–1953.

Bizzarro, B., Barros, M.S., Maciel, C., Gueroni, D.I., Lino, C.N., Campopiano, J., Kotsyfakis, M., Amarante-Mendes, G.P., Calvo, E., Capurro, M.L., et al. (2013). Effects of *Aedes aegypti* salivary components on dendritic cell and lymphocyte biology. Parasit Vectors *6*, 329.

Chauvaux, S., Rosso, M.-L., Frangeul, L., Lacroix, C., Labarre, L., Schiavo, A., Marceau, M., Dillies, M.-A., Foulon, J., Coppée, J.-Y., et al. (2007). Transcriptome analysis of *Yersinia pestis* in human plasma: an approach for discovering bacterial genes involved in septicaemic plague. Microbiology (Reading, Engl) *153*, 3112–3124.

Churchill, G.A., Airey, D.C., Allayee, H., Angel, J.M., Attie, A.D., Beatty, J., Beavis, W.D., Belknap, J.K., Bennett, B., Berrettini, W., et al. (2004). The Collaborative Cross, a community resource for the genetic analysis of complex traits. Nat Genet *36*, 1133–1137.

Gage, K.L., and Kosoy, M.Y. (2005). Natural history of plague: perspectives from more than a century of research. Annu Rev Entomol *50*, 505–528.

Gonzalez, R.J., Weening, E.H., Frothingham, R., Sempowski, G.D., and Miller, V.L. (2012). Bioluminescence imaging to track bacterial dissemination of *Yersinia pestis* using different routes of infection in mice. BMC Microbiol *12*, 147.

Guinet, F., and Carniel, E. (2003). A technique of intradermal injection of *Yersinia* to study *Y. pestis* physiopathology. Adv Exp Med Biol *529*, 73–78.

Leitner, W.W., Wali, T., and Costero-Saint Denis, A. (2013). Is arthropod saliva the achilles' heel of vector-borne diseases? Front Immunol *4*, 255.

Peters, N.C., Kimblin, N., Secundino, N., Kamhawi, S., Lawyer, P., and Sacks, D.L. (2009). Vector transmission of leishmania abrogates vaccine-induced protective immunity. PLoS Pathog *5*, e1000484.

Shannon, J.G., Hasenkrug, A.M., Dorward, D.W., Nair, V., Carmody, A.B., and Hinnebusch, B.J. (2013). *Yersinia pestis* subverts the dermal neutrophil response in a mouse model of bubonic plague. MBio *4*, e00170–13.

Spinner, J.L., Winfree, S., Starr, T., Shannon, J.G., Nair, V., Steele-Mortimer, O., and Hinnebusch, B.J. (2013). *Yersinia pestis* survival and replication within human neutrophil phagosomes and uptake of infected neutrophils by macrophages. J Leukoc Biol.

Weening, E.H., Cathelyn, J.S., Kaufman, G., Lawrenz, M.B., Price, P., Goldman, W.E., and Miller, V.L. (2011). The dependence of the *Yersinia pestis* capsule on pathogenesis is influenced by the mouse background. Infect Immun *79*, 644–652.

Zhou, J., Bi, Y., Xu, X., Qiu, Y., Wang, Q., Feng, N., Cui, Y., Yan, Y., Zhou, L., Tan, Y., et al. (2013). Bioluminescent tracking of colonization and clearance dynamics of plasmid-deficient *Yersinia pestis* strains in a mouse model of septicemic plague. Microbes Infect.